Polymer Dynamics Studied by Dynamic Light Scattering

A thesis presented in partial fulfilment of

the requirements for the degree of

Master of Science

in Physics at

Massey University

by

David Thomas CLARK

1998

Abstract

Theoretical treatments of dynamic properties of polymer solutions are reviewed. Particular emphasis is placed on the discussion of diffusion in polymer solutions. The relationship between the slow diffusion coefficient found by Dynamic Light Scattering (DLS) and the Self Diffusion Coefficient is shown.

An introduction to DLS theory is given. The experimental techniques involved in DLS measurements are discussed.

Concentration dependencies of the DLS observed slow diffusion coefficient in ternary polymer solutions of polystyrene-poly vinyl methyl ether-solvent have been measured. Solvents used were toluene, carbon tetrachloride and tetrachloroethylene and the polymer molar masses were 110 000 $gmol^{-1}$ for both polystyrene (PS) and poly vinyl methyl ether (PVME). Solvents were chosen to be very nearly isorefractive with PVME. Toluene is very nearly an equally good solvent for the polymer pair PS and PVME, while tetrachloroethylene is equally poor for both polymers. Carbon tetrachloride is an unequal quality solvent for this polymer pair. The results of these DLS measurements are reported.

Four sets of experiments are described. The first is the effect on the relationship between D_I (the slow mode diffusion coefficient found by DLS) and D_S (the self diffusion coefficient) of different mass fractions in the polymer solution. It is found the mass fraction, x, has little effect on the observed diffusion coefficient. Secondly the effect of the polymer-polymer interaction parameter, χ, on the relationship between D_I and D_S is investigated. It is found solutions formed with equal quality solvents have D_I nearly equal to D_S. But solutions formed with unequal quality solvents have D_I considerably less than D_S and that these solutions suffer phase separation at lower concentration. Thirdly the effect of polymer molar mass on the relationship between D_I and D_S is investigated. These are found to be in line with those expected from literature.

Fourthly the considerable discrepancy between D_I and D_S which is manifest in 110 000 $gmol^{-1}$ PS/ 110 000 $gmol^{-1}$ PVME/ toluene solutions at polymer volume fractions greater than 0.4 is investigated. The diffusion coefficient found, D_I, does not fit a unique concentration power law. Two unique regions are seen with concentration exponents of -11±4 and -14.9±0.7 for the low and high concentration regions respectively. This is found to agree with results found in literature.

Acknowledgments

I wish to express my sincere gratitude to the following people for their involvement in this work:

Firstly to Jesus, the Author and Perfector of my faith, who gives people a second chance. To you goes the glory.

My supervisor Assoc. Professor Neil Pinder, for providing both theoretical and experimental "know how", and infinite patience. Your enthusiasm was greatly appreciated, as was your advice and proof reading.

The Staff and Students of the Dept. of Physics who have greatly encouraged and enthused myself for the things of physics as well as put up with me for more than a decade.

Dr Hedwig of the Dept. of Chemistry for the use of his warm room and balance.

The Mechanical Workshop Staff for construction of the high concentration transferral apparatus.

GAF for supplying the poly vinyl methyl ether used in this work free of charge. Having worked with this polymer, I now see why, it sticks everywhere.

My Mum and Dad who have provided the example and the enthusiasm to achieve anything. Thanks.

And of course Kerry Wallace, my girlfriend at the time of writing, whose unfailing love and support provides an all-win situation in everything I do. Who patiently proof-read this manuscript, and whose proofed manuscripts I always looked forward to receiving.

Table of Contents

List of Figures

Chapter 2 Polymer and DLS Theory

Chapter 3 Experimental Set-up

List of Tables

Chapter 3 Experimental Set-Up

Chapter 4 Results and Discussion

Chapter 1
Introduction

1.1 Polymers and Dynamic Light Scattering

Since the dawn of the laser, Laser Light Scattering has allowed the investigation of molecular size movements within solutions. Recently ternary polymer solutions containing two polymers and a single solvent have been investigated using Dynamic Light Scattering (DLS). The lack of suitable theory, and apparatus of sufficient quality has limited these investigations to diffusion coefficient dependence on molar mass and concentration. Generally these investigations have utilised special polymers and solvents in order to reduce the complexity of the results found.

Benmouna and Borsali et al [1] [2] [3] [4] have recently produced a theory of diffusion specifically for polymer solutions, which they have extended in ternary polymer solutions. This theory makes several predictions which are easily verifiable by experiment. Daivis [5] has briefly examined various aspects of this theory experimentally, however these results require confirmation and expansion, as well as experimental investigation into recent theoretical advances of this theory.

Daivis's work advanced understanding of diffusion in polymer solutions, however understanding was left incomplete in several areas. In his work Daivis compared diffusion in an equally good solvent for the polymer pair polystyrene (PS) and poly vinyl methyl ether (PVME) with that for the same polymer pair in an unequal quality solvent. The comparison of this diffusion data with data collected with the same polymer pair in an equally poor quality solvent would reveal much about polymer motion in solutions, yet this work was not attempted by Daivis. Daivis noted that the diffusion coefficient measured by DLS deviated from that obtained by Pulse Gradient Spin Echo Nuclear Magnetic Resonance Spectroscopy (PGSE NMR) at high polymer concentrations. This work was not pursued by Daivis. This work investigates aspects of

Daivis's work which have been left incomplete or require further investigation for resolution.

1.2 Thesis Organisation

Chapter 2 summarises existing theories of diffusion in polymer solutions, and DLS theory. This chapter also explains what polymers are and gives a basic understanding of the properties of polymers critical to understanding this thesis.

Chapter 3 summarises experimental procedures for both the DLS equipment and also for solution preparation. This chapter also summarises some of the theoretical background for the DLS equipment, and the sources of polymers and solvents utilised in this work.

Chapter 4 summarises investigations into four aspects of the work previously presented by Daivis et al [5] [6] [7] [8] [9]. The first is the effect on the relationship between D_I and D_S of different mass fractions in the polymer system 110 000 Dalton PS/ 110 000 Dalton PVME/ solvent (where three different solvents were utilised:- toluene, carbon tetrachloride and tetrachloroethylene). Secondly the effect of the polymer-polymer interaction parameter, χ, on the relationship between D_I and D_S is investigated. Thirdly the effect of polymer molar mass on the relationship between D_I and D_S is investigated. Fourthly the considerable discrepancy between D_I and D_S which is manifest in 110 000 Dalton PS/ 110 000 Dalton PVME/ toluene solutions at polymer volume fractions greater than 0.4. The results presented in this chapter are also discussed and compared to results found in literature.

Chapter 5 summarises the main conclusions which can be drawn from this study.

Chapter 2
Polymer and DLS Theory

2.1 Polymer Outline

2.1.1 Polymers-What are they?

Polymers are very large molecules that are made by chemically bonding together many smaller identical molecules called monomers which may be simple or complex in structure. The number, N, of monomers in the polymer chain is called the degree of polymerisation.

Polymers are characterised by high molecular weight M_W, but also have some unusual properties, which make them of interest. Polymers may appear in liquid, solid or viscous form depending on temperature.

The liquid polymer state is characterised by a viscosity which strongly increases with the molecular mass. In contrast to this, the response of the polymer liquid to a mechanical constraint, at the beginning is of the elastic type, the viscous flow appearing only after a time delay which increases with the molecular mass. While polymer liquids will flow, they usually have high viscosity in melts or solution, while the large inter and intra bond interactions allow such a flowing medium to remain, as in the case of paint, stuck to a wall. The transition between the viscous state and the solid state is characterised by a temperature T_g called the glass transition temperature. This temperature corresponds to a discontinuity of physical parameters and in particular of the thermal expansion coefficient. The discontinuity observed when T decreases seems to result from the freezing (for $T<T_g$) of rotation and of large motions of chain elements.

Polymers may be designed to have high strength, or withstand high strain, yet still have the ability to withstand huge deformation (ie. modern car bumpers). One of the most useful aspects is the ability of some polymers to stretch significantly beyond their own

length (ie. bungee cord), yet still return to their original length. Articles traditionally made of metal for strength reasons are increasingly being made of polymeric materials.

The many and varied properties of polymers and the ability to tailor make a polymer to fulfil the requirements of a specified material with a specified set of physical parameters, have meant that polymers have become increasingly important in today's world. Yet surprisingly there has not yet been developed a single unified, all embracing theoretical basis to account for all the physical properties of polymeric materials in terms of the chemical structure of the individual molecules [10]. However there are a number of theories which can be applied quantitatively to approximate some polymer specific phenomena: Entropy-elasticity, viscosity, glassy solidification, particular deformation and failure mechanisms, mixing behaviour, crystallisation and melting, and solution dynamics.

With the increasing use of polymer blends to make "high-tech" polymeric materials (ie. therm-plastics) the need to explain the dynamics of polymeric interaction has increased so that one can quantitatively know the properties of a polymer blend without having to mix it. Previously this has had a rather empirical basis (more along the lines of trial and error). However over the last few decades huge strides have been made in describing solution and melt dynamics (resulting in "designer" polymers). Even so polymer science is still very much in the theoretical and experimental conformation stage of its growth.

2.1.2 Polymeric Structure

As has been previously mentioned, polymers are long chain molecules made up of repeating units called monomers. The degree of polymerisation and the make up of the monomer have a major influence on the properties of the polymer. Large degrees of polymerisation can lead to flexible polymers, but monomers with large coulombic interaction between structural units of the monomer will become rigid.

Once in solution or in melt, these properties change depending on the polymer's compatibility with the solvent. If a polymer is compatible with a solvent then the chains

of the polymer will tend to spread out to allow maximum contact with the solvent. However in a poor solvent the polymer chains contract to allow maximum self contact, resulting in a highly coiled polymer (in the extreme case, the polymer "drops out" of solution and a two phase system is formed). As the temperature rises the thermal energy k_BT of the chains overcomes the inhibitive effect of the poor solvent, and the polymer slowly untangles. While as the temperature decreases, the polymer will tangle more tightly until such time as the critical solution temperature T_C is reached-at which time two distinct phases are formed, either

a) solvent/polymer precipitate, or

b) solvent/polymer with reduced mass fraction, and a polymer phase on its own.

A useful static property is the root mean square radius of gyration, R_g, which is a measure of the average size of a polymer molecule (or the root mean square distance that the elements of the chain are from the centre of gravity, not the linear end to end distance of the polymer molecule). This will reveal the "quality" of solvent, and also what is happening in solution.

Chapter 2.2 Properties of Polymers in Solution

2.2.1 Compatibility of Polymers

Mixtures of polymers generally do not form thermodynamically stable single-phase systems unless the free energy of mixing is negative

ie $$\Delta G_m = \Delta H_m - T\Delta S_m < 0 \qquad (2.2.1)$$

where ΔH_m is the enthalpy of mixing and ΔS_m is the entropy of mixing, and T is the absolute temperature. These are generally positive for pairs of polymers, so only if

$$\Delta H_m < T\Delta S_m \qquad (2.2.2)$$

will the two polymers mix to form a single homogeneous phase. This defines the lower limit for the enthalpy of mixing above which the two polymers are not miscible. An additional, necessary and sufficient condition for compatibility is given by

$$\left[\frac{\partial^2 \Delta G_m}{\partial \phi_i^{\,2}}\right]_{T,p} > 0 \qquad (2.2.3)$$

where ϕ_i is the volume fraction of the ith component. The three possible forms for binary systems are shown in figure 2.2.1

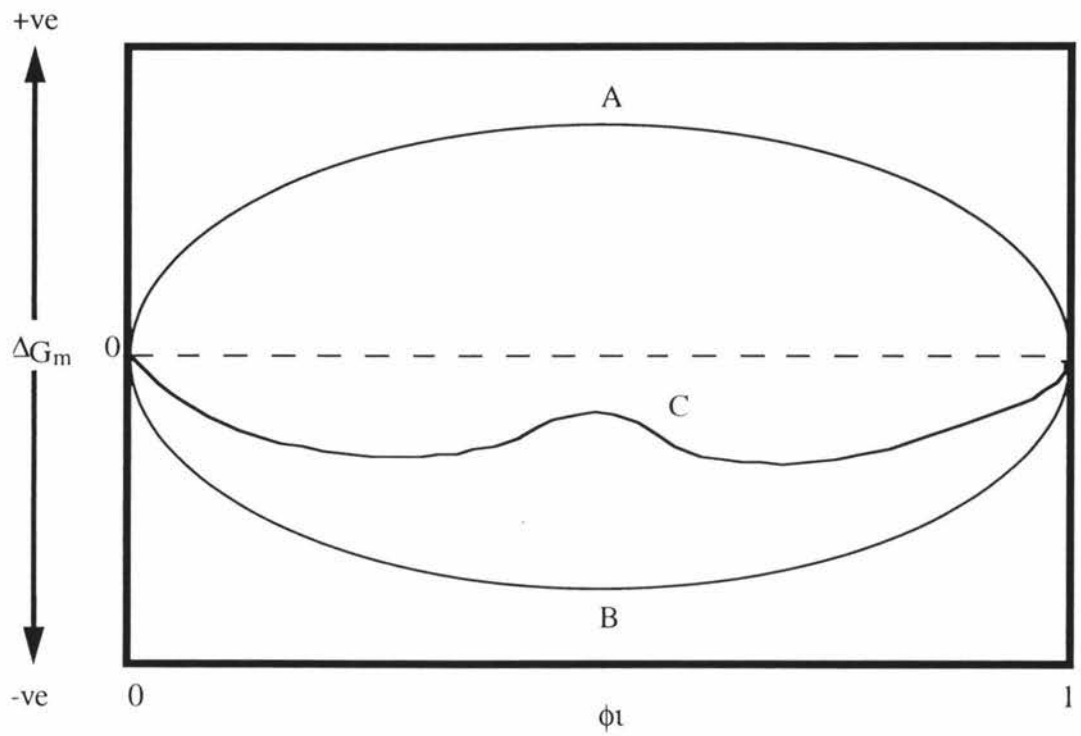

Figure 2.2.1 Free Energy of Mixing for Binary mixtures versus their composition A) Incompatibility, B)Total Miscibility, C) Partial Miscibility.

The behaviour of binary systems can best be described by their phase diagrams as shown in figures 2.2.2 and 2.2.3. In the single phase region only one distinct phase is found in which the solution is completely compatible. At the Binodal curve the solution breaks up into two separate stable phases, the border between stable and unstable regions is called the binodal. Further into the two phase region, there is reached a state where the interfacial energy vanishes (and/or changes sign). It is then favourable for the system to break up into many small domains, this threshold defines what is called the spinodal curve. Beyond this curve phase separation occurs (in the shaded regions). As the molar mass of the polymer is increased the Upper Critical Point (UCP) moves up and to the left. In the limit of infinite molecular mass, the UCP approaches the T axis. The limiting value of T is called the theta temperature, θ.

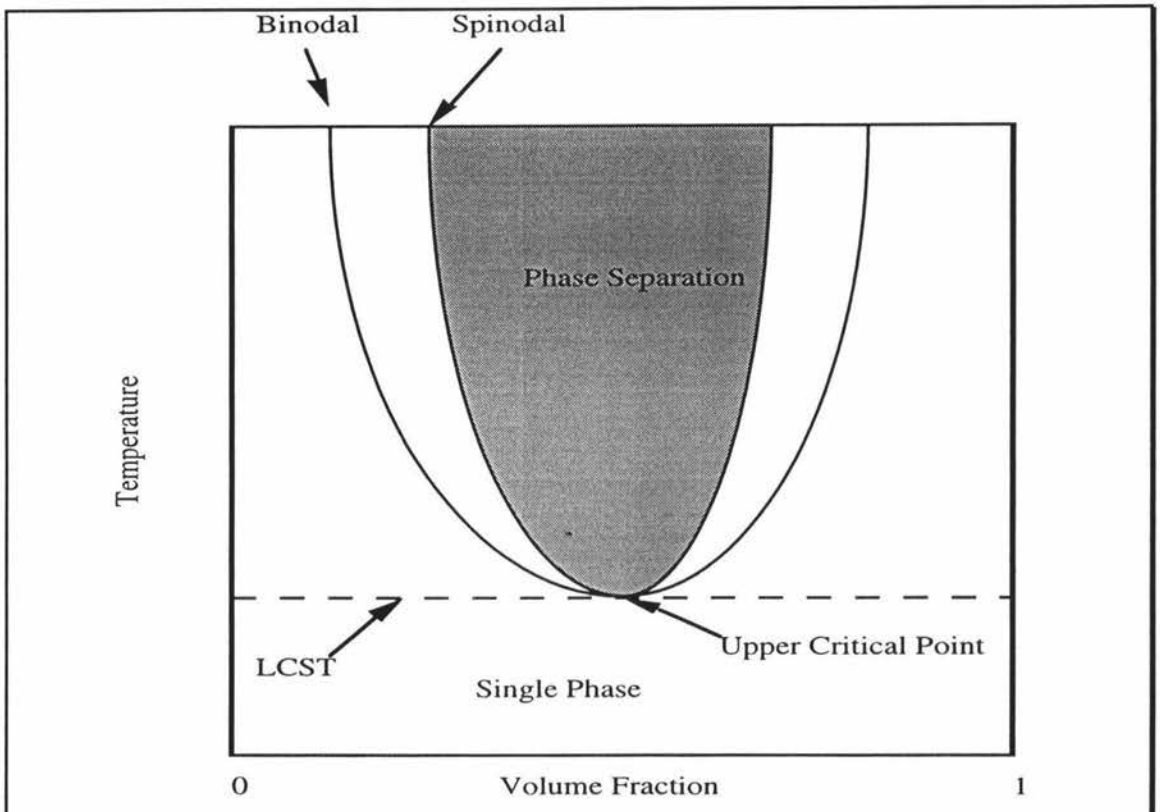

Figure 2.2.2 Phase diagram of a binary system showing the Upper Critical Point (UCP)

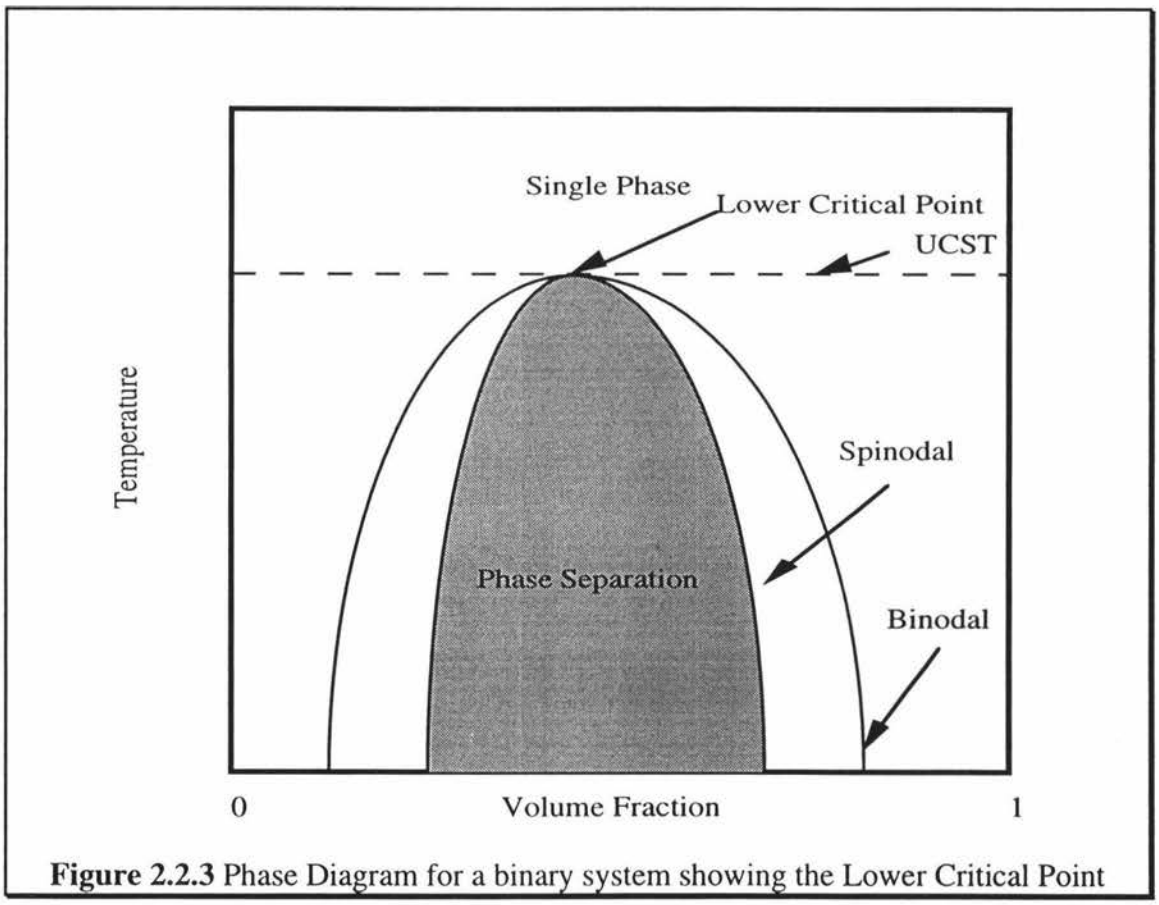

Figure 2.2.3 Phase Diagram for a binary system showing the Lower Critical Point

Daoud and Jannink [11] in their 1976 paper deduced the temperature-concentration diagram for a solution with no lower critical solution temperature (LCST) (or a LCST far from the Upper Critical Solution Temperature (UCST)), this diagram is shown in figure 2.2.4.

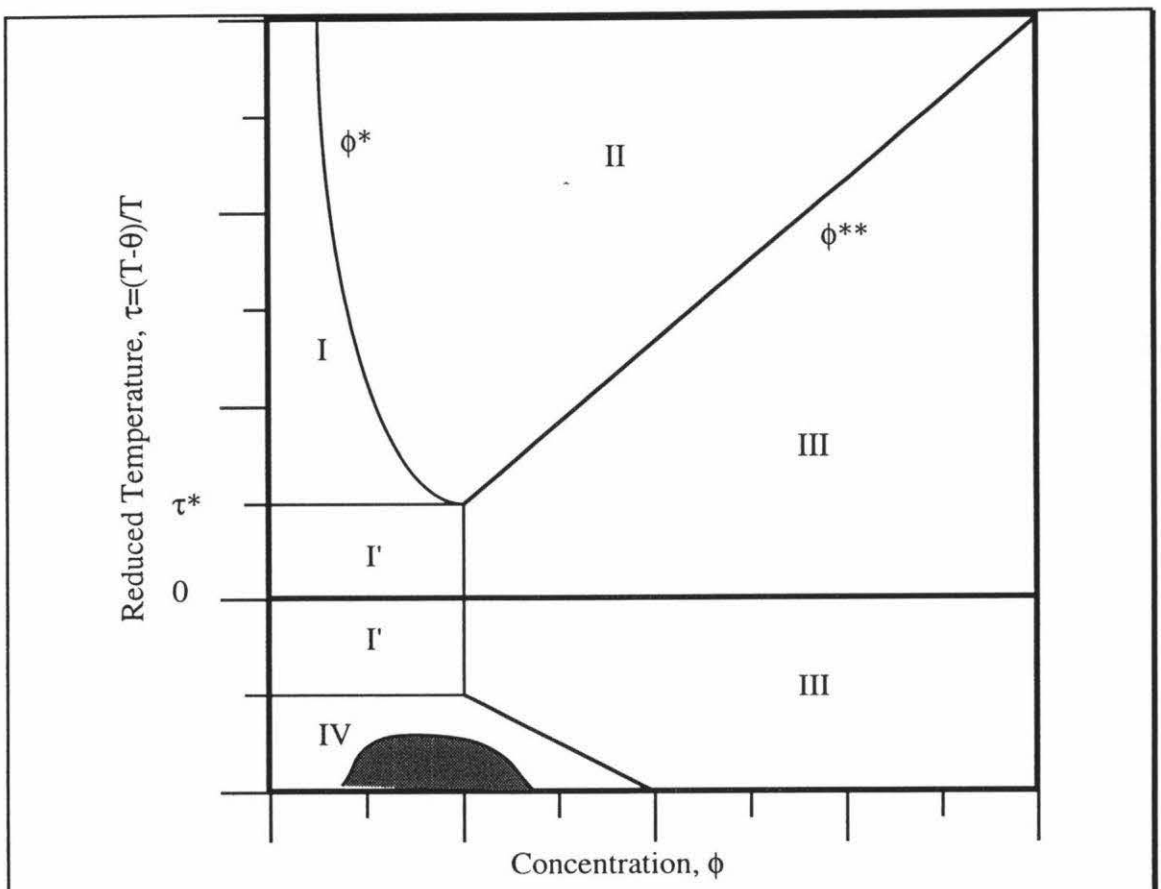

Figure 2.2.4 Temperature-concentration diagram for a polymer solution far from the Lower Critical Point (LCP) according to Daoud and Jannick [11]. The regions are:- I) Dilute good solvent, I') Dilute theta, II) Semi dilute good solvent, III) Semi dilute theta solvent, IV) Collapsed Chain. The shaded region corresponds to the two phase region of figure 2.2.3. For a polymer of infinite mass, the dilute theta region I' is vanishingly small and the UCST corresponds to the theta temperature.

2.2.2 Ideal Polymer Chain Model

Summaries of Ideal Chain statistics can be found in most works on polymer solution theory [12] [13] [14] [15] the reader is referred to these for a more detailed analysis, however a brief summary of the important points of this theory are given here.

In this model the monomers or base units of the polymer are covalently bonded together in a linear fashion. In general each monomer is given freedom of rotation about the axis of its proceeding monomer unit, and this freedom allows the chain to potentially take on a huge range of different conformations. The only restrictions on the conformation come from the steric hindrances of the neighbouring monomers. Long range interactions are expressly ignored in this model.

These flexible polymer molecules may be modelled by a hypothetical chain which is made up of rigid thin rods of equal length connected linearly by universal joints. This model is called the Random Flight Chain. The random flight chain no longer retains any information about the primary chemical structure and local interactions of the actual polymer molecule. It is therefore only useful for formulating the global or large scale behaviour.

Because the chain may take any direction with equal probability, gaussian statistics are assumed. Doi and Edwards [12] give the probability that the chain has an end to end vector $\underline{R}$ as

$$\Phi(\underline{R},N)=\left(\frac{3}{2\pi Nb^2}\right)^{\frac{3}{2}}\exp\left(\frac{-3R^2}{2Nb^2}\right) \qquad (2.2.4)$$

where N is the number of links or monomers per polymer and b is the effective bond length (ie. the monomer length).

Doi and Edwards [12] also give the scattering function of such a chain as

$$S(\underline{q}) = N(1 - \frac{q^2 R_g}{3}) \text{ for } |q|R_g \langle\langle 1 \quad (2.2.5)$$

$$S(\underline{q}) = \frac{2N}{q^2 R_g^2} \text{ for } |q|R_g \rangle\rangle 1 \quad (2.2.6)$$

which is called the Debye function and is often approximated

$$S(\underline{q}) = \frac{N}{1 + (q R_g)^2/2} \quad (2.2.7)$$

where R_g is the radius of gyration and takes the form

$$R_g = \frac{b}{\sqrt{6}} N^{1/2} \quad (2.2.8)$$

in this model and $\underline{q}$ is the scattering vector whose magnitude is given by $q = \frac{4\pi n}{\lambda} \sin(\theta/2)$ where n is the refractive index of the sample λ the wavelength of the incident light and θ the scattering angle. Each of these quantities will be defined in later sections of this chapter, and are included now only for completeness.

de Gennes [13] gives a summary of ideal chains as being characterised by gaussian statistics, end to end vector (size) <R> being proportional to $N^{1/2}$ and the scattering law following a q^{-2} relationship.

2.2.3 Excluded Volume and the Self Avoiding Walk

The excluded volume effect was first discussed by Kuhn [16] and was developed by Flory [17].

The basic concept is that in ideal polymer interactions, only interactions within a few neighbouring monomers along the chain cause any effect on the orientation or structural configuration of the monomer. However segments distant from the original monomer do interact if they come close to each other in space. Since each segment has finite volume, other segments cannot come into this region. The motion is called a "Self Avoiding Walk," since the polymer "avoids" contact with itself. This interaction

"swells" the polymer; the coil size of the chain with such interactions is larger than that of an ideal chain, which has no such interaction. The size of this swelling depends upon the solvent quality, and the potential monomer-monomer interaction strength. This effect is called the "Excluded Volume Effect."

It has been recognised by Flory and Kuhn that such long range interactions change the statistical properties of the chain, an example being the relationship between the end to end vector $\underline{R}$ of the polymer to the degree of polymerisation, N. In ideal random flight statistics

$$\langle R^2 \rangle \propto N \tag{2.2.9}$$

however if we take into account the excluded volume effect we find

$$\langle R^2 \rangle \propto N^{2\upsilon} \tag{2.2.10}$$

where υ is called the "critical exponent," which Flory has calculated to have the value $\upsilon \approx 3/5$ for a good solvent, which is close to the renormalisation theory result of 0.588.

This critical exponent is not to be confused with the segment-segment excluded volume v, which is an indicator of solvent quality (it is proportional to the solvent quality). The segment-segment excluded volume parameter is related to the Flory interaction parameter, χ, by the following relationship

$$1 - 2\chi = \frac{v}{b^3} \tag{2.2.11}$$

where b^3 is the volume of a polymer segment or solvent molecule (assumed to be equal in lattice models). The excluded volume can also be written [18] [19] in terms of the reduced temperature $\tau = (T - \theta)/T$ as

$$\left(\frac{v}{b^3}\right)^2 = \frac{\tau^2}{k_1} \tag{2.2.12}$$

where k_1 is a constant expected to weakly depend on the solvent and monomer type.

2.2.4 Theta Solutions

The osmotic pressure Π, of a dilute solution (below ϕ^* in figure 2.2.4 (in the dilute regions I and I')) of a mono disperse polymer with molecular weight M, can be expressed as a power series of polymer mass concentration c, as

$$\frac{\Pi}{RT} = \frac{c}{M} + A_2 c^2 + A_3 c^3 + \ldots \qquad (2.2.13)$$

where R is the gas constant and T the absolute temperature. This series is usually referred to as the osmotic virial expansion, with A_i (i=2,3,...) referred to as the ith virial coefficient of the solution. Experimentally A_2 can be evaluated by determining the initial slope of (Π/RTc) plotted against c. However A_3 and higher coefficients are not so easy to determine.

For a series of homologous polymers A_2 depends on M as well as T and the solvent species. Experimental studies have shown repeatedly that for a given polymer there is a combination of poor solvent and temperature, θ, for which A_2 vanishes regardless of M. Because the concentration is low, the higher order coefficients need not be considered. This special poor solvent at θ is called the theta solvent, and θ the theta temperature.

Under theta conditions coil expansion due to the intramolecular excluded volume effect and coil contraction due to attraction between non-neighbouring segments (so called long range interactions) in the same chain cancel out precisely. In this respect the theta temperature is an analogue of the Boyle point for non-ideal gases. The theta temperature of a polymer-solvent combination is a point of ideal behaviour, hence much experimental work is carried out under theta conditions.

From the thermodynamics of polymer solutions it is known that A_2 is proportional to $(\frac{1}{2} - \chi)$ where χ is the Flory interaction parameter, and it is also related to the (excluded) volume of the solute molecules. Hence the so called theta conditions are A_2=0 and χ=1/2 for T=θ.

Experimentally the theta temperature of a polymer-solvent combination can easily be found by osmomotry at different temperatures: $T=\theta$ when Π/c becomes independent of polymer concentration.

2.2.5 Flory-Huggins Mean Field Theory

Both Flory [14] and Huggins [20] independently worked to describe the mixing behaviour of polymers in low molar mass solvents.

As a solvent mixes into a polymer there is an entropy increase to the total system, while the internal energy of the system remains essentially constant. Flory showed a simple approach to calculate the entropy of mixing.

He assumed that the solvent molecules are ordered as a 3-D lattice, where each lattice point is occupied either by a solvent molecule or a single polymer segment.

Let N be the total number of lattice sites, and n be the number of polymer molecules with x segments, and $m=N-xn$ be the number of solvent molecules.

The problem Flory faced of describing the mixing behaviour of polymers in low molar mass solvents, essentially becomes one of calculating the number of different possible confirmations of the n polymer molecules and N-xn solvent molecules.

Initially, to begin with, individual segments of polymer molecules are arranged such that consecutive polymer segments have to be sited at neighbouring lattice sites, then the remaining sites must be filled with solvent molecules. Hence for n_i polymer molecules in the lattice the first segment of the $(i+1)$ molecule can be put in any one of the remaining N-xn_i vacant sites. The second segment of this molecule is restricted to those free lattice sites immediately adjacent to the site occupied by the first segment. The fraction of lattice sites not occupied by polymer segments is given by $(n\text{-}xn_i)/N$. Let z be the number of sites adjacent to that occupied by the first segment, then the number of available lattice sites for the second segment is given by $z(N - xn_i)/N$, similarly for the third segment $(z-1)(N - xn_i)/N$ lattice sites are available.

Flory then approximated that for the fourth and remaining polymer segments, an equal number of lattice sites were available

$$y = (z-1)\frac{N - xn_i}{N} \tag{2.2.14}$$

hence the total number of configurations for an individual polymer is then

$$v_{i+1} = \frac{N - xn_i}{2}\frac{zy^{x-1}}{z-1} \approx \frac{(N - xn_i)^x}{2}\left[\frac{z-1}{N}\right]^{x-1} \tag{2.2.15}$$

The total number of different configurations for an ensemble of n polymer molecules in a lattice is given by

$$W = \frac{1}{n!}\prod_{i=1}^{n} v_i \tag{2.2.16}$$

from equations (2.2.15) and (2.2.16) and the Boltzman equation $S=k\ln W$ we find

$$S = -k\left[m\ln\frac{m}{m+xn} + n\ln\frac{n}{m+xn}\right] + k(x-1)n[\ln(z-1)-1] - kn\ln 2 \tag{2.2.17}$$

the entropy of mixing ΔS_m is given by the difference between S and the configurational entropy for the undissolved polymer, which is found by setting $m=0$ in equation (2.2.17). Hence

$$\Delta S_m = -k\left[m\ln\frac{m}{m+xn} + n\ln\frac{xn}{m+xn}\right] \tag{2.2.18}$$

or since $m+xn=N$

$$\Delta S_m = -k[m\ln\phi_m + n\ln\phi_n] \tag{2.2.19}$$

where ϕ_i is the volume fraction of the component of interest. If this expression is differentiated with respect to m the molar entropy of mixing is obtained

$$\Delta s_m = -R[\ln(1-\phi_n) + (1-1/x)\phi_n] \tag{2.2.20}$$

To find the free energy of mixing the enthalpy of mixing also needs to be found. The exact calculation of the enthalpy is not possible by analytic methods since it is a multi particle problem with a large number of potential parameters. Hence only interactions between adjacent solvent molecules and polymer segments are taken into account as a first approximation. In terms of enthalpy of mixing, only the difference between the total energy of interaction in the solution and the energy of interaction of the pure components is relevant.

If w_{11} and w_{22} are the interactions between similar entities and w_{12} as those of different components, the energy on contact between two components has the form

$$\Delta w_{12} = w_{12} - \frac{1}{2}(w_{11} + w_{22}) \tag{2.2.21}$$

On the formation of p_{12} contact pairs in solution, the enthalpy of mixing is

$$\Delta H_m = p_{12}\Delta w_{12} \tag{2.2.22}$$

The probability that a lattice site adjacent to a given polymer segment is occupied by a solvent molecule is assumed to be proportional to the volume of the solvent present. The number of possible contacts per polymer molecule consisting of x segments is zx. Hence the enthalpy of mixing is

$$\Delta H_m = zxn\phi_m\Delta w_{12} = zm\phi_n\Delta w_{12} \tag{2.2.23}$$

if we allow

$$\chi = \frac{z\Delta w_{12}}{k_B T} \tag{2.2.24}$$

then equation (2.2.23) becomes

$$\Delta H_m = k_B T m\chi\phi_n \tag{2.2.25}$$

χ is a dimensionless parameter known to depend on temperature and pressure. Good solvents have low χ values while poor solvents have high values of χ. de Gennes [13]

has suggested that χ=1/2 is the borderline between good and poor solvents. In most cases χ is positive because the interactions are mainly Van der Waals type interactions (χ is proportional to the electronic polarisability).

If we compare equations (2.2.21) and (2.2.24) we see

$$\chi = \chi_{12} - \frac{1}{2}(\chi_{11} + \chi_{22}) \qquad (2.2.26)$$

where χ_{12} is the monomer-solvent interaction parameter, χ_{11} is the monomer-monomer interaction parameter and χ_{22} is the solvent-solvent interaction parameter.

Gundert et al have shown that the following characteristic behaviour can be shown for χ.

a) χ very often increases strongly with polymer concentration particularly in the case of poor solvents.

b) In some cases χ seems to be independent of concentration. This is mainly found in good solvents.

c) In a few cases, mostly in highly exothermic systems, χ decreases with increasing concentration. Gundert et al [21] give the system toluene/polystyrene as an example of this.

Pouchly and Patterson [22] have extended the interaction parameter to include the case of a mixed solvent and a polymer. They give the result for this system that the overall interaction parameter is given by

$$\overline{\chi} = u_1\chi_{13} + u_2\chi_{23} - u_1u_2\chi_{12} \qquad (2.2.27)$$

where $u_1 = \phi_1 / (\phi_1 + \phi_2)$, with ϕ_1, and ϕ_2 being the volume fractions of the two solvents respectively. In the above equation χ_{13} refers to the interaction parameter of solvent one and the polymer, χ_{23} is the interaction parameter of solvent two and the polymer and

χ_{12} is the interaction parameter between the two solvents. Hence a mixed solvent may be a better solvent for a polymer if $\chi_{12}>0$. This theory does not designate that the species 1 and 2 must be solvents, hence this result is valid if it is assumed species 1 and 2 are two different polymers and species 3 is a common solvent.

From equations (2.2.19) and (2.2.25) we find the free energy of mixing to be

$$\Delta G_m = \Delta H_m - T\Delta S_m = k_B T\left(m\ln\phi_m + n\ln\phi_n + \chi m\phi_n\right) \qquad (2.2.28)$$

or in molar terms

$$\Delta g_m = RT\left[\ln\left(1-\phi_n\right) + \left(1-1/x\right)\phi_n + \chi\phi_n^{\,2}\right] \qquad (2.2.29)$$

which is known as the Flory-Huggins equation

If the number of chain segments $x>>1$ the term $1/x$ can be neglected and equation (2.2.29) simplifies to

$$\Delta g_m = RT\left[\ln\left(1-\phi_n\right) + \phi_n + \chi\phi_n^{\,2}\right] \qquad (2.2.30)$$

This theory can be developed to the mixing of two polymers. By analogy to equations (2.2.19) and (2.2.25) we find

$$\Delta S_m = -k\left[n_1\ln\left(\phi_1\right) + n_2\ln\left(\phi_2\right)\right] \qquad (2.2.31)$$

and $$\Delta H_m = k_B T\chi_{12} N\phi_1\phi_2 \qquad (2.2.32)$$

where ϕ_i is the volume fraction of polymer i, and $N=n_1+n_2$ is the total number of polymer molecules present in the mixture.

de Gennes [13] gives the following critique of the Flory-Huggins Mean Field theory. "The mean field calculation replaces the monomer-monomer interaction by a certain self-consistent potential which is uniform in space; such a potential cannot induce any swelling of the chains (as is known to happen in good solvents or polymer mixes). Thus

the mean field for polymer solutions is intrinsically associated with ideal chains, which is clearly not acceptable at low concentrations."

Doi and Edwards [12] give the result for the mean end to end vector for the mean field case as

$$\langle R \rangle = \sqrt{N} b \left(\frac{\sqrt{N} v}{b^3} \right)^{\frac{1}{5}} \propto N^{3/5} \qquad (2.2.33)$$

while they also indicate that the scattering function at high q will follow the form

$$S(\underline{q}) \propto q^{-5/3} \text{ for } qR_g >> 1 \qquad (2.2.34)$$

2.2.6 Polymer Motion

2.2.6a The Rouse Model

The Rouse model represents a polymer by a set of beads connected by springs. It is natural to model the dynamics of the polymer solution by the Brownian motion of such beads. Such a model was first proposed by Rouse [23], and has been the basis of the dynamics of dilute polymer solutions. The Rouse model describes the motion of unentangled polymers, or the motion of entangled polymers over a short time.

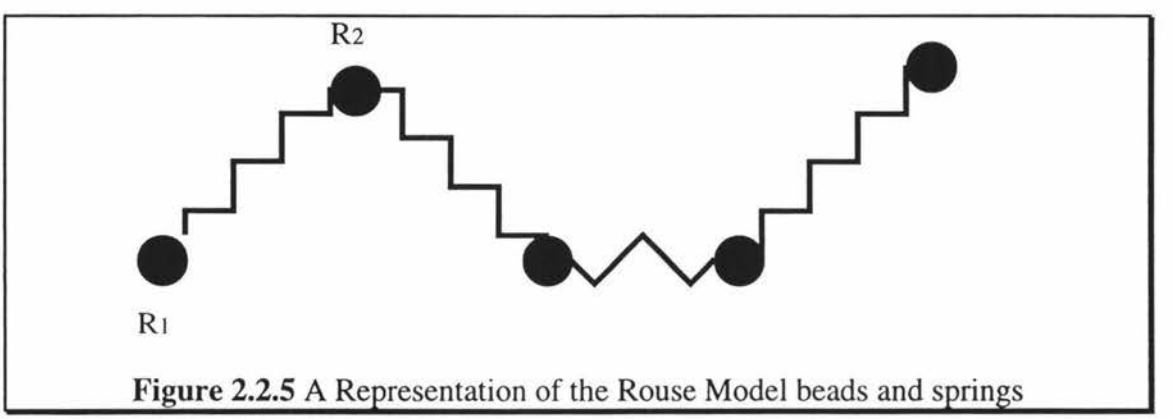

Figure 2.2.5 A Representation of the Rouse Model beads and springs

The idea behind the model is as follows, suppose we divide the backbone atoms of a polymer into N-1 groups (or monomers), each consisting of N_s consecutive backbone atoms. Each group is called a sub molecule. Let $\underline{R}_i$ (i=$1,2,...N$) be the position vector of

the backbone atom at the boundary of the sub molecules. If N_s is taken to be large, the distribution of the end to end vector of each sub molecule at equilibrium is gaussian.

$$\Psi_{eq}(\{R_i\}) \propto \exp\left[\frac{-3}{2b^2}\sum(R_i - R_{i-1})^2\right] \tag{2.2.35}$$

where b is the statistical segment length. This distribution is equivalent to the Boltzmann distribution $\exp(-U/k_BT)$ of the bead-spring model whose potential energy is given by

$$U = \frac{3}{2b^2}k_BT\sum(R_i - R_{i-1})^2 \tag{2.2.36}$$

It is assumed that each bead experiences a drag as it moves through the surrounding polymers and that drag is described by Stokes Law. The Rouse model also neglects excluded volume interactions and hydrodynamic interactions.

If we consider the macroscopic flow

$$v(r,t) = \mathbf{x}(t)r \tag{2.2.37}$$

where $\mathbf{x}(t)$ is the velocity gradient tensor, then the drag is proportional to the difference between the segment velocity $\frac{\partial R_i}{\partial t}$ and the average velocity at the point of the segment $\mathbf{x}R_i$. Hence the equation of motion is

$$m\frac{\partial^2 R_i}{\partial t^2} = -\zeta\left(\frac{\partial R_i}{\partial t} - \mathbf{x}R_i\right) - \frac{\partial U}{\partial R_i} + f_i \tag{2.2.38}$$

where ζ is the friction constant of the bead and f_i represents the random force due to the thermal motion. The friction term of equation (2.2.38) may be ignored, and from equations (2.2.36) and (2.2.38) we find

$$\frac{\partial R_i}{\partial t} = -\frac{1}{\zeta}\frac{\partial U}{\partial R_i} + \frac{1}{\zeta}f_i + \mathbf{x}R_i \tag{2.2.39}$$

If we allow $$\tau_s = \frac{\zeta b^2}{3k_B T} \tag{2.2.40}$$

then $$\frac{\partial R_i}{\partial t} = \frac{1}{\tau_s}\left(R_{i+1} + R_{i-1} - 2R_i\right) + \frac{1}{\zeta} f_i + \mathbf{x} R_i \tag{2.2.41}$$

τ_s is known as the characteristic relaxation time of a sub molecule.

We must also consider the end beads for their equation of motion is slightly different: for i=1 the equation becomes

$$\frac{\partial R_1}{\partial t} = -\frac{1}{\tau_s}\left(R_2 - R_1\right) + \frac{1}{\zeta} f_i + \mathbf{x} R_i \tag{2.2.42}$$

this may be regarded as a special case of equation (2.2.41) if R_0 is defined by making

$$R_0 \equiv R_1 \tag{2.2.43}$$

similarly the equation for R_N is obtained from equation (2.2.41) if R_{N+1} is defined by

$$R_{N+1} = R_N \tag{2.2.44}$$

Equations (2.2.41)-(2.2.44) are the basic equations for the Rouse model.

In the continuous limit equation (2.2.41) can be rewritten

$$\frac{\partial}{\partial t} R(i,t) = \frac{1}{\tau_s}\frac{\partial^2 R}{\partial i^2} + \frac{1}{\zeta} f(i,t) + \mathbf{x} R(i,t) \tag{2.2.45}$$

The time correlation function of f_i is given by Doi and Edwards [12] as

$$\left\langle f(i,t) f(j,t) \right\rangle = 2\zeta k_B T \delta(i-j)\delta(t-t') \tag{2.2.46}$$

Equation (2.2.45) is supplemented by the boundary conditions from equations (2.2.43) and (2.2.44)

$$\frac{\partial R}{\partial i} = 0 \text{ at } i = 0 \text{ and } i = N \tag{2.2.47}$$

The Rouse model gives a linear equation for $R(i,t)$. A standard way of treating such a system is to use normal co-ordinates each capable of independent motion. The normal co-ordinates in this model are given by

$$X_p = \frac{1}{N}\int_0^N di \cos\left(\frac{p\pi i}{N}\right) R(i,t) \quad (\text{for } p = 0,1,2,...) \tag{2.2.48}$$

From equation (2.2.45) it follows that

$$\frac{\partial}{\partial t} X_p = \frac{1}{\zeta_p}\left(-k_p X_p + f_p\right) + \mathbf{x} X_p \quad (\text{for } p = 1,2,...) \tag{2.2.49}$$

where $\zeta_0 = N\zeta$ and $\zeta_p = 2N\zeta$ for $p=1,2,..$ and

$$k_p = \frac{6\pi^2 k_B T}{Nb^2} p^2 \quad (\text{for } p = 0,1,2,...) \tag{2.2.50}$$

and f_p's are the random variables satisfying

$$\left\langle f_{p\alpha} \right\rangle = 0 \quad (\text{for } p = 0,1,2,..) \tag{2.2.51}$$

and

$$\left\langle f_{p\alpha}(t) f_{q\beta}(t') \right\rangle = 2\delta_{\alpha\beta}\delta_{pq}\zeta_p k_B T \delta(t-t') \tag{2.2.52}$$

From equation (2.2.49) the characteristic relaxation time of X_p is $\zeta_p/k_p = \tau_R/p^2$ where

$$\tau_R = \frac{\zeta_1}{k_1} = \frac{\zeta N^2 b^2}{3\pi^2 k_B T} \tag{2.2.53}$$

which is the longest relaxation time of the Rouse model, and is called the Rouse relaxation time. Since N is proportional to the molecular weight M it is found

$$\tau_R \propto M^2 \tag{2.2.54}$$

At equilibrium a polymer molecule moves around by thermal motion and its speed is characterised by the self diffusion constant defined by

$$D_s = \lim_{t\to\infty} \frac{1}{6t}\left\langle \left(R_g(t) - R_g(0)\right)^2 \right\rangle \tag{2.2.55}$$

where $R_g(t)$ is the centre of mass of the molecule. For the Rouse chain, $R_g(t)$ is given by

$$R_g(t) = \frac{1}{N}\int_0^N diR(i,t) = X_0 \tag{2.2.56}$$

and from equation (2.2.49) it follows that

$$R_g(t) - R_g(0) = \int_0^t dt' f_0(t') \tag{2.2.57}$$

If this equation is substituted into equation (2.2.38) and equation (2.2.41) used, we find

$$\left\langle \left(R_g(t) - R_g(0)\right)^2 \right\rangle = \int_0^t dt_1 \int_0^t dt_2 \left\langle f_0(t_1) f_0(t_2) \right\rangle = \frac{6k_B T}{N\zeta} t \tag{2.2.58}$$

hence from equation (2.2.55) we find

$$D_s = \frac{k_B T}{N\zeta} \tag{2.2.59}$$

Equations (2.2.53) and (2.2.59) indicate $D_s \propto M^{-1}$ and $\tau_R \propto M^2$ This prediction is not consistent with experimental results, which in theta conditions are summarised by $D_s \propto M^{-1/2}$ and $\tau_R \propto M^{3/2}$. This failure comes from the neglect of the hydrodynamic interaction [12] however the model is conceptually quite important, and has turned out to be a useful model in the dynamics of polymer melts.

2.2.6b The Zimm Model

The Zimm model differs from the Rouse model in that it includes the hydrodynamic interactions among the various beads in one chain. This interaction can be accounted for approximately, by using the equilibrium-averaged Oseen-Burgers tensor, as was originally done by Zimm [24] who was guided by the formalism developed by Kirkwood and collaborators [25].

To describe the dynamics of polymers in dilute solutions hydrodynamic interaction have to be taken into account, which is expressed by the mobility matrix

$$\mathbf{M}_{nm} = \frac{\mathbf{I}}{\zeta} \tag{2.2.60}$$

where $\mathbf{I}$ is the unit tensor ($I_{\alpha\beta}=\delta_{\alpha\beta}$) and ζ is the friction constant of the particle. Doi and Edwards [12] show

$$\mathbf{M}_{nm} = \frac{1}{8\pi\eta_s|r_{nm}|}\left[\hat{\mathbf{r}}_{nm}\hat{\mathbf{r}}_{nm} + \mathbf{I}\right] \text{ for } n \neq m \tag{2.2.61}$$

where $\underline{r}_{nm}=\underline{R}_n-\underline{R}_m$ and $\hat{\mathbf{r}}_{nm}$ is the unit vector in the direction of $\underline{r}_{nm}$.

For the tensor equation (2.2.61) it can be shown [12] that

$$\frac{\partial}{\partial \underline{R}_n}.\mathbf{M}_{nm} = 0 \tag{2.2.62}$$

hence the Langevin equation describing Rouse motion becomes

$$\frac{\partial}{\partial t}\underline{R}_n = \sum_m \mathbf{M}_{nm}.\left(-\frac{\partial U}{\partial \underline{R}_m} + f_m(t)\right) \tag{2.2.63}$$

Under theta conditions equations (2.2.36) and (2.2.62) give (in the continuous limit)

$$\frac{\partial}{\partial t}\underline{R}_n = \sum_m \mathbf{M}_{nm}.\left(k\frac{\partial^2}{\partial m^2}\underline{R}_m + f_m(t)\right) \tag{2.2.65}$$

Because equation (2.2.65) is a non-linear function of R_n-R_m, Zimm simplified the analysis by introducing the pre-averaged approximation which replaces $\underline{M}_{nm}$ by its average

$$\underline{M}_{nm} \rightarrow \langle M_{nm}\rangle = \int d\{R_n\} M_{nm}\Psi(\{R_n\},t) \tag{2.2.66}$$

If we consider problems near equilibrium then the equilibrium distribution function $\Psi_{eq}(\{R_n\})$ may be used in (2.2.66) and since the distribution of $\hat{\mathbf{r}}_{nm}$ is independent of $|r_{nm}|$

$$\langle M_{nm}\rangle_{eq} = \frac{1}{8\pi\eta_s}\left\langle\frac{1}{|r_{nm}|}\right\rangle_{eq}\langle\hat{\mathbf{r}}_{nm}\hat{\mathbf{r}}_{nm} + \mathbf{I}\rangle_{eq} \tag{2.2.67}$$

and using $\langle\hat{\mathbf{r}}_{nm}\hat{\mathbf{r}}_{nm}\rangle_{eq} = \frac{\mathbf{I}}{3}$

$$\langle M_{nm} \rangle_{eq} = \frac{1}{6\pi\eta_s} \left\langle \frac{1}{|R_n - R_m|} \right\rangle_{eq} \tag{2.2.68}$$

Under the theta condition, the distribution of R_n-R_m is gaussian with $|n\text{-}m|b^2$ as its variance, hence

$$\langle M_{nm} \rangle_{eq} = \int_0^\infty dr 4\pi r \left(\frac{3}{2\pi|n-m|b^2} \right)^{3/2} \exp\left(\frac{-3r^2}{2|n-m|b^2} \right) \frac{\mathbf{I}}{6\pi\eta_s r} \tag{2.2.69}$$

$$\langle M_{nm} \rangle_{eq} = \frac{\mathbf{I}}{\left(6\pi^3|n-m|\right)^{1/2}\eta_s b} \equiv h(n-m)\mathbf{I} \tag{2.2.70}$$

Thus in the pre-averaging approximation equation (2.2.65) becomes a linear equation for $\underline{R}_n$.

$$\frac{\partial}{\partial t}\underline{R}_n(t) = \sum_m h(n-m)\left(k\frac{\partial^2}{\partial m^2}\underline{R}_m(t) + f_m(t) \right) \tag{2.2.71}$$

To analyse equation (2.2.71) it is rewritten in terms of the Rouse normal coordinates X_p defined by equation (2.2.48)

$$\frac{\partial}{\partial t}X_p(t) = \sum_q h_{pq}(-k_q X_q + f_q) \tag{2.2.72}$$

where k_q is defined by equation (2.2.50) and

$$h_{pq} = \frac{1}{N^2}\int_0^N dn \int_0^N dm \cos\left(\frac{p\pi n}{N}\right)\cos\left(\frac{q\pi m}{N}\right) h(n-m) \tag{2.2.73}$$

which Doi and Edwards [12] give as

$$h_{pq} = \frac{\sqrt{N}}{\left(3\pi^3 p\right)^{1/2}\eta_s b}\frac{1}{2N}\delta_{pq} \tag{2.2.74}$$

h_{pq} is nearly diagonal, if the off diagonal component of h_{pq} is neglected, the resulting equation will have the same structure as that of the Rouse model

$$\zeta_p \frac{\partial}{\partial t}X_p(t) = -k_p X_p + f_p(t) \tag{2.2.75}$$

where $$\zeta_p = \left(h_{pp}\right)^{-1} = \left(12\pi^3\right)^{1/2}\eta_s\left(Nb^2p\right)^{1/2} \text{ (for } p = 1,2,..) \tag{2.2.76}$$

$$\zeta_0 = \frac{3}{8}\left(6\pi^3\right)^{1/2}\eta_s b\sqrt{N} \tag{2.2.77}$$

and $$k_p = \frac{6\pi^2 k_B T}{Nb^2}p^2 \text{ (for } p = 0,1,2...) \tag{2.2.78}$$

From these the diffusion coefficient and the relaxation times are obtained

$$D_s = \frac{k_B T}{\zeta_0} = \frac{8k_B T}{3\left(6\pi^3\right)^{1/2}\eta_s b\sqrt{N}} \tag{2.2.79}$$

and $$\tau_p = \frac{\zeta_p}{k_p} = \tau_1 p^{-3/2} \tag{2.2.80}$$

where $$\tau_1 = \tau_R = \frac{\eta_s\left(\sqrt{N}b\right)^3}{\sqrt{3\pi}k_B T} \tag{2.2.81}$$

From equations (2.2.79) and (2.2.81) we note the molecular weight dependence of D_s and τ_R

$$D_s \propto M^{-1/2}, \tau_R \propto M^{3/2} \tag{2.2.82}$$

which agrees with experimental results under theta conditions unlike the Rouse model. This may be partially explained by the fact that in the Zimm model the interaction among the segments is not localised.

In a good solvent the excluded volume interaction needs to be taken into account. This is done if we add the potential

$$U_1 = \frac{1}{2}\upsilon k_B T\sum_{n,m}\delta\left(\underline{R}_n - \underline{R}_m\right) \tag{2.2.83}$$

This results in the Langevin equation becoming non-linear, however this may be solved by using the linear Langevin equation of equation (2.2.75) and including the excluded volume effects in the parameters ζ_p and k_p.

From equations (2.2.68) and (2.2.73) ζ_p is determined as

$$\zeta_p = \left(h_{pp}\right)^{-1} = \left[\frac{1}{N^2}\int_0^N dn \int_0^N dm \cos\left(\frac{p\pi n}{N}\right)\cos\left(\frac{p\pi m}{N}\right)\frac{1}{6\pi\eta_s}\left\langle\frac{1}{|R_n - R_m|}\right\rangle_{eq}\right]^{-1} \tag{2.2.84}$$

To evaluate ζ_p the distribution of R_n-R_m of the excluded volume chain must be approximated. For simplicity it is assumed [12] the distribution will have the same form as the distribution of the end to end vector of the excluded volume chain with n-m segments, this has the functional form

$$\Psi_{nm}(R_n - R_m) = F\left(\frac{|R_n - R_m|}{|n-m|^{\upsilon} b}\right) \tag{2.2.85}$$

This distribution function gives

$$\left\langle\frac{1}{|R_n - R_m|}\right\rangle_{eq} \approx \frac{1}{|n-m|^{\upsilon} b} \tag{2.2.86}$$

from which follows

$$\zeta_0^{-1} \approx \frac{1}{\eta_s N^{\upsilon} b} \tag{2.2.87}$$

and

$$\zeta_p^{-1} \approx \frac{N^{-\upsilon}}{\eta_s b} p^{\upsilon-1} \tag{2.2.88}$$

Doi and Edwards [12] give

$$k_p \approx \frac{N^{-2\upsilon}}{b^2} k_B T p^{2\upsilon+1} \tag{2.2.89}$$

which leads to the diffusion coefficient

$$D_s \approx \frac{k_B T}{\eta_s N^{\upsilon} b} \tag{2.2.90}$$

and the relaxation times

$$\tau_p = \frac{\zeta_p}{k_p} = \frac{\tau_1}{p^{3\upsilon}} \tag{2.2.91}$$

and

$$\tau_1 = \tau_R = \frac{\zeta_1}{k_1} \approx \frac{\eta_s N^{3\upsilon} b^3}{k_B T} \tag{2.2.92}$$

Hence we find that the molecular weight dependence of the diffusion coefficient and the relaxation time are

$$D_s \propto M^{-\upsilon} \text{ and } \tau_R \propto M^{3\upsilon} \tag{2.2.94}$$

2.2.6c Reptation

The basic idea of the reptation model was first given by de Gennes [13] and expanded by Doi and Edwards [12]. If we consider the motion of a polymer in a strongly entangled system. If the test polymer attempts to move perpendicularly to its own length, it will encounter large resistance from the surrounding polymers. If however the polymer moves along its own length (backward or forward) it will encounter significantly less resistance. Dynamically the polymer can be considered to be confined in a tube which represents a mean field potential created by the other polymers.

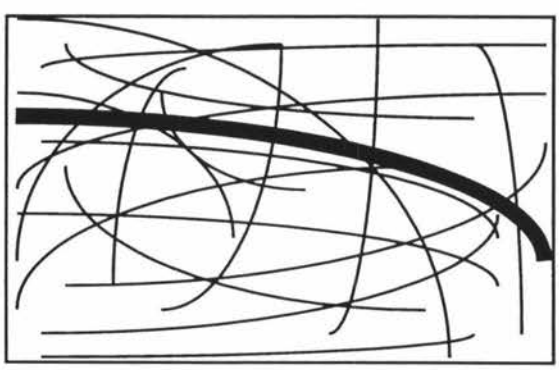

Figure 2.2.6 A single polymer entangled in the polymeric matrix of other polymers

A simple version of the model assumes the tube to be fixed in the material. The motion of the polymer perpendicular to the tube is restricted by the tube wall, but its motion

along the tube is free. This situation is represented by the Rouse chain confined to a tube.

At equilibrium, the tube axis is a randomly connected tube segment of length a. Since there are $Z=L/a$ tube segments (L is the tube contour length), the mean end to end distance of the tube axis is Za^2. This must be equal to the mean square end to end distance of the polymer Nb^2.

If the lateral and longitudinal fluctuations are neglected, it is found that it may be assumed that the movement is along the tube, with diffusion constant

$$D_c = \frac{k_B T}{N\zeta} \tag{2.2.95}$$

As the polymer moves along the tube, one end moves out of the tube, then a new part of the tube is created in a random direction such that the length of the new tube segment is a. When the tube segment is created on one end, the tube segment on the other end becomes empty of the polymer. Such a segment will not impose any constraint on the polymer and can be considered destroyed. Thus the one dimensional diffusion of the polymer is accompanied by the creation and destruction of the tube.

The characteristic time of reptation can be estimated by the time needed for the polymer to disengage from a certain tube, or the time needed for the polymer to move over the distance L along the tube, thus the reptation relaxation time (called the reptation time) is given by

$$\tau_d \approx \frac{L^2}{D_c} \approx ZN^2\tau_s \tag{2.2.96}$$

where $\tau_s = \frac{\zeta b^2}{3k_b T}$ is the characteristic relaxation time of a sub molecule.

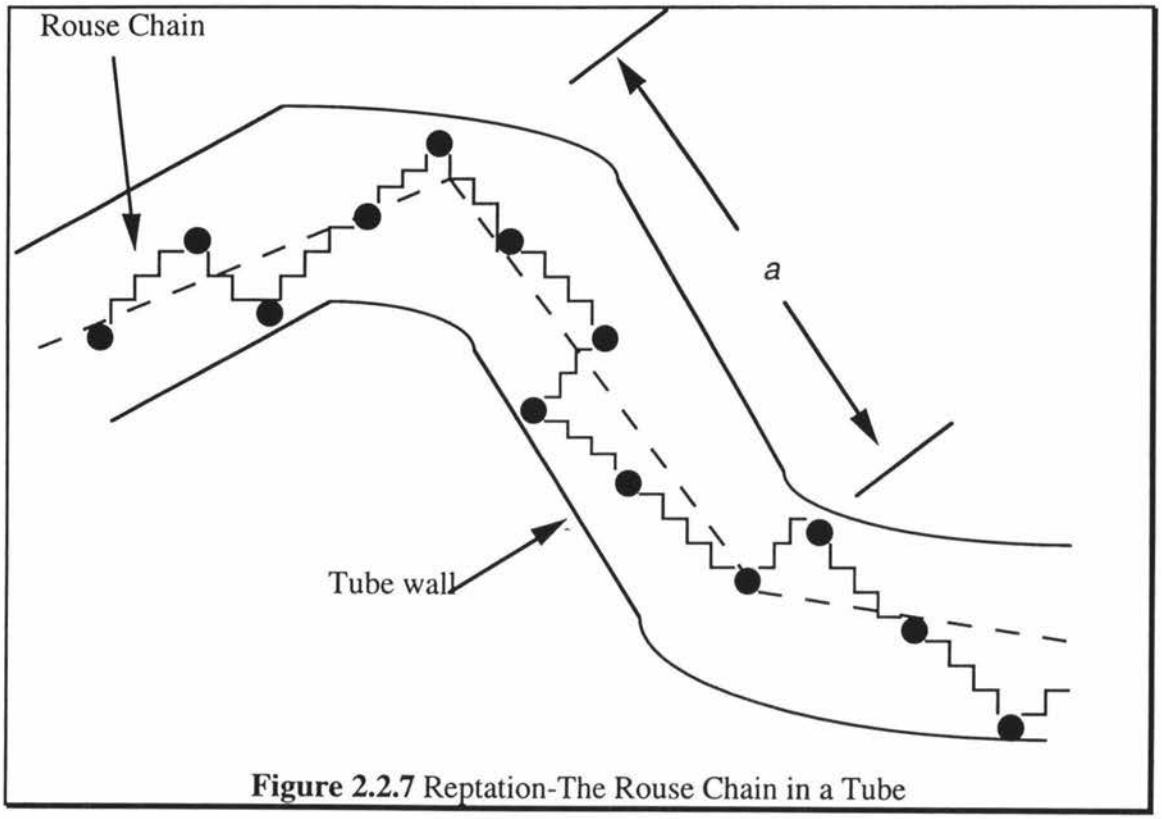

Figure 2.2.7 Reptation-The Rouse Chain in a Tube

The equation of motion for reptation is obtained as follows. If we let $\underline{R}(s,t)$ be the position of the polymer at the contour length $s(o<s<L)$ and time t. Consider that the polymer moves a distance Δs along itself in a time interval Δt. Δs may take positive or negative values randomly, hence it's mean variance is given by

$$\langle \Delta s \rangle = 0 \; ; \; \langle \Delta s^2 \rangle = 2D_c \Delta t \tag{2.2.97}$$

Since the polymer moves along itself, the time evolution of $\underline{R}(s,t)$ is given by

$$\underline{R}(s,t+\Delta t) = \underline{R}(s+\Delta s,t) \tag{2.2.98}$$

Special consideration is needed for the chain end. If $\Delta s>0$, the segment at $s=L$, moves out of the tube and can go in a random direction, i.e.

$$\underline{R}(L,t+\Delta t) = R(L,t) + \underline{v}(t) \tag{2.2.99}$$

where $v(t)$ is the random vector whose mean variances are given by

$$\langle \underline{v} \rangle = 0 \; ; \; \langle \underline{v}(t)^2 \rangle = a\Delta s \tag{2.2.100}$$

Similarly if $\Delta s<0$, $\underline{r}(0,t)$ changes as

$$\underline{R}(0,t+\Delta t) = \underline{R}(0,t) - \underline{v}(t) \tag{2.2.101}$$

If we consider the mean square displacement of the centre of mass

$$R_g(t) = \frac{1}{L}\int_0^L ds\underline{R}(s,t) \tag{2.2.102}$$

and from equation (2.2.98) we have

$$R_g(t+\Delta t) - R_g(t) = \frac{1}{L}(\underline{R}(L,t) - \underline{R}(0,t))\Delta s \tag{2.2.103}$$

where we have neglected the terms of order v/L. If we take the average of the square of equation (2.2.103) and use the fact that Δs is independent of $\underline{R}(s,t)$ then

$$\left\langle \left(R_g(t+\Delta t) - R_g(t)\right)^2 \right\rangle = \frac{1}{L}\left\langle (\underline{R}(L,t) - \underline{R}(0,t))^2 \right\rangle \left\langle \Delta s^2 \right\rangle \tag{2.2.104}$$

The first average is equal to Nb^2 (where b is the length of the statistical chain segment) and the second average is given by equation (2.2.97), hence

$$\left\langle \left(R_g(t+\Delta t) - R_g(t)\right)^2 \right\rangle = \frac{Nb^2}{L^2} 2D_c\Delta t \tag{2.2.105}$$

From Rouse motion it is known that the self diffusion coefficient is defined as

$$D_s = \lim_{t\to\infty}\frac{1}{6t}\left\langle \left(R_g(t) - R_g(0)\right)^2 \right\rangle \tag{2.2.106}$$

from this it is found

$$D_s = \frac{Nb^2}{3L^2} D_c = \frac{a^2}{b^2}\frac{k_B T}{2N^2\zeta} \tag{2.2.107}$$

hence $$D_s \propto M^{-2} \tag{2.2.108}$$

2.2.6d The Blob Model

de Gennes [13] considered that in solutions where chains overlap, not individual polymer chains, but their sub chains may behave independently of one another. de Gennes postulated that sub chains whose end distance is of the order of the correlation length ξ would move independently of one another. He named the domain occupied by each of them the "blob." This idea assumes there is no thermodynamic interaction between chain segments separated by more than ξ.

Only the important results will be shown here

$$D_s \propto M^{\upsilon(3\upsilon-1)} \tag{2.2.109}$$

in the semi-dilute regime, while for good solvents

$$D_s \propto M^{0.75} \tag{2.2.110}$$

and for theta solvents

$$D_s \propto M^{1.0} \tag{2.2.111}$$

2.3 Basic Dynamic Light Scattering Theory

The theory of Dynamic Light Scattering is discussed in detail by Berne and Pecora [26]. The following is a summary of the theory pertinent to the work presented here.

Consider the scattering geometry of **Figure 2.3.1**. The light incident on the sample has an electric field vector of the form

$$E_i = \underline{n}_i E_0 \exp[i(\underline{k}_i.r - w_i t)] \qquad 2.3.1$$

where $\underline{n}_i$ is a unit vector in the direction of the incident electric field.

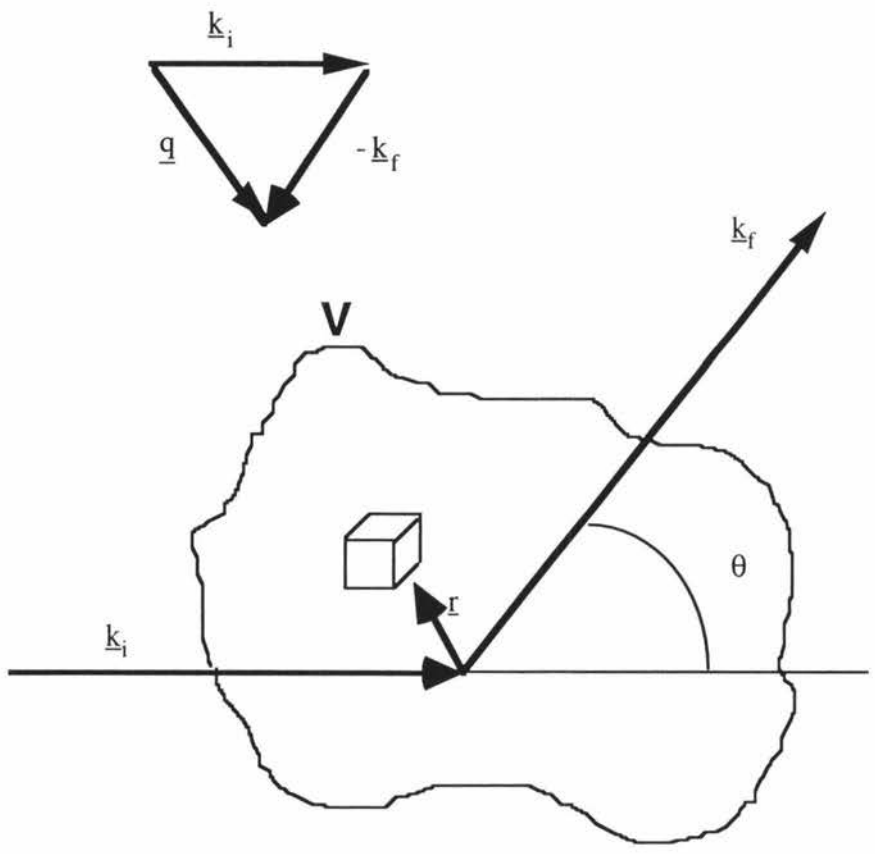

Figure 2.3.1 Typical scattering geometry in a Dynamic Light Scattering Experiment. The scattering vector $\underline{q}$ is obtained by the subtraction of $\underline{k_f}$ from $\underline{k_i}$.

The instantaneous electric field at a point can be represented as the sum of the electric fields due to the individual scattering events from small volume elements within the scattering volume *V*.

If we consider a non-magnetic, non-conducting, non-absorbing medium, this medium may be characterised by a local permittivity, $\varepsilon(\underline{r},t)$ which varies in space and time. The local value of ε can be written as the mean value plus a fluctuation;

$$\varepsilon(\underline{r},t) = \varepsilon_0 + \delta\varepsilon \tag{2.3.2}$$

Berne and Pecora [26] have shown the scattered field detected at a distance R $(|R|>>|r|>>\lambda)$ from the sample is

$$E_s(R,t) = \frac{E_0}{4\pi R\varepsilon_0}\exp(ik_f R\int_V d^3r\exp[i(\underline{q}.\underline{r}-\varpi_i t)]\{\underline{n}_f.[k_f\times(\delta\varepsilon(\underline{r},t).\underline{n_i})]\} \tag{2.3.3}$$

where $\underline{q} = \underline{k}_i - \underline{k}_f$. For the conditions of this work $|\underline{k}_i| \cong |\underline{k}_f|$ then the magnitude of the scattering vector is given by

$$q = \frac{4\pi n}{\lambda_i}\sin(\theta/2) \tag{2.3.4}$$

where n is the refractive index of the sample and θ the scattering angle.

Equation (2.3.3) can be expressed in terms of the spatial Fourier transform of the permittivity fluctuation

$$\delta\underline{\varepsilon}(\underline{q},t) = \int_V d^3r\exp(i\underline{q}.\underline{r})\delta\underline{\varepsilon}(\underline{r},t) \tag{2.3.5}$$

as

$$E_s(\underline{R},t) = \frac{E_0}{4\pi R\varepsilon_0}\exp[i(k_f R-\varpi_i t)]\{\underline{n}_f[\underline{k}_f\times(\underline{k}_f\times(\delta\underline{\varepsilon}(\underline{q},t).\underline{n}_i))]\} \tag{2.3.6}$$

which may be simplified by expanding the cross products as

$$\delta\underline{\varepsilon}_{if} = \underline{n}_f \delta\underline{\varepsilon}(\underline{q},t).\underline{n}_i \qquad (2.3.7)$$

hence

$$E_s(\underline{R},t) = \frac{-E_0 k_f^{\ 2}}{4\pi R\varepsilon_0}\exp[i(k_f R - \varpi_i t)\delta\underline{\varepsilon}_{if}(\underline{q},t)] \qquad (2.3.8)$$

The dependence of the permittivity fluctuations on time can be studied by measuring the electric field auto correlation function, which written in normalised form is

$$g^{(1)}(\tau) = \frac{< E_s^{\ *}(\underline{R},0)E_s(\underline{r},\tau) >}{< |E_s|^2 >} \qquad (2.3.9)$$

ie.

$$g^{(1)}(\tau) =< \delta\underline{\varepsilon}_{if}^{\ *}(\underline{q},0)\delta\underline{\varepsilon}_{if}(\underline{q},\tau) > \exp(-i\omega_i\tau) \qquad (2.3.10)$$

To make a connection between molecular properties and light scattering measurements it is convenient to introduce the assumption that the light is scattered from particles and the permittivity fluctuations are due to fluctuations in the number density of the particles only.

An incident monochromatic beam of light impinging on a single molecule which has an anisotropic polarisability specified by a polarisability tensor $\underline{\alpha}$ induces a dipole moment

$$\underline{\mu}(t) = \underline{\alpha}.\underline{E}(t) \qquad (2.3.11)$$

which varies with time. Here $\underline{E}(t)$ is the electric field vector of the incident light wave.

The fluctuation in the polarisability density is given by Berne and Pecora [26] as

$$\delta\alpha_{ij}(\underline{r},t) = \sum_{j=1}^{N} \underline{\alpha}_{if}^{\ j}(t)\delta(\underline{r} - \underline{r}_j(t)) \qquad (2.3.12)$$

where $\underline{\alpha}_{if} = \underline{n}_i.\underline{\alpha}.\underline{n}_f$ is the component of the molecular polarisability tensor along $\underline{n}_i$ and $\underline{n}_f$, the incident and detected polarisations.

The spatial Fourier transform of the polarisability fluctuation is

$$\delta\alpha_{if}(\underline{q},t) = \sum_{j=1}^{N} \underline{\alpha}_{if}{}^{j} \exp[i\underline{q}.\underline{r}_j(t)] \tag{2.3.13}$$

hence the electric field auto correlation function can be expressed

$$g^{(1)}(\tau) = \frac{<\delta\alpha_{if}{}^{*}(\underline{q},0)\delta\alpha_{if}(\underline{q},\tau)>}{<\left|\delta\alpha_{if}(\underline{q})\right|^2>} \tag{2.3.14}$$

If all the particles have the same polarisability $\alpha_{if}{}^{j}$, then $g^{(1)}(\tau)$ can be written as

$$g^{(1)}(\tau) = \frac{S(\underline{q},\tau)}{S(\underline{q})}\exp(-i\varpi_i\tau) \tag{2.3.15}$$

where $S(\underline{q},\tau)$ is the Dynamic Structure Factor;

$$S(\underline{q},\tau) = \frac{1}{N}\sum_{i=1}^{N}\sum_{j=1}^{N}\left\langle \exp[i\underline{q}.\underline{r}_i(\tau) - \underline{r}_j(0)]\right\rangle \tag{2.3.16}$$

Note $S(\underline{q}) = S(\underline{q},0)$ is the static structure factor

If we consider a dilute solution of small non interacting random flight polymer molecules each with the same molar mass (each molecule considered to be a Rayleigh scatterer satisfying the condition $qR_G \leq 1$), and intramolecular interference is negligible, then (2.3.15) and (2.3.16) can be simplified and the electric field auto correlation function has a single exponential decay, ie.

$$\left|g^{(1)}(\tau)\right| = \exp(-D_0 q^2 \tau) \tag{2.3.17}$$

where D_0 is the infinite dilution diffusion coefficient.

For large non-interacting polymer molecules, the summation in equation (2.3.16) must be performed over all of the segments (in a single molecule, since the cross terms between segments of different molecules vanish for non-interacting systems) and $P(\underline{q})=S(\underline{q})$ for a single molecule is called the particle form (or scattering) factor.

In a more realistic case polymer molecules have a range of molar masses (or are said to be poly disperse). For the case of a dilute poly disperse solution (of polymer dissolved in solvent) equation (2.3.17) can easily be generalised. The field auto correlation function becomes a weighted sum of exponentials.

$$\left|g^{(1)}(\tau)\right| = \int_0^\infty G(\Gamma)e^{-\Gamma\tau}d\Gamma \qquad (2.3.18)$$

where $\Gamma=D_0q^2$ and $G(\Gamma)d\Gamma \propto P(\underline{q},M)\alpha^2 n(M)dM$ is the fraction of the scattering intensity due to particles having decay rates in the range Γ to $\Gamma+d\Gamma$.

The molecular polarisability can be written in terms of the polarisability per unit mass (which is constant) as

$$\alpha \propto \alpha_m M$$

and hence

$$G(\Gamma)d\Gamma \propto P(\underline{q},M)M^2 n(M)dM \qquad (2.3.19)$$

Koppel [27] and Pusey [28] have found that $\ln\left|g^{(1)}(\tau)\right|$ can be expressed as a power series (commonly called the cumulant expansion)

$$\ln\left|g^{(1)}(\tau)\right| = -\langle\Gamma\rangle\tau + \frac{1}{2}\frac{\mu_2}{\langle\Gamma\rangle^2}\langle\Gamma\rangle^2\tau^2 - \frac{1}{3!}\frac{\mu_3}{\langle\Gamma\rangle^3}\langle\Gamma\rangle^3\tau^3 + \frac{1}{4!}\frac{\mu_4 - 3\mu_2^{\,2}}{\langle\Gamma\rangle^4}\langle\Gamma\rangle^4\tau^4 + \ldots \qquad (2.3.20)$$

with $$\langle\Gamma\rangle = \int_0^\infty \Gamma G(\Gamma)d\Gamma \qquad (2.3.21)$$

and $$\mu_n = \int_0^\infty (\Gamma - \langle\Gamma\rangle)^n G(\Gamma)d\Gamma \qquad (2.3.22)$$

hence we may extract an average diffusion coefficient <D> given by $\langle D\rangle = {\langle\Gamma\rangle}/{q^2}$, and hence <$D$> takes the form

$$\langle D\rangle = \frac{1}{q^2}\int_0^\infty \Gamma G(\Gamma)d\Gamma$$

ie. $$\langle D \rangle = \frac{\int_0^\infty D(M)M^2 n(M)P(\underline{q},M)dM}{\int_0^\infty M^2 n(M)dM} \qquad (2.3.23)$$

King et al [29] have shown that when $P(q,M)=1$ for all species (satisfied by taking measurements at small q), then the z-average diffusion coefficient $\langle D \rangle_z$ is obtained from the initial slope.

In dilute solutions the correlations between segments from different molecules are negligible and equation (2.3.16) can be simplified. In semi dilute solutions correlations between segments from different molecules cannot be neglected, hence the summation in $S(q,\tau)$ must be performed over all segments. de Gennes [13] [30] has shown that if the field auto correlation function (equation (2.3.14)) is written in terms of the Fourier components of the number density of the segments then

$$S(\underline{q},\tau) = \exp(-D_c q^2 \tau) \qquad (2.3.24)$$

where D_c is the co-operative diffusion coefficient.

Dynamic Light Scattering can also be used to provide useful information about the polydispersity of any given sample. Bloomfield [31] provides a useful review of this area of DLS theory and practice.

2.4 DLS Theory-Ternary Polymer Solutions

2.4.1 Benmouna et al Mean Field RPA Theory

The dynamic structure factor for scattering from a system consisting of a solvent and two different spherical solutes was considered by Philles [32]. He discovered that the dynamic structure factor $S(\underline{q},\tau)$ was composed of two exponential decay rates, these decay rates were not simply related to the diffusion coefficient of either of the solutes. Pusey et al [33] calculated the mode amplitudes using the hard sphere model. This treatment is summarised below.

When the time dependent part of equation (2.3.14) is rewritten in terms of the fluctuations in the refractive index $\delta n(\underline{q},t)$, the dynamic structure factor becomes,

$$S(\underline{q},\tau) \propto \left\langle \delta n(-\underline{q},0)\delta n(\underline{q},\tau) \right\rangle \tag{2.4.1}$$

where the right hand side is the spatial Fourier transform of the space-time correlation function for refractive index fluctuations, $\langle \delta n(0,0)\delta n(\underline{r},\tau)\rangle$. This space-time correlation function may be rewritten in terms of the number density fluctuation.

The number density may be assumed to decay according to a similar form to that of Fick's Law (ie. similarly to mutual diffusion in a binary solution) which states that if a concentration, c, is not uniform, there is a flux of particles, J, which is proportional to the spatial gradient of the concentration,

$$J_i^{\,a} = -\sum_{j=1}^{n-1} D_{ij} grad(c_j) \tag{2.4.2}$$

where D is called the diffusion coefficient. Hence the number density decays as

$$\frac{\partial}{\partial t}\delta p_1(\underline{r},t) = D_{11}\nabla^2\delta p_1(\underline{r},t) + D_{12}\nabla^2\delta p_2(\underline{r},t) \tag{2.4.3}$$

$$\frac{\partial}{\partial t}\delta p_2(\underline{r},t) = D_{21}\nabla^2\delta p_1(\underline{r},t) + D_{22}\nabla^2\delta p_2(\underline{r},t) \tag{2.4.4}$$

The matrix of diffusion coefficients can be diagonalised which reveals two uncorrelated modes

$$\delta p_+ = \alpha_+ \delta p_1 + \delta p_2 \tag{2.4.5}$$

$$\delta p_- = \alpha_- \delta p_1 + \delta p_2 \tag{2.4.6}$$

which decay as

$$\frac{\partial}{\partial t}\delta p_+(\underline{r},t) = D_+ \nabla^2 \delta p_+ \tag{2.4.7}$$

$$\frac{\partial}{\partial t}\delta p_-(\underline{r},t) = D_- \nabla^2 \delta p_- \tag{2.4.8}$$

The values of $\alpha_\pm$ and $D_\pm$ are determined by

$$\alpha_\pm = \frac{(D_{11}-D_{22})^2 \pm [(D_{11}-D_{22})^2 + 4D_{11}D_{21}]^{1/2}}{2D_{12}} \tag{2.4.9}$$

and

$$D_\pm = \frac{1}{2}(D_{11}-D_{22})^2 \pm \frac{1}{2}[(D_{11}-D_{22})^2 + 4D_{12}D_{21}]^{1/2} \tag{2.4.10}$$

If constants are ignored (which would later be normalised out), the refractive index fluctuations are related to the density fluctuations by the relationship

$$\delta n(\underline{r},t) = f_1 \delta p_1(\underline{r},t) + f_2 \delta p_2(\underline{r},t) \tag{2.4.11}$$

where f_1 and f_2 are scattering amplitudes

If equations (2.4.5) and (2.4.6) are substituted into equation (2.4.11) and this result Fourier transformed (see equation (2.4.1)) the form of the Dynamic Structure Factor $S(\underline{q},t)$ is found. The final form of $S(\underline{q},\tau)$ is

$$S(\underline{q},\tau) = A_+ \exp(-D_+ q^2 \tau) + A_- \exp(-D_- q^2 \tau) \tag{2.4.12}$$

where the diffusion coefficients D_+ and D_- represent the rates of decay of two different types of density fluctuation. Thus the theory predicts that the field auto correlation function of the scattered light comprises two decay processes. Borsali et al [1] [34] [35]

have proven experimentally that at least two decay modes exist (Borsali et al could only resolve two modes), a fast decay due to a diffusion coefficient D_+ and a slow decay due to the diffusion coefficient D_-.

The + mode is interpreted as "compression-dilation"; where the relative concentrations are fixed ($\delta p_1/p_1 = \delta p_2/p_2$). D_+ is often called the co-operative diffusion co-efficient D_C.

The - mode until recently was interpreted as an exchange of species, at fixed total number density (ie. $\delta p_1 + \delta p_2 = 0$), and is often called the interdiffusion mode, and the diffusion coefficient that results, D_I.

Recently Akcasu et al [36] have shown that in general these diffusion coefficients cannot be identified with the cooperative diffusion and interdiffusion coefficients, respectively.

Benmouna et al [2] and Foley and Cohen [3] in their theoretical papers on Dynamic Light Scattering from multi component solutions both found that for a ternary solution two modes of relaxation for $S(q,\tau)$ could be identified. Benmouna et al, identified one mode as cooperative and the other as inter diffusive (under specific system conditions).

Their approach was to use the random phase approximation (RPA) to find an approximate expression for the effect of interactions on $S(q,\tau)$. This theory, being a mean field theory, is only valid above c^*, the overlap concentration [1]. For static properties, the use of RPA results in the Flory-Huggins expression for $S(0)$ [4]. The initial slope of $\ln S(q,\tau)$ is found and it is assumed that both modes decay exponentially. Moreover it is also assumed that hydrodynamic interactions are totally screened [2]. Zimm type hydrodynamic interactions are screened in semi dilute and concentrated regimes, this implies one neglects intramolecular hydrodynamic interactions as well. One could remove this restriction by the use of the blob model, but for simplicity all monomers are assumed to have the same friction coefficient ζ.

From this theory two special cases were considered.

Case A:- two interacting polymers with equal molar mass and size, one having no optical contrast with the solvent, in a solvent of the same quality for both polymers

Case B:- a solution of two polymers, differing only in their molar masses

In Case A two decay rates are found

$$\Gamma_I = q^2 D_I(\underline{q}) = \Gamma_S(\underline{q})[1 - 2x(1-x)\phi\chi NP(\underline{q})] \qquad (2.4.13)$$

and

$$\Gamma_C = q^2 D_C(\underline{q}) = \Gamma_S(\underline{q})[1 + \upsilon\phi NP(\underline{q})] \qquad (2.4.14)$$

In the small q limit, the diffusion coefficients D_I and D_C are analogous to D_- and D_+ in equation (2.4.12). In equation (2.4.14) x is the relative concentration of the visible polymer (ie. $c_1/(c_1+c_2)$ where c is the polymer concentration), ϕ is the polymer volume fraction and χ $(=\chi_{12})$ is the Flory interaction parameter for polymer-polymer interactions. Also υ is the excluded volume parameter (assumed to be the same for both polymers). $\Gamma_S(q)$ is the "bare" relaxation frequency characterising the time decay of the self scattering function $S^0(q,t)$. given in [2] This leads to an expression for $\Gamma_S(q)$ as given by [34]

$$\Gamma_S(\underline{q}) = q^2 \frac{kT}{\zeta NP(\underline{q})} = q^2 \frac{D_S}{P(\underline{q})} \qquad (2.4.15)$$

where $P(q)$ is the form factor of a simple chain in the system and can generally be assumed to have the form of the Debye function, N is the number of monomers per polymer molecule, ζ is the friction coefficient (which may depend on concentration) and D_S is the self diffusion coefficient.

Unless $P(q)$ is equal to one, a q-dependent effective diffusion coefficient is obtained, however in the limit of small q, the self diffusion coefficient is found.

The limiting forms of (2.4.13) and (2.4.14) are consistent with the known limits of ternary diffusion coefficients [37]

$$\lim_{C_1 \to 0} D_{12} = 0 \qquad (2.4.16)$$

$$\lim_{C_2 \to 0} D_{11} = D_{10} \qquad \text{(mutual diffusion)} \qquad (2.4.17)$$

$$\lim_{C_1 \to 0} D_{11} = D_1(c_2) \qquad (2.4.18)$$

where $D_1(c_2)$ represents the self diffusion coefficient of a trace of component 1 in the presence of a variable concentration c_2 of component 2. Equation (2.4.18) is equivalent to equation (2.4.13) with $x \to 0$. This is the condition which must be satisfied in order to perform an "optical tracer" DLS experiment.

Using the standard notation $\upsilon\phi N = 2A_2Mc$, where A_2 is the second generalised viral coefficient which may depend on c (A_2 expresses the dependence of the osmotic pressure on the total polymer concentration) and M is the molar mass, Borsali et al [34] expressed equations (2.4.13) and (2.4.14) as

$$\Gamma_1 = q^2 D_1(\underline{q}) = \Gamma_S(\underline{q})[1 - 4A_2Mcx(1-x)P(\underline{q})\chi/\upsilon] \quad (2.4.19)$$

$$\Gamma_C = q^2 D_C(\underline{q}) = \Gamma_S(\underline{q})[1 + 2A_2McP(\underline{q})] \qquad (2.4.20)$$

Equation (2.4.19) indicates that the degree to which D_1 approximates D_S depends not only on the value of x, but also upon the thermodynamic quantities A_2 and χ/v. An interesting limit of equation (2.4.19) is found when χ/v tends to zero. Then Γ_1 becomes equal to $\Gamma_S(\underline{q})$ regardless of the value of x. Such a situation is realised when the polymers are compatible and the solvent is good both of them.

Borsali et al [34] showed that when the only component 1 is visible $S(\underline{q},t)$ is given by

$$S(\underline{q},t) = S_{11}(\underline{q},t) = (\partial n/\partial\varphi)_1^2 (a_C e^{-\Gamma_C \tau} + a_1 e^{-\Gamma_1 \tau}) \qquad (2.4.21)$$

where $(\partial n/\partial\varphi)_1$ is the increment of refractive index of polymer 1 and φ is its total volume fraction

Assuming N is the same for both polymers, and that χ is small compared to v, the following expressions are obtained for the amplitudes

$$a_C = x^2 \varphi NP(\underline{q}) \frac{1 - \chi/\chi_C(\underline{q})}{1 + v\varphi NP(\underline{q})[1 - \chi/\chi_C(\underline{q})]} \tag{2.4.22}$$

$$a_I = x(1-x)\varphi NP(\underline{q}) \frac{1 + v\varphi NP(\underline{q})}{1 + v\varphi NP(\underline{q})[1 - \chi/\chi_C(\underline{q})]} \tag{2.4.23}$$

where $$\chi_C(\underline{q}) = [2\varphi Nx(1-x)P(\underline{q})]^{-1} \tag{2.4.24}$$

and x is the relative composition of the visible polymer.

They also were able to show the frequencies as

$$\Gamma_C = \Gamma_S[1 + v\varphi NP(\underline{q})] \tag{2.4.25}$$

and $$\Gamma_I = \Gamma_S[1 - \chi/\chi_C(\underline{q})] \tag{2.4.26}$$

where Γ_S is described in equation (2.4.15)

In the limit of small x, the amplitude of the co-operative mode approaches zero, hence only the inter diffusive mode is measured. When x is finite both modes are expected to contribute to $S(q,\tau)$, even though only one of the polymers is visible.

Giebel et al [13] using a ternary system of poly (methyl methacrylate) and poly (dimethyl siloxane) dissolved in a tetrahydrofuran solvent, observed experimentally two distinct modes in the auto correlation function obtained from DLS measurements. These relaxation modes were found to be in good agreement with theoretical calculations based on the RPA theory developed by Benoit and Benmouna.

They showed that this theory predicted phase separation to occur for some values of x and c_T since at high concentration this theory predicted D_I to become negative.

Case B:- Borsali et al [34] also considered the case where a solvent with "zero average contrast" is used. This corresponds to the following conditions, x=1/2 and

$$(\partial n/\partial\varphi)_1 = -(\partial n/\partial\varphi)_2 \qquad (2.4.27)$$

Benmouna et al [2] give the result

$$A_C = \frac{\varphi NP(\underline{q})(1-\chi/\chi_C(\underline{q}))}{1+\upsilon\varphi NP(\underline{q})(1-\chi/\chi_C(\underline{q}))}\left\{x^2\left(\frac{\partial n}{\partial\varphi}\right)_1^2 + (1-x)^2\left(\frac{\partial n}{\partial\varphi}\right)_1^2 + 2x(1-x)\left(\frac{\partial n}{\partial\varphi}\right)_1\left(\frac{\partial n}{\partial\varphi}\right)_2\right\} \qquad (2.4.28)$$

which is the extension of equations (2.4.21) and (2.4.22) with both components 1 and 2 visible and component 1 having relative composition x.

If $(\partial n/\partial\varphi)_2 = 0$ then the result of Case A is recovered (equation (2.4.22)). If however $(\partial n/\partial\varphi)_1 = -(\partial n/\partial\varphi)_2$ then A_C=0 for x=1/2 ie. the cooperative mode disappears and the inter diffusive mode alone survives. Its amplitude is given by

$$A_I = \left(\frac{\partial n}{\partial\varphi}\right)_1^2 \varphi NP(\underline{q})\frac{1+\upsilon\varphi NP(\underline{q})}{1+\upsilon\varphi NP(\underline{q})[1-\chi/\chi_C(\underline{q})]} \qquad (2.4.29)$$

This result is of particular interest as it allows the precise determination of the interpenetrative diffusion coefficient, and hence allows the consistency of the theory to be checked experimentally (experimental evidence to support this finding is presented by Borsali et al in [34]).

2.4.2 Extensions to Benmouna Theory

Daivis et al [6] Pinder et al [8] and Pinder [38] have extended the Benmouna theory to include ternary polymer systems with different polymer molecular weights, scattering functions and solvent quality (for each polymer).

It is useful to revisit the Benmouna theory (and it's basic premises) in order to understand these extensions.

Benmouna et al [2] expressed the total scattered intensity by various species in the system by taking into account their interactions in terms of the scattered intensity of the

individual molecules. If we let $S_{ii}(\underline{q})$ denote the static intensity scattered by molecules of species i. $S_{ii}(\underline{q})$ is generally a sum of the intensity $S_{ii}^{0}(\underline{q})$ scattered by individual molecules and the contribution $Q_{ii}(\underline{q})$ due to interactions between these molecules ie.

$$S_{ii}(\underline{q}) = S_{ii}^{0}(\underline{q}) + Q_{ii}(\underline{q}) \tag{2.4.30}$$

Furthermore, interactions between different species i and j contribute to the total intensity through the quantity

$$S_{ij}(\underline{q}) = Q_{ij}(\underline{q}) \qquad (i \neq j) \tag{2.4.31}$$

Similarly, the same formalism can be applied to inelastic scattering intensities or intermediate scattering functions. If we use the Kronecker delta function δ_{ij}, this may written as

$$S_{ij}(\underline{q}) = \delta_{ij} S_{ij}^{o}(\underline{q},t) + Q_{ij}(\underline{q},t) \tag{2.4.32}$$

$S_{ii}^{0}(\underline{q})$ and $S_{ii}^{0}(\underline{q},t)$ are referred to as the bare static structure factor and the bare intermediate scattering function, respectively. The total intermediate scattering function is

$$S(\underline{q},t) = \sum_{i}\sum_{j} a_i a_j S_{ij}(\underline{q},t) \tag{2.4.33}$$

a_i and a_j are increments of refractive indices for light relative to polymers i and j respectively. The heart of the theory is to use RPA to express the Q_{ij}'s in terms of the S_{ii}^{0}'s

Benmouna et al were led to introduce the use of matrix notation to account for the relative contribution of each of the partial dynamic scattering functions. They defined a dynamic scattering matrix $\mathbf{S}(\underline{q},t)$ as

$$\mathbf{S}(\underline{q},t) = \begin{bmatrix} S_{11}(\underline{q},t) & S_{12}(\underline{q},t) \\ S_{21}(\underline{q},t) & S_{22}(\underline{q},t) \end{bmatrix} \tag{2.4.34}$$

They assumed that this matrix evolved over time following the simple exponential form

$$\mathbf{S}(\underline{q},t) = \mathbf{S}(\underline{q}).e^{-\Omega t} \tag{2.4.35}$$

where $\mathbf{\Omega}(q)$ is defined as the first cumulant matrix

$$\Omega(\underline{q}) = -\lim_{t\to 0}\frac{\partial}{\partial t}\mathbf{S}(\underline{q},t).\mathbf{S}^{-1}(\underline{q}) \tag{2.4.36}$$

which neglects the "memory matrix" in the framework of the generalised Langevin equation satisfied by $\mathbf{S}(\underline{q},t)$, and hence any hydrodynamic interactions.

Equation (2.4.35) is easily resolved and yields the following results

$$S_{11}(\underline{q},t) = a_I e^{-\Gamma_I t} + a_C e^{-\Gamma_C t} \tag{2.4.37}$$

$$S_{21}(q,t) = b_I e^{-\Gamma_I t} + b_C e^{-\Gamma_C t} \tag{2.4.38}$$

where the amplitudes a_I, a_C, b_I and b_C are

$$a_I = \frac{(\Gamma_I - \Omega_{22})S_{11}(\underline{q}) + \Omega_{12}S_{21}(\underline{q})}{\Gamma_I - \Gamma_C} \tag{2.4.39}$$

$$a_C = \frac{(\Gamma_C - \Omega_{22})S_{11}(\underline{q}) + \Omega_{12}S_{21}(\underline{q})}{\Gamma_C - \Gamma_I} \tag{2.4.40}$$

$$b_I = \frac{(\Gamma_I - \Omega_{11})S_{21}(\underline{q}) + \Omega_{21}S_{11}(\underline{q})}{\Gamma_I - \Gamma_C} \tag{2.4.41}$$

$$b_C = \frac{(\Gamma_C - \Omega_{11})S_{21}(\underline{q}) + \Omega_{21}S_{11}(\underline{q})}{\Gamma_C - \Gamma_I} \tag{2.4.42}$$

and Γ_I and Γ_C are the eigenvalues of $\mathbf{\Omega}$ ie.

$$\Gamma_I = \Omega_{av} - \left(\Omega_{av}{}^2 - \Delta(\Omega)\right)^{1/2} \tag{2.4.43}$$

and

$$\Gamma_C = \Omega_{av} + \left(\Omega_{av}{}^2 - \Delta(\Omega)\right)^{1/2} \tag{2.4.44}$$

where $\Omega_{av} = (\Omega_{11} + \Omega_{22})/2$ and $\Delta(\Omega) = \Omega_{11}\Omega_{22} - \Omega_{12}\Omega_{21}$ and Ω_{ij} are the matrix elements of $\mathbf{\Omega}$ and $S_{22}(\underline{q},t)$ and $S_{12}(\underline{q},t)$ are deduced from equations (2.4.37) and (2.4.38) by a proper interchange of indices.

Benmouna et al [2] give the result

$$\Omega = qk_BT\mathbf{M}(\underline{q}).\mathbf{S}^{-1}(\underline{q}) \tag{2.4.45}$$

where **M** is the generalised mobility matrix defined by

$$\mathbf{M}(\underline{q}) = q^{-2}\lim_{s\to\infty} s\chi(\underline{q},s) \tag{2.4.46}$$

If we use the Rouse model then $M_{ii} = \phi_i/\zeta$. Where ϕ_i is the number of monomers per unit volume of type i and all the monomer units are assumed to have the same friction factor, ζ. All the cross terms vanish ie. M_{12}=M_{21}=0, and hence

$$\Omega_{11} = \frac{q^2k_bT\phi_1}{\zeta}.\frac{1}{S(\underline{q})} \tag{2.4.47}$$

Akcasu et al [36] give the result

$$\frac{1}{\mathbf{S}(\underline{q})} = \frac{1}{\mathbf{S}^0(\underline{q})} + \mathbf{v}(\underline{q}) \tag{2.4.48}$$

where $\mathbf{v}(\underline{q})$ is the excluded volume matrix, hence dropping the $(\underline{q})$ dependency term

$$\Omega_{11} = \frac{q^2k_BT\phi_1}{\zeta}\left[\frac{1}{S_{11}{}^0} + \upsilon_{11}\right] \tag{2.4.49}$$

and by the appropriate translation of indices

$$\Omega_{22} = \frac{q^2k_BT\phi_2}{\zeta}\left[\frac{1}{S_{22}{}^0} + \upsilon_{22}\right] \tag{2.4.50}$$

By noting $S_{12}{}^0$=$S_{21}{}^0$=0 we find

$$\Omega_{12} = \frac{q^2k_BT\phi_1\upsilon_{12}}{\zeta} \tag{2.4.51}$$

and

$$\Omega_{21} = \frac{q^2k_BT\phi_2\upsilon_{21}}{\zeta} \tag{2.4.52}$$

If we let x be the mass fraction of polymer 1 and let polymer 2 be isorefractive with the solvent, then ϕ_1=$x\phi$ and ϕ_2=(1-x)ϕ.

Benmouna et al [39] have noted

$$S_{11}^{\ 0} = x\phi N_1 P_1 \tag{2.4.53}$$

and $$S_{22}^{\ 0} = (1-x)\phi N_2 P_2 \tag{2.4.54}$$

where S_{ii}^0 are the "bare" structure factors. Also we note

$$\upsilon_{12} = \upsilon_1\left(1 + \chi/\upsilon_1\right) = \upsilon_{21} \tag{2.4.55}$$

where υ_1 is the excluded volume parameter for polymer 1, and $\chi = \chi_1 = \chi_2$. (i.e. the polymers are "equally good")

Hence $$\Omega_{11} = \frac{q^2 k_B T}{\zeta}\left[\frac{1}{N_1 P_1} + x\phi\upsilon_{11}\right] = \frac{q^2 k_B T}{\zeta}[A] \tag{2.4.56}$$

$$\Omega_{22} = \frac{q^2 k_B T}{\zeta}\left[\frac{1}{N_2 P_2} + (1-x)\phi\upsilon_{22}\right] = \frac{q^2 k_B T}{\zeta}[B] \tag{2.4.57}$$

$$\Omega_{12} = \frac{q^2 k_B T}{\zeta}\left[x\phi\upsilon_{12}\right] = \frac{q^2 k_B T}{\zeta}[C] \tag{2.4.58}$$

similarly $$\Omega_{21} = \frac{q^2 k_B T}{\zeta}\left[(1-x)\phi\upsilon_{21}\right] = \frac{q^2 k_B T}{\zeta}[D] \tag{2.4.59}$$

hence from equations (2.4.43) and (2.4.44) we obtain a general expression for the relaxation modes

$$\Gamma_{\pm} = \frac{q^2 k_B T}{\zeta}\left[\frac{A+B}{2} \pm \left\{\left(\frac{A+B}{2}\right)^2 - (AB - CD)\right\}^{1/2}\right] \tag{2.4.60}$$

where Γ_+ is identified with Γ_C and Γ_- is identified with Γ_I and where

$$[A] = \left(\frac{1}{N_1 P_1} + x\phi\upsilon_{11}\right) \tag{2.4.61}$$

$$[B] = \left(\frac{1}{N_2 P_2} + (1-x)\phi\upsilon_{22}\right) \tag{2.4.62}$$

$$[C] = x\phi\upsilon_{12} \tag{2.4.63}$$

$$[D] = (1-x)\phi\upsilon_{21} \tag{2.4.64}$$

2.4.2a Ternary systems containing polymers of equal molar mass and a solvent of equal quality

Let us consider the case of equal molar mass polymers in a solvent of equal quality for both polymers (such a system might be polystyrene (PS) and poly vinyl methyl ether (PVME) in toluene, toluene being an equally good solvent for the polymers, or the system PS and PVME in tetrachloroethylene where the tetrachloroethylene is equally poor for the polymers).

Here $N_1=N_2=N$, $P_1(q)=P_2(q)=P$ and $\nu_{11}=\nu_{22}=\nu$ and $\nu_{12}=\nu(1+\chi/\nu)=\nu_{12}$, and the resultant mode frequencies are

$$\Gamma_{\pm} = \frac{q^2 k_B T}{\zeta}\left[\frac{2+NP\phi\upsilon}{2NP} \pm \left\{\frac{\phi^2\upsilon^2}{4} - x(1-x)\phi^2\upsilon^2\left[1-\left(1+\frac{\chi}{\upsilon}\right)^2\right]\right\}^{1/2}\right] \tag{2.4.65}$$

which is the general result for a ternary solution, where the solvent is of equal quality for both polymers in the system.

We will look at two special cases

CASE A:- the solvent is of equally good quality for both polymers 1 and 2. Here $\chi/\nu \rightarrow 0$ and hence the frequency modes reduce to

$$\Gamma_{\pm} = \frac{q^2 k_B T}{\zeta}\left[\frac{2+NP\phi\upsilon}{2NP} \pm \frac{\phi\upsilon}{2} \pm 2x(1-x)\phi\upsilon\,\chi/\upsilon\right] \tag{2.4.66}$$

In most experimental work, the conditions are set so that the slow (or -) mode is overwhelmingly dominant hence we are interested primarily in the results of this slow mode. The conditions are such that according to Akcasu et al [36] we may identify this slow mode with the interpenetration or interdiffusion mode Γ_I, hence

$$\Gamma_1 = \frac{q^2 k_B T}{\zeta}\left[\frac{1}{NP} - 2x(1-x)\phi\chi\right] \tag{2.4.67}$$

or $$\Gamma_1 = \frac{q^2 k_B T}{\zeta NP}\left[1 - 2x(1-x)\phi NP\chi\right] \tag{2.4.68}$$

Recalling the results

$$D_S = \frac{q^2 k_B T}{\zeta N} \tag{2.4.69}$$

and $$\Gamma_1 = \frac{q^2 D_S}{P(\underline{q})} \tag{2.4.70}$$

we find $$D_1 = D_S(1 - 2x(1-x)\phi NP\chi) \tag{2.4.71}$$

Since χ is negative for good solvents we note $D_1 > D_S$. This fits with experimental observation [7] [9] .

CASE B:- The case of an equally bad solvent for polymers 1 and 2 of the same molar mass and form factor.

In this case χ/v is not small (i.e χ/v large), then generally

$$\Gamma_{\pm} = \frac{q^2 k_B T}{\zeta}\left[\frac{1}{NP} + \frac{\phi\upsilon}{2} \pm \frac{\phi\upsilon}{2}\left\{1 + 4x(1-x)\frac{\chi^2}{\upsilon^2}\right\}^{1/2}\right] \tag{2.4.72}$$

i.e. $$\Gamma_{\pm} = \frac{q^2 k_B T}{\zeta NP}\left[1 + \phi\upsilon NP\left\{\frac{1}{2} \pm \frac{1}{2}\left(1 - 4x(1-x)\frac{\chi^2}{\upsilon^2}\right)^{1/2}\right\}\right] \tag{2.4.73}$$

we may look at two sub cases

Case i) $x\chi^2/v^2$ comparatively small, then

$$\Gamma_1 = \frac{q^2 k_B T}{\zeta NP}\left[1 - xNP\phi\upsilon\left(\frac{\chi}{\upsilon}\right)^2\right] \tag{2.4.74}$$

Case ii) $x\chi^2/v^2$ is large then

$$\Gamma_1 = \frac{q^2 k_B T}{\zeta NP}\left[1 - \phi \upsilon NP\left(\frac{\chi}{\upsilon}\right)\{x(1-x)\}^{1/2}\right] \qquad (2.4.75)$$

2.4.2b Ternary systems containing polymers of unequal molar mass and a solvent of unequal quality.

Daivis et al [6] and Pinder et al [8] have made two further extensions of the Benmouna theory.

CASE A:- Systems in which the solvent is of unequal solvent quality for the two polymers of unequal molar mass. This first extension must be viewed with extreme caution as Flory Huggins theory cannot account for such challenges to polymer compatibility posed by such a solvent.

Their basic premise is that the major effect of the use of such a solvent is an increase in the effective value of the polymer-polymer interaction parameter. They present one special case in which the solvent is poor for polymer 1 and good for polymer 2. Both x and χ/v are considered small. They give the result

$$\Gamma_1 = \frac{q^2 k_B T}{\zeta N_1 P_1}\left[1 - \frac{x(1-x)N_2P_2(\phi[\upsilon + 2x]N_1P_1)^2}{4(\phi[1+x]N_1P_1N_2P_2 + N_1P_1 - N_2P_2}\right] \qquad (2.4.76)$$

where N_1, P_1 are respectively the degree of polymerisation of the visible polymer and the scattering function for this polymer. N_2 and P_2 refer to these quantities for the isorefractive polymer.

We note that systems consisting of PS and PVME in a solvent of carbon tetrachloride approximate the conditions specified.

We also note that Saeki et al [40] have shown that χ can assume large positive values for the "compatible" polymers PS in poly(α-methyl-styrene) when in a ternary solution with a solvent of unequal quality for both polymers. Thus the assumption that χ/v is small is no longer valid.

CASE B:- The second extension is to a system in which the solvent is equally good (or equally poor) and the polymers have unequal molar mass.

Daivis et al [6] give the result

$$\Gamma_I = \frac{q^2 k_B T}{2\zeta N_1 P_1}\left[F_1 - \sqrt{\left(F_1^2 - F_2\right)}\right] \tag{2.4.77}$$

where $$F_1 = 1 + \frac{N_1 P_1}{N_2 P_2} + N_1 P_1 \phi \upsilon \tag{2.4.78}$$

and

$$F_2 = \frac{4N_1 P_1}{N_2 P_2} + 4[N_1 P_1 \phi \upsilon]^2 x(1-x) + 4N_1 P_1 \phi \upsilon\left[\frac{xN_1 P_1}{N_2 P_2} + (1-x)\right] - 4x(1-x)[N_1 P_1 \phi \upsilon]^2\left[1 + \frac{\chi}{\upsilon}\right]^2 \tag{2.4.79}$$

which if x and χ/ν are both small reduces to

$$\Gamma_I = \frac{q^2 k_B T}{\zeta N_1 P_1}\left[1 + \frac{N_1 P_1 \phi \upsilon x(N_1 P_1 - N_2 P_2) - 2x(1-x)\phi^2 \upsilon \chi (N_1 P_1)^2 N_2 P_2}{\phi \upsilon N_1 P_1 N_2 P_2 + N_1 P_1 - N_2 P_2}\right] \tag{2.4.80}$$

We note that such a system is approximated by the solution formed by PS and PVME in a tetrachloroethylene.

2.4.3 Ternary solutions close to phase separation

Investigations of the properties of ternary solutions in the past few decades have centred on investigating the self diffusion coefficient, D_S, and its scaling behaviour with concentration and molecular weight to confirm the reptation model of both de Gennes [13], and Doi and Edwards [12]. Experiments have generally been carried out in a temperature and concentration range in which the system remains far from phase separation (i.e. in a stable monophasic state far from the critical point). However it has become necessary to explore the behaviour of ternary solutions at all temperatures and concentrations in order to obtain understanding of what critical phenomena occur far

from, around and beyond phase separation. Also since some of our experimental observations were made at or close to phase separation, we include a brief overview of the recent theoretical advances.

Some characteristic phenomena are known about solutions close to phase separation, which any theory would have to accommodate. It is known that ternary polymer solutions close to phase separation are characterised by the correlation length ξ diverging, this implies long range hydrodynamic effects are significant in this critical region. It is known ξ varies with reduced temperature as

$$\xi \propto \varepsilon^{-n} \tag{2.4.81}$$

where $$\varepsilon = \frac{(T - T_C)}{T} \tag{2.4.82}$$

here T and T_C are the temperature and the critical temperature of the solution. The critical exponent n (normally ν but to save confusion with the excluded volume parameter we have used n here) has a mean field theory of 0.5, while 3-dimensional Ising and the Fisher renormalisation values are 0.63 and 0.71 respectively.

Far from the critical point, the solutions behave in a manner well described by the Benmouna theory (i.e. with Rouse-type mechanics), hence any theory must contain an hydrodynamic term and a Rouse term, with suitable mechanics to explain the interchange between these two different interaction types.

Benmouna et al [39] in 1993 presented an approach in an attempt to explain system behaviour around phase separation. Their basic approach was to use the frame work of the earlier Benmouna theory, but to recognise that the mobilities, μ, of the polymers would be modified to some extent due to "memory effects."

They assumed that the decay frequencies could be taken as

$$\Gamma_{\pm} = q^2 k_B T \frac{\mathbf{M}(\underline{q}) \pm \mathbf{M}'(\underline{q})}{\mathbf{S}(\underline{q}) \pm \mathbf{S}'(\underline{q})} \tag{2.4.83}$$

where $\mathbf{M}(\underline{q})$ and $\mathbf{M}'(\underline{q})$ represent the components of the mobility matrix including both the Rouse and hydrodynamic terms. Similarly $\mathbf{S}(\underline{q})$ and $\mathbf{S}'(\underline{q})$ represent the same components of the intermediate scattering function $S(\underline{q},t)$.

Borsali [41] states that the mobility matrix is symmetric and $\mathbf{M}(\underline{q})$ and $\mathbf{M}'(\underline{q})$ which represent its elements can both be written in terms of the Rouse and hydrodynamic terms as

$$\mathbf{M}(\underline{q}) = \mathbf{M}_0(Rouse) + \frac{1}{(2\pi)^2 \eta_0} \int_0^\infty dk \; f\left(\frac{k}{q}\right) s(k) \qquad (2.4.84)$$

where η_0 is the viscosity of the solvent and

$$f(w) = w^2 \left\{ \frac{w^2+1}{2w} \log\left|\frac{w+1}{w-1}\right| - 1 \right\} \qquad (2.4.85)$$

where $w=(k/q)$. $\mathbf{M}_0(Rouse)$ is the mobility in the Rouse limit, and its elements are $M_{ii}^0 = \frac{\phi_i}{\zeta_i}$ and $M_{ij}^0 = 0$. This is not a new approach and has previously been suggested by Doi and Edwards [12], de Gennes [13] and Akcasu [42].

Benmouna et al [39] reported that for a symmetric solution ($N_1=N_2=N$ and $P_1=P_2=P$) in zero average contrast (or optical theta) conditions they found

$$\Gamma_T = \Gamma_C = q^2 D_0 \left\{ \frac{1}{P(\underline{q})} + \left(\upsilon + \frac{\chi}{2}\right)\phi N \right\} + \frac{q^2 k_B T}{(2\pi)^2 \eta} \int_0^\infty dk \; f\left(\frac{k}{q}\right) \frac{\dfrac{1}{P(k)} + \left(\upsilon + \dfrac{\chi}{2}\right)\phi N}{P(q) + \left(\upsilon + \dfrac{\chi}{2}\right)\phi N} \qquad (2.4.86)$$

and

$$\Gamma_I = q^2 D_0 \left\{ \frac{1}{P(\underline{q})} - \frac{\chi}{\chi_C} \right\} + \frac{q^2 k_B T}{(2\pi)^2 \eta} \int_0^\infty dk \; f\left(\frac{k}{q}\right) \frac{P(k)}{P(q)} \frac{\left[1 - \dfrac{\chi}{\chi_C} P(q)\right]}{\left[1 - \dfrac{\chi}{\chi_C} P(k)\right]} \qquad (2.4.87)$$

where $D_0 = \dfrac{k_B T}{N\zeta}$

In optical theta conditions the initial decay rate $S_I(\underline{q},t)$ gives directly the inter diffusive relaxation frequency, hence we shall concentrate on this term. The first term of this equation gives the standard Rouse contributions (as predicted by the original Benmouna theory) while the second term represents the long range hydrodynamic back flow effects.

To solve the equation for Γ_I we note

1) $P(\underline{q})$ may be given by the Debye function

$$P(\underline{q}) = \frac{2}{u^2}\left(e^{-u} + u - 1\right) \tag{2.4.88}$$

where $u = q^2 R_g^{\,2}$ and R_g is the radius of gyration. $P(\underline{q})$ may be simplified to

$$P(\underline{q}) = \frac{1}{1 + \frac{1}{2} q^2 R_g^{\,2}} \tag{2.4.89}$$

where the arbatory factor 1/2 is used to empirically fit high qR_g data for solutions far from phase separation.

2) That

$$\frac{1}{(2\pi)^2 \eta} \int_0^\infty dk\, f\left(\frac{k}{q}\right) \frac{1 + q^2\xi^2}{1 + k^2\xi^2} = \frac{F(q,\xi)}{6\pi\eta\xi} \tag{2.4.90}$$

where $F(x)$ is the Kawasaki function

$$F(x) = \frac{3}{4} \frac{1 + x^2}{x^3} \left[x + x^2 - 1\right] \arctan x \tag{2.4.91}$$

which has the values i) $3/4 + x$ for $x \geq 2$

ii) $3/4$ as x approaches zero

This leads to

$$\Gamma_I = q^2 D_0 \left\{ \frac{1}{P(q)} - \frac{\chi}{\chi_C} \right\} + \frac{q^2 k_B T}{6\pi\pi\xi} F(q,\xi) \tag{2.4.92}$$

The first term represents Rouse contributions as predicted by the simple Benmouna theory, while the second term represents long range hydrodynamic back flow effects. It should be noted that as the critical temperature is reached, the Rouse term vanishes. The behaviour of the second term depends on the magnitude of $q\xi$. For $q\xi<<1$ this term is independent of q and displays a critical slowing down.

Luo [43] in his 1996 Ph D thesis presents two special cases of this theory.

CASE A:- a solution satisfying the following conditions

I) both polymers sufficiently small that $P(q)$ tends to unity

II) $N_1=N_2=N$

III) polymer 1 is isorefractive with the solvent

IV) polymer 2 is present in a trace amount

under these conditions

$$\frac{\Gamma_1}{q^2} = D_1 = D_0\left\{1-\frac{\chi}{\chi_C}\right\}+\frac{k_BT}{6\pi\eta\xi}F(q,\xi) \qquad (2.4.93)$$

a) if $q\xi\leq 0.5$ then $F(q,\xi)\approx 3/4$, and hence

$$D_1 = D_0\left\{1-\frac{\chi}{\chi_C}\right\}+\frac{3}{4}\frac{k_BT}{6\pi\eta\xi} \qquad (2.4.94)$$

from this we may note

i) D_1 is q independent

ii) as the solution approaches phase separation χ tends to χ_c, and ξ diverges and hence D_1 is expected to display a critical slowing down

iii) hydrodynamic effects are of the same nature as "Rouse effects"

b) if $q\xi>2$ then $F(q,\xi) \approx q\xi$, hence

$$D_I = D_0\left\{1-\frac{\chi}{\chi_C}\right\}+\frac{qk_BT}{6\pi\eta} \qquad (2.4.95)$$

from this we may note

i) D_I is now q dependent due to the hydrodynamic component

ii) the Rouse contribution displays a "critical slowing down" and in the limit q tends to zero $\lim_{q\to 0} D_I = D_0\left\{1-\frac{\chi}{\chi_C}\right\}$

CASE B:- a solution satisfying the following conditions

I) the minority polymer has a molar mass so large that $\frac{1}{P(q)} \approx 1+\frac{q^2R_g{}^2}{3}$

II) $N_2>>N_1$

III) the majority polymer is isorefractive with the solvent

IV) The polymer relative abundances are 3:1 by mass

In this case no equivalent expression to equation (2.4.87) has yet been obtained.

Both the fast and slow modes will be expected to contribute to the total relaxation behaviour of the solution. Benmouna et al [39] note that as the temperature is increased, one reaches the critical temperature for polymer-polymer phase separation first, before the critical temperature for polymer-solvent separation is reached (i.e. the solution separates into two polymer phases, before it separates by precipitation). This implies the critical dynamics in phase separation are in composition fluctuations rather than in concentration fluctuations, hence the important decay rate will be the slow decay rate.

In general one can expect D_I to be composed of two terms (similar to that in equation (2.4.87)), one a Rouse term, given by the simple Benmouna theory, and a hydrodynamic term similar in form to that given in equation (2.4.87)

If we use the assumption $\frac{1}{P(q)} \approx 1+\frac{q^2 R_g{}^2}{3}$ and that $R_g{}^2$ can be expressed as $2\xi^2\left(1-\frac{\chi}{\chi_C}\right)$ then the form of D_I will be

$$\frac{\Gamma_I}{q^2} = D_I = D_0\left\{1-\frac{\chi}{\chi_C}\right\}\left\{1+\frac{2}{3}q^2\xi^2\right\}+\frac{k_B T}{6\pi\eta\xi}F(q,\xi) \qquad (2.4.96)$$

where $F(q,\xi)=\frac{3}{4}+q\xi.$

Since ξ is expected to be large (the minority polymer has large molar mass) we can expect D_I to take the form

$$D_I = \frac{\Gamma_I}{q^2} = D_0\left\{1-\frac{\chi}{\chi_C}\right\}\left\{1+\frac{2}{3}q^2\xi^2\right\}+\frac{k_B T}{6\pi\eta}q \qquad (2.4.97)$$

It is interesting to note

i) as $\chi \Rightarrow \chi_C$, the hydrodynamic term will become more significant

ii) the Rouse term gives D_I a q^2 dependence

iii) as phase separation is approached a q dependence will emerge as the hydrodynamic term becomes more dominant

iv) as the small q asymptote of Γ/q^2 is $D_0\left\{1-\frac{\chi}{\chi_C}\right\}$, it should demonstrate a critical slowing down as phase separation is approached

v) at high temperature where $\chi<\chi_C$ and the hydrodynamic term is negligible, then Γ/q^2 versus q^2 should be a straight line with slope $R_g{}^2 D_0/3$ and intercept D_0 since $D_I \approx D_0\left\{1+\frac{q^2 R_g{}^2}{3}\right\}$

vi) at low temperature, close to phase separation Γ/q^2 vs q^2 is expected to be non-linear due to the q dependence of the hydrodynamic term

Chapter 3
Experimental Set-up

3.1 Dynamic Light Scattering

3.1.1 Historical Overview

The use of light scattering to study the properties of materials has a long history, dating back to Tyndall in 1869 [44]. These studies were severely limited by the resolution of the classical light source and of the detection systems employed. With the advent of the laser (and the extra resolution that mono-chromatic light sources allow), and the photomultiplier in the field of light scattering, the study of particles diffusing through a media could finally reach its potential. The first experiments of this type, however, just predate the dawn of the laser era [45].

The laser era allowed new experiments to be designed. In 1964 Pecora [46] showed that the frequency distribution of light scattered from macromolecular solutions would yield values of the macromolecular diffusion coefficient. These frequency changes were so small that "conventional" monochromators could not be used to resolve the frequency distribution of the scattered light. This problem was solved by Cummins *et al* [47] who used an "optical-mixing" technique (which is the optical analog of the beating technique developed in radio-frequency spectroscopy) to spectrally resolve the light scattered from dilute suspensions of polystyrene spheres. Light scattering has since become a major research field, and a routine method in the characterisation of compounds in solution.

3.1.2 The Dynamic Light Scattering System

The light scattering equipment used in this study has previously been described by Daivis [5], Daivis and Pinder [6] [7] and O'Driscoll and Pinder [48]. This apparatus is

shown in Fig 3.1.1, and the components that make up the system will be described in the following sections

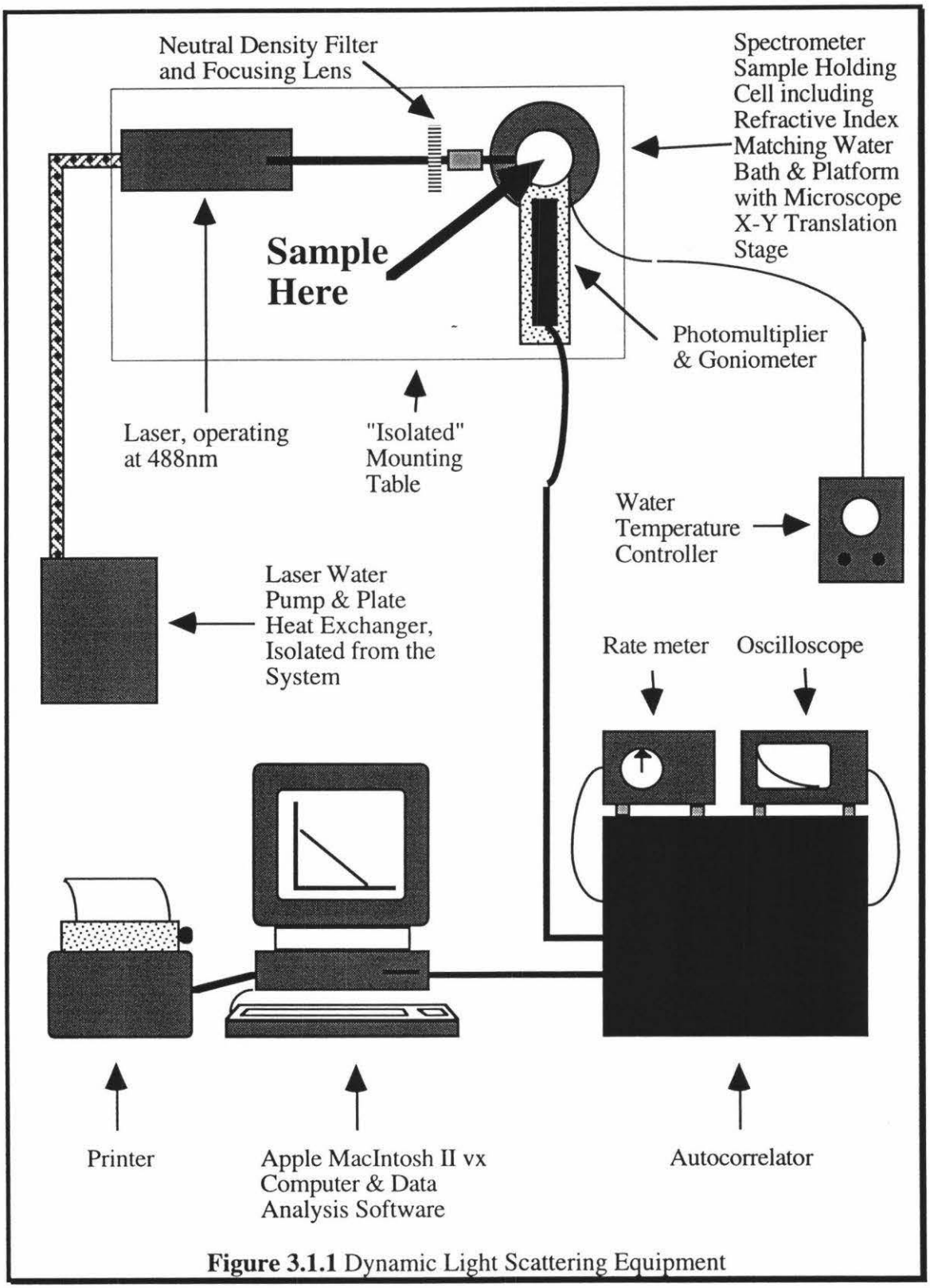

Figure 3.1.1 Dynamic Light Scattering Equipment

The laser and spectrometer are mounted on a massive table free from vibrational motion. The table consists of a steel frame filled with concrete, and surfaced with steel plate (this allows the fixation of optical components by either magnetic mounts or screwing the component directly to the table surface). This frame then rests on thick foam rubber and is supported by steel legs.

The light scattering apparatus was contained within a temperature (25 °C) and humidity controlled environment.

3.1.3 Laser Operation

A Spectra Physics 165-08 Argon Ion laser was used as the scattering light source in this study. This laser was chosen for its tunability (frequency selections available), however for this study it was kept at 488.0 nm (blue), being the strongest of the Ar^+ lasing transitions available. The laser was used well above threshold, and a neutral density filter was nearly always used to attenuate the light source. This is essential to prevent multiple scattering of the incident light within the scattering volume and also localised heating of the sample. The incident beam was weakly focused by a 10 cm focal length lens to limit the scattering volume, this also increases the beam intensity within the scattering volume.

A closed circuit cooling system is used to cool the laser when in operation. This consisted of a water pump and a plate heat exchanger. The pump circulates distilled water, which is in thermal contact with both the laser and the plate heat exchanger. The heat exchanger cools the distilled water by thermal contact with tap water via metal plates separating the two water flows. The pump and heat exchanger are vibrational isolated from the laser and optics table.

3.1.4 Spectrometer and Photomultiplier

Measurements were made with a Malvern Instruments RR 102 spectrometer. This consisted of a refractive index matching bath with temperature control unit, a spectrometer goniometer unit and photomultiplier assembly.

3.1.4a Refractive Index Matching Bath

A refractive index matching bath was used to reduce unwanted reflections and flare from the glass cell used to contain the sample. Water, which had been triply filtered using a Millipore cartridge system, was used as the refractive index matching medium. While water's refractive index is too low for complete matching, it provides good control while having practical physical characteristics (high boiling point, low viscosity, and could readily be filtered to remove particulate contamination). It is also harmless, taken in small quantities. The matching fluid was recirculated and filtered using a Malvern Instruments RR 98 recirculation pump when the light scattering equipment was not in active use. The recirculation pump allowed filtration of the medium via a Millipore filter (the filter papers used were surfactant free 0.22μm Millipore GVWP 047 00, Lot No. C7K20179).

The refractive index matching bath has been modified to accept a microscope stage with x and y translation verniers, allowing precise movement in the horizontal plane. This enables accurate positioning of the sample holders (normally NMR tubes) within the incident light beam. The NMR tubes are held in a nylon collar which was then clamped to the x-y translation stage. The position of the NMR tube was carefully adjusted using the following procedure: Each time a tube was inserted in the nylon collar the position perpendicular to the direction of the incident beam (in the horizontal plane) was adjusted so that back reflections from the tube wall returned along the direction of the incident beam. The position parallel to the incident beam was adjusted by setting the photomultiplier to 90° and noting the tube positions, on the vernier scales, when the count rate decreased to zero. This was achieved using a digital-analogue rate meter,

designed and built by Trotter [49], connected to the detection optics. The count rate decreased to zero twice, once for each wall of the NMR tube. The tube was then returned to the exact centre of these two measurements.

A Malvern instruments RR 56 temperature controller was used to control the temperature of the water bath and hence the temperature of the sample. This was connected to a copper block within the water bath assembly.

3.1.4b Spectrometer Goniometer and Photomultiplier

The spectrometer goniometer and photomultiplier assembly contained; collection optics, photomultiplier tube and a photoelectron pulse amplifier and discriminator. An ITT FW 130 photomultiplier was used. This particular photomultiplier was chosen for minimal after pulsing and low dark current, after tests by ITT on a selection of FW 130 photomultiplier tubes. It was operated at the recommended voltage of -1740 V, and was mounted in the standard Malvern Instruments photomultiplier housing within the spectrometer. The housing also contains all the collection optics and the pulse amplifier and discriminator. The collection optics were designed to provide coherent detection of the scattered light, while the amplifier and discriminator produce standardised pulses corresponding to photoelectron detection. Jolly and Eisenberg provide a discussion of the collection optics used in the Malvern Instruments spectrometer [50].

3.1.4c Optical Alignment of the Spectrometer

It is important to ensure the correct optical alignment of the spectrometer before measurements are made, the following procedure was employed: The input lens was removed, as was the vat containing the refractive index matching fluid. This vat was then cleaned. The incident light beam was then aligned to the optical axis of the spectrometer, after which the vat was replaced, and its position and the incident beam direction adjusted until the back reflections from the entrance and exit windows of the vat were symmetric and centred. The vat was then filled with refractive index matching fluid. This was followed by the replacement of the input lens, which was aligned so the

back reflections from both the front and back surfaces were centralised. The incident beam was then focused in the centre of the vat. A strongly scattering sample was placed in the spectrometer and the angle of the detection optics set to 90°. The vertical alignment of the detection optics was adjusted for maximum count rate. This was aided by the use of the Trotter digital-analogue rate meter (see section 3.1.4a), which utilised signal direct from the detection optics. The laser power was then reduced to minimum and the beam attenuated. The photomultiplier assembly was slowly moved to 0°, and the beam attenuated further if required. Here the angle was adjusted for maximum count rate, and the horizontal and vertical alignment of the detection optics also set for maximum count rate. At this point the angle vernier was set to zero.

The optical alignment was checked before serious measurements were taken, in a series of experiments using (0.091 ±0.006) μm polystyrene latex spheres (supplied by Dow Chemicals, Run No. LS-1132-B) in distilled water. According to basic light scattering theory

$$\Gamma_S = \frac{q^2 D_S}{P(q)} \qquad (3.1.1)$$

where Γ_S is the first cumulant on the expansion of the correlation function, D_S is the diffusion coefficient, $P(q)$ is the structure factor (and is normally taken as having a value of unity), q is the scattering vector (or q-vector) where $q = \left(\frac{4\pi}{\lambda}\right) n \sin\left(\frac{\theta}{2}\right)$, here λ is the wavelength of incident light, n is the refractive index of the solution and θ is the scattering angle. If $P(q)$ is not equal to unity then the Γ_S is q-dependent. The solutions prepared have previously been characterised [51] [52] [53] and no q-dependence has been found. Hence a plot of D_S vs q should give a straight line parallel to the x-axis if the detection optics are in correct alignment. Also a plot of the Γ_S vs q^2 should be a straight line through the origin with slope equal to the diffusion coefficient. Figs 3.1.2 and 3.1.3 show the plots obtained after optical alignment.

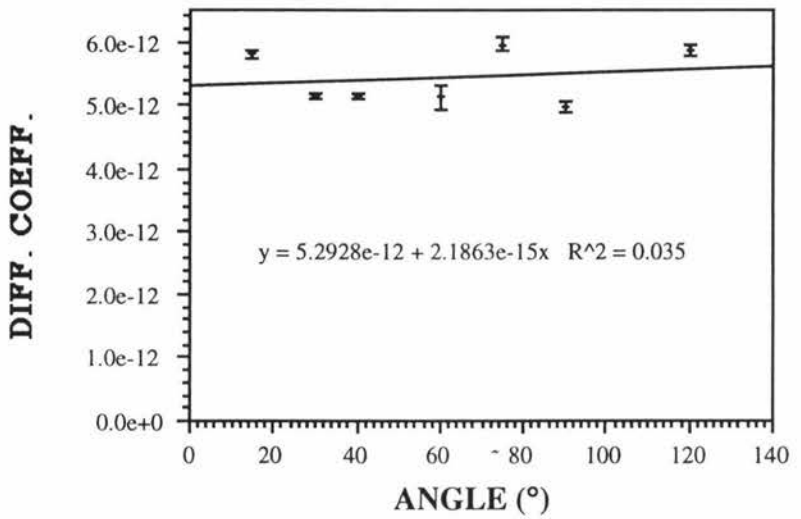

Figure 3.1.2 The diffusion coefficient of 0.091μm polystyrene latex solution at various angles of scatter

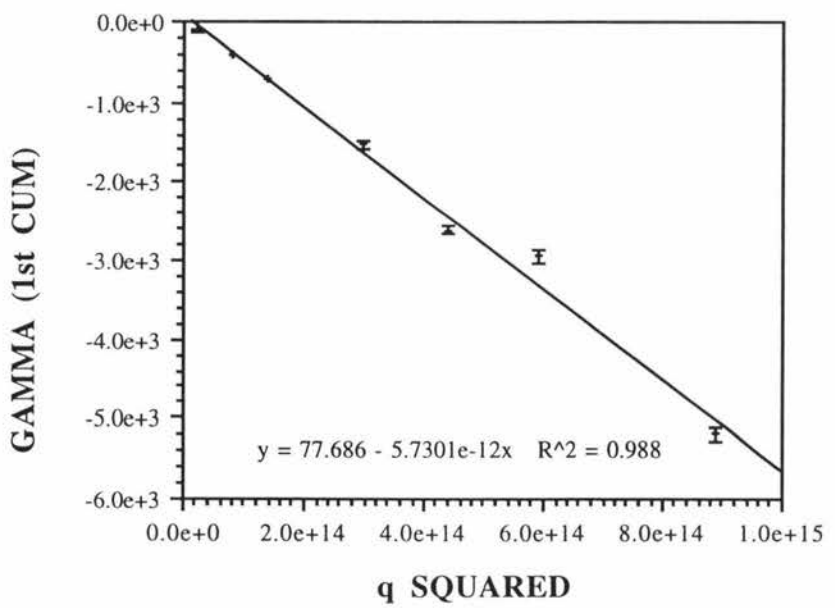

Figure 3.1.3 The first cumulant of a 0.091 μm polystyrene solution vs q^2

Both figures 3.1.2 and 3.1.3 show a that the self diffusion coefficient does not very systematically with q, and hence that the optical alignment of the detection optics is more than adequate. Indeed the data analysis package gave a hydrodynamic radius of

(4.6 ± 0.3) x 10^{-8} m, which compares favourably with the stated diameter of (9.1 ± 0.6) x 10^{-8} m.

3.1.5 The Autocorrelator

The clipped photon-counting technique was introduced by Foord *et al* [54] in 1970. The operating principles are discussed by Oliver [55] and a detailed description of a correlator of this type is given by Mole and Giessler [56].

The standardised pulses emitted from the detection optics are processed by a digital correlator built by O'Driscoll [48] [51]. This correlator has been previously described [48] [51], and the principle characteristics will now be briefly discussed. The instrument has been designed to have specifications similar to the commercially available (in the late 1970's) Malvern Instruments 4300 correlator. The correlator has 48 correlation channels each with 10^8 count capacity, with sample times ranging from 0.05 μm to 9.95 x 10^5 μm. Four monitor channels each of 10^{10} count capacity, are provided for normalisation of the correlation function. The correlator operates with zero dead time.

The design of the digital correlator is simplified by "allowing" the input pulses to occur at certain times only. This is achieved using a derandomiser. The derandomiser defines time intervals equal to the shortest sample time (50 ns), and shifts the input pulses in the time domain so that they are synchronised to the master 20 MHz clock. This time shift does not affect the correlator operation it is only necessary to know the number of pulses occurring in a given sample period and not the actual time they occurred.

These incoming data are then reduced to binary form before the correlation function is computed. The reduction to "one bit" form is achieved by "clipping" or "scaling" the data. Clipping is achieved by setting the output at one if the input level exceeds a certain count number, k, in a given sample time, T. If the level is less than k then the output is set to zero. Scaling is achieved by outputting one count for every s counts that enter the scaler. Clipping is available in the range 0-99 and scaling in the range 1-99. In practice scaling always followed clipping at zero.

The auto correlation function $G^{(2)}(T)$ is found by storing and delaying the data from the sampling counter and then multiplying these by the undelayed data. The digital correlator calculates the correlation function of the photo detection pulses by accumulating the products

$$NG^{(2)}(iT - rT) = \sum_{i=1}^{N} n(iT)n_k(iT - rT) \qquad (3.1.2)$$

where T is the sample time, r is the delay channel number, N is the number of samples and n and n_k are the unclipped and clipped numbers of the photo detections counted in a given sampling period. For a stationary, ergodic process, the time average is equal to the ensemble average, so

$$NG^{(2)}(iT - rT) = N\langle n(iT)n_k(iT - rT)\rangle \qquad (3.1.3)$$

is independent of the time origin iT. The lag time (iT-rT) is usually labeled τ and the correlation function is even so that $G^{(2)}(-\tau) = G^{(2)}(\tau)$.

The normalised intensity auto correlation function $g^{(2)}(\tau)$ is equal to the normalised photo count correlation function [57] and the estimator for $g^{(2)}(\tau)$ obtained in an experiment is given by

$$\hat{g}^{(2)}(\tau) = \frac{\langle n(iT)n_k(iT - rT)\rangle}{\langle n\rangle\langle n_k\rangle}$$

hence

$$\hat{g}^{(2)}(\tau) = N \times \frac{NG^{(2)}(\tau)}{B} \qquad (3.1.4)$$

where B is the product of the measured values of $N<n>$ and $N<n_k>$. It is appropriate to think of the measured $\hat{g}^{(2)}(\tau)$ as one member of an ensemble which has the population mean $g^{(2)}(\tau)$.

All of the quantities in equation (3.1.4) are available from the stores and monitor channels of a digital correlator. This normalisation method is sometimes called self-normalisation.

If the scattered field has gaussian statistics, the electric field auto correlation function is related to the intensity auto correlation function by the Siegert relation [57]

$$g^{(2)}(\tau) = 1 + C\left|g^{(1)}(\tau)\right|^2 \qquad (3.1.5)$$

where the constant C is an experimental factor which accounts for the effects of clipping (or scaling), the finite area of the detector and the finite length of the sample time. In the analysis, C is treated as a free parameter.

The O'Driscoll correlator has incorporated into the hardware a device designed to prevent the detection of dust, and hence the distortion of the correlation function. This device uses an intensity monitor to detect unusually high input pulse rates, which suggest the presence of dust. This intensity monitor then stops the correlator. A delay circuit delays the input pulses sufficiently for the spurious signals to be detected by the intensity monitor and the correlator to be stopped, before these spurious signals can be processed. This "blinker" sense circuit compares the number of channel A pulses in a sample period with some preset number, the blinker level. If this level is exceeded a logic '1' is entered into a four stage shift register and if not a logic '0' is loaded. This shift register is also clocked by the sample time clock. Three consecutive '1's in the shift register generate a correlator 'stop' command. Four consecutive '0's generate a 'start' command. The number of times the correlator stops/starts is recorded in a monitor channel. It is important to give the dust time to move through the sample area, so a one second delay time is allowed for the particle to move, then an additional 128 sample times are delayed to allow the main correlator shift register delay line to fill with data and so acquire the history of the current data before correlation is recommenced. The introduction of software control of the correlator has made the use of the blinker unnecessary, however the basic principles of the blinker are used in the correlator control software to reduce dust distortion of the correlation function.

After correlation, the data is stored in the accumulator, from which it can be displayed, one channel at a time or transferred via the data bus to a computer.

3.1.6 Computer and Software

The data from the autocorrelator are transferred to a computer via a RS 232 serial port using an interface constructed by O'Driscoll [51], the transfer rate is 9600 baud.

The data are collected and analysed by a Macintosh II vx computer. The data are collected using a program called "dlsEXPRESS2L" (written in Fortran 77 and compiled using Absoft's MacFortran compiler, version 2.3). The program uses standard toolbox routines to control the serial port. The program also initiates the start, and the termination of "live" accumulations on the autocorrelator. "dlsEXPRESS2L" corrects the angle of scattered light (compensating for the refractive index of the matching medium), the sample solvent viscosity, the sample cell shape, the temperature, and wavelength of the incoming laser light; and records the autocorrelator sample time, whether the signal is scaled or clipped (and by how much), and the number of runs averaged with the data. The program plots and updates the auto correlation function after each data collection run, and stores the processed data in a temporary file called "$$$express."

The software also incorporates a run rejection scheme, which is similar to the "blinker" facility in the hardware of the autocorrelator (see section 3.1.5). This is designed to reject runs in which the count rate shows evidence of unusually high scattering intensity. The scheme first allows ten preliminary runs. These are measured for the mean number of counts per run. Each run provides an estimate of the mean number of counts per sample time, $\hat{n}$. The values of $\hat{n}$ obtained in the ten preliminary runs are stored in an array and their average calculated. Each time a run is completed, the new value of $\hat{n}$ is compared to the mean value. If this is within five standard deviations of the mean value, the new run is included in a running average of $\hat{g}^{(2)}(\tau)$ and the new value replaces the oldest value of $\hat{n}$ in the array. This process is continued until a predetermined number of runs has been accepted. The scheme has the advantage that the mean value of $\hat{n}$ is self-correcting, and will adapt to small drifts in average intensity.

The experimental data stored in the temporary file $$$express, were then analysed by a second program called "dlsfit006L" (also written in Fortran 77 and compiled by Absoft's MacFortran, version 2.3). This program allows the option of fitting the data with cumulant fits, or single or double exponential fits (with or without a floating base line).

The intensity auto correlation function is normally written [58]

$$g^{(2)}(\tau) = 1 + \left(C\left|g^{(1)}(\tau)\right| + \Delta_1\right)^2 + \Delta_2 \qquad (3.1.6)$$

where $g^{(1)}(\tau)$ is a model provided by the theory and Δ_1 and Δ_2 are constants which are included to allow for artefacts which cannot be eliminated experimentally. Δ_1 can be thought of in terms of the constant scattering function obtained from "stationary dust" in the scattering volume, while Δ_2 could represent drifts in the source intensity or the "detection optics" gain, which would lead to the misnormalisation of $g^{(2)}(\tau)$ [59], or a number fluctuation term resulting from large particles (dust) passing through the scattering volume [58]. Provincher et al [59] noted that Δ_1 appears to be more important than Δ_2 in data analysis. In their work they used a dust discrimination scheme, so it is expedient to ignore Δ_2 under such conditions. Since a "dust discrimination" scheme (which effectively removes any "sudden" increases in the detected intensity from the data set) is employed in the software controlling data collection, it is reasonable to ignore Δ_2 in the analysis. Indeed in practice the most straight forward method of data analysis is to fit

$$S_i = \left(\hat{g}^{(2)}(\tau_i) - 1\right)^{1/2} \qquad (3.1.7)$$

or ln S_i directly. This has the advantage that when a complicated model for $g^{(1)}(\tau)$ is being fitted, it may be fitted directly rather than its square which would be fitted if $g^{(2)}(\tau)$ were fitted.

All the cumulant fits used the method of least squares to fit the data as described in [5]. For single exponential fits, the data were fitted to the equation

$$C\exp(-\Gamma\tau)+\Delta_1 \tag{3.1.8}$$

with Δ_1 being optional, while for double exponential fits

$$C\left[A\exp(-\Gamma_1\tau)+(1-A)\exp(-\Gamma_2\tau)\right]+\Delta_1 \tag{3.1.9}$$

is fitted, with Δ_1 optional. The details of which are given in [5] and expanded on by Bevington [60] .

Two methods are provided in "dlsfit006L" to assess the quality of fit. In the first the value of the reduced χ^2 is computed using

$$\chi_F^{\,2}=\frac{\chi^2}{F} \tag{3.1.10}$$

where F is the number of degrees of freedom in the fit, i.e. the number of data points minus the number of parameters in the fit. A value of χ_F^2 close to one indicates that the fit is good while a value greater than one indicates a poor fit [60] .

The second method of assessing the fit involves plotting the weighted residuals. In this method the difference between the predicted (theoretical) value and the obtained data are plotted for each data point of the auto correlation function. This difference is then plotted against the channel (time) at which the original data point occurred. If the fit is poor, a plot of residuals will show a trend, while a good fit will show a random distribution of points above and below the abscissa.

"dlsfit006L" can neglect the first few points of a data set in the analysis if required. This may be necessary because of photomultiplier after pulsing, especially when using very low count rates or short sample times. "dlsfit006L" will also allow several runs on the same sample to be averaged (which allows runs from several days work to be averaged). Since individual runs may have different values of C (see equation 3.1.6),

individual runs are first fitted with a cumulant fit to determine C and then each run is renormalised to a intercept of 1 (for S_i) before averages are calculated.

From the linear-quartic cumulant fits, the diffusion coefficient, the polydispersity of the sample, and the hydrodynamic radius can be calculated and printed out (via a laser printer), and the auto correlation function plotted via a Hewett-Packard 7470A plotter.

3.1.7 Running Samples

In running samples the following steps were taken: The detection optics were switched on and left for a period greater than 24 hours, so that the dark current of the photomultiplier would reduce to a constant level. Initially the set-up was thoroughly checked for optical alignment by checking the hydrodynamic radius of a 0.091μm polystyrene latex in water (see section 3.1.4c). This step was not repeated subsequently, as the Malvern cell was left undisturbed.

The current sample was taken from the sample preparation room (25 °C) and allowed to come into equilibrium in the Malvern cell (25 °C). The laser was switched on, and operated above threshold, and the computer set to run. Using the Trotter rate meter connected to the detection optics, the sample was aligned in the cell, so that the cell was centrally located. The detection optics were then attached to the autocorrelator (the output of which was displayed directly on an oscilloscope). The sample time of the autocorrelator was then adjusted until the correlation function had decayed to a value of approximately e^{-3} at the largest value of τ. The parameters required by the computer software were then set and the computer allowed to run the autocorrelator "live" for a few sample periods, after which the sample time was reassessed (and adjusted where necessary). The computer program was then set and left to run the experiment for several hours or days depending on the strength of the scattered signal.

At the completion of a run (or set of runs) the data were then retrieved from a temporary data file ($$$express), and analysed using the program "dlsfit006L."

From the analysis various parameters were extracted, printed and plotted and further analysed (i.e. with further runs of this series of solutions). The data files were renamed and kept for later perusal as required.

3.2 Sample Preparation

3.2.1 Glassware Cleansing Procedures

Particulate contamination in light scattering cells can lead to severe distortion of data [61] [62], so every effort must be expended to produce dust free samples. This is most easily achieved by ensuring that all apparatus used in sample preparation is scrupulously clean.

Sample containers, glassware and all other apparatus associated with the preparation of samples were subjected to the following procedures to ensure freedom from particulate contamination: The apparatus was first cleaned in detergent and tap water. It was then left to soak in chromic acid overnight, before being thoroughly rinsed in tap water. The apparatus was next soaked overnight in Decon 90 detergent solution. After rinsing in tap water, it was then rinsed in 0.22 μm filtered, distilled and deionised water. It was then rinsed in analytical grade acetone, and left to dry in a dust free environment. The apparatus was then flushed using condensing acetone vapour, and allowed to dry in a vacuum desiccator overnight to remove the last traces of liquid. The apparatus was then stoppered, or removed to a dust free environment for storage until later use.

Any apparatus that could not withstand chromic acid was instead soaked in detergent solution for a longer period to loosen contaminants.

Acetone flushing was carried out using the apparatus shown in Fig. 3.2.1

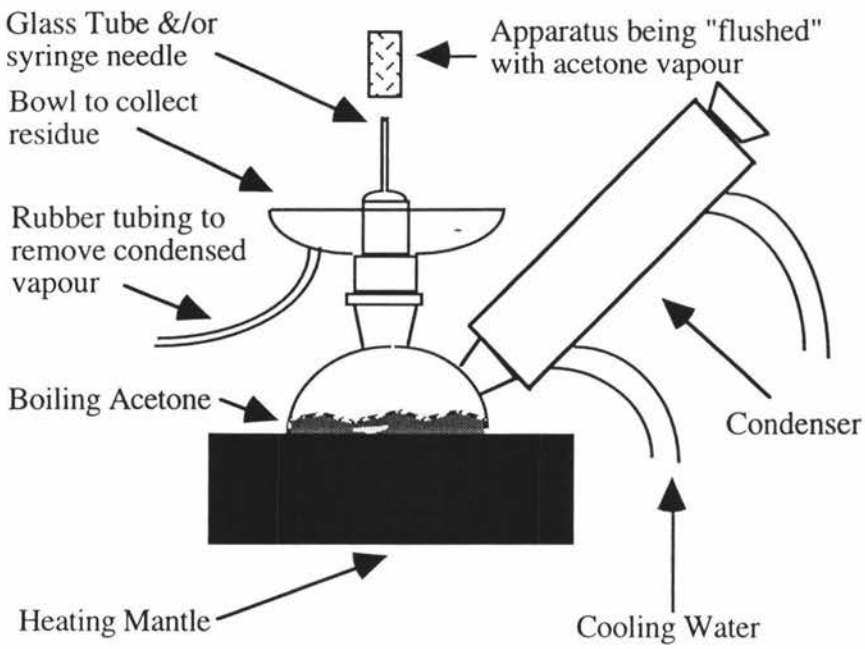

Figure 3.2.1 Apparatus for cleaning glassware

This is based on a design discussed by Tabor [61], it consists of a heating mantle on which a triple necked flask rests. Analytical grade acetone was heated and kept at boiling point in this triple necked flask. The acetone vapour pressure within the flask was relieved through a narrow glass tube in one of the necks of the flask, creating a jet of moderate pressure acetone vapour which could then be directed onto the apparatus being cleaned. A small catch bowl was attached below the narrow glass tube, to catch the condensed acetone vapour from the flushed apparatus. A piece of rubber tubing carried this condensed acetone way from the heating mantle and flushing apparatus. A condenser was fitted to a second neck of the flask so that the acetone vapour could be recycled when not required. The third neck of the flask was used for replenishment of acetone as required.

3.2.2 Polymers used in this study

3.2.2a Polymer Characteristics

This study examines solutions containing the two random coil polymers, polystyrene (PS) and poly (vinyl methyl ether) (PVME). The structure diagrams of PS and PVME are given in figures 3.2.2, and 3.2.3 respectively, and the characteristics of the polymers used in this study are given in table 3.2.1.

Polymer	Source	M_w	M_w/M_n	Catalogue No.	Lot No.
Polystyrene	Pressure Chemicals	110, 000	≤ 1.06		4b
PVME as supplied	GAF	102, 000	4	Gantrez	M-555
PVME as used	GAF	110, 000	1.3	Gantrez	M-555

Table 3.2.1 Polymers used in this study

Polystyrene was supplied by Polysciences with a molar mass of 110, 000 $gmol^{-1}$ and was in the form of minus 6-Mesh granules. The polystyrene was used as obtained.

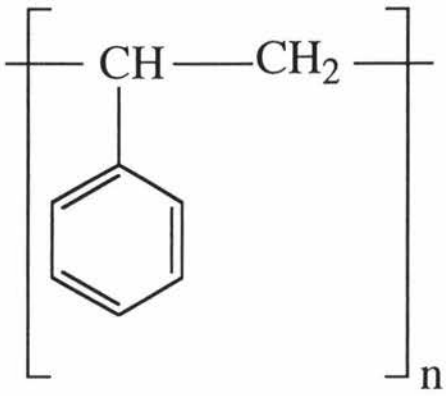

Figure 3.2.2 The structure of polystyrene

Polystyrene was added to the appropriate solvent, in sufficient quantity to prepare a standard solution, which was then filtered (see below) and sealed until required.

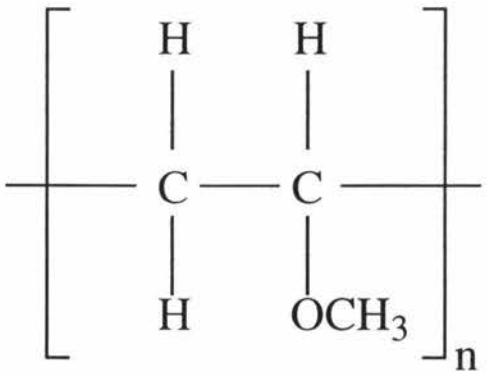

Figure 3.2.3 The structure of poly (vinyl methyl ether)

PVME was obtained as a 50:50 PVME/toluene solution, Daivis [5] has determined the molar mass of the polymer in this state to be 102, 000 $gmol^{-1}$ with a polydispersity of 4. Such a large polydispersity is unacceptable for this study, so polymer fractionation was used to reduce the polydispersity following the method described by Daivis [5]. This procedure reduced the polydispersity to a value of 1.3, and increased the molecular mass of the polymer to 110, 000 (10, 000) $gmol^{-1}$. While the polydispersity is still high it is acceptable since this polymer acts only as a "mesh" through which the "visible" PS is monitored as it diffuses.

3.2.2b Fractionation of PVME

Flory [14] has discussed general fractionation techniques. The main objective of fractionation is to reduce the polydispersity of the a polymer by as much as possible with the minimum of effort. The fractionation method used is described by Mason and Arquette [63]. The principle involves the addition of sufficient non-solvent to a solution of the polymer dissolved in a good solvent to precipitate the higher molecular mass molecules. In this case the PVME was dissolved in the good solvent toluene and the non-solvent Petroleum Spirit (40-60 °C) was added to cause precipitation. If the solution is allowed to attain equilibrium it separates into two phases, the higher molar mass PVME precipitates and settles to the bottom of the flask. This separation (or fractionation) can be completed by the removal of either the supernatant or the precipitate. This process was completed twice, the first time the large molar mass precipitate was discarded, the second time the low molar mass supernatant was discarded. Only the so-called "middle fraction" of the PVME was retained for use in the dynamic light scattering experiments.

The procedure used in fractional precipitation was as follows: First approximately 20 g of the M-555 PVME/toluene solution as obtained from GAF was put into a flask. This was then dissolved in 60-70 g of analytical grade toluene. This solution was left overnight to attain equilibrium and then transferred to a 2 litre triple necked flask. The flask was then placed in a temperature controlled water bath. Temperature control was achieved by a precise temperature controller (Thermomix 1460, B. Braun, Melsungen AG, West Germany). The flask's contents were stirred constantly, using an overhead stirrer, and allowed to stabilise at 25 °C overnight. Approximately 750 ml of analytical grade Petroleum Spirit (40-60 °C) was then added and the solution allowed to stabilise. At this point the solution should have been cloudy. More Petroleum Spirit (40-60 °C) was added, carefully, if the solution wasn't cloudy (the amount of precipitate formed depends on the quantity of the non-solvent added) until lasting cloudiness was achieved. The temperature was increased to 28 °C and allowed to stabilise (the solution should

have cleared at this point, if it hadn't then a little toluene was added, and the above temperature related steps repeated until at 25 °C the solution was cloudy, and at 28 °C the solution was clear). The stirrer was removed, the flask stoppered, the temperature decreased to 25 °C, and solution left overnight to equilibrate. The solution now existed in two phases. However, the dividing line between these two phases was sometimes difficult to see. Careful and gentle swirling would disturb the two phases around this dividing line and allow this line to be clearly contrasted. Due care was needed in this process so the two phases were not redispersed. The supernatant was removed and the precipitate layer was redissolved in toluene and discarded (it is preferable to remove the supernatant to a one litre round bottomed flask in the water bath, otherwise the addition of toluene is necessary to redissolve the precipitate formed as this solution cools). The supernatant was then returned to the 2 litre flask. Approximately 230 ml Petroleum Spirit (40-60 °C) (this quantity depends on the amount of precipitate desired) was added and the solution stirred and then left overnight. The precipitate (middle fraction) in this case was retrieved from the two phased solution that resulted.

3.2.2c PVME Handling

The solvents used in fractionation were most effectively removed by the following method. The middle fraction was diluted and filtered (see below) into a series of 100 ml flasks which had been previously weighed, these where then "dried" using a rotary evaporator for a few hours at 90 °C, a fast rotation rate was required to spread the polymer in a thin layer around the flask for the most effective "drying". The flasks were then connected to a vacuum pump (0.2 mm Hg) and left overnight, after which the flasks were transferred to the weighing room and allowed to come into thermal equilibrium before the mass of dry PVME was determined. The PVME was then redissolved in toluene.

Redispersion in other solvents was readily achieved by drying the PVME solution several times, as detailed above, each time resolvating in the solvent of choice.

Particular care is needed in handling PVME because it is very susceptible to oxidative and photochemical degradation resulting in a dark brown appearance. Precautions included wrapping the flasks containing PVME in silver foil (to keep out light) and storing under a dry nitrogen atmosphere in a cool place. These precautions were followed at all stages of processing and subsequent solution preparation and preservation. PVME is also susceptible to absorbing moisture, to avoid this PVME was stored in an organic solvent. Toluene seems to be a particularly good solvent, keeping the polymer from appreciable oxidation and contamination.

3.2.3 Solvents used in this study

Solutions were made with analytical grade solvents as listed in table 3.2.2, these solvents were used as obtained with the addition of 0.2 μm filtration.

Solvent	Source	Product Number	Lot Number	$\bar{v}$ (m^3kg^{-1})	$\partial n/\partial C$ (cm^3g^{-1})
Toluene	Ajax Chemicals	551	111587	1.1597	0.111
Carbon Tetra-chloride	Ajax Chemicals	143	909330	0.63111	0.161
Tetrachloro-ethylene	BDH (Aust)	10407 6T	2015480 L	0.6192	
Petroleum Spirit (40-60 °C)	Ajax Chemicals	10178	4998760		

Table 3.2.2 Solvents used in sample preparation

3.2.4 Sample filtration

The clarification of solutions is hindered by the overlapping dispersities of particle size, density, and refractive index of the polymers and the extraneous material [61]. Fortunately the major contribution to extraneous scattering is from gross particles, and these are easiest to remove. Two methods are usually employed in removing particulate contamination; centrifugation and filtration. Filtration was chosen in this study because of its relative ease of operation and quickness of use, which is important when using volatile solvents which may evaporate (and hence change the solution concentration).

Samples were filtered using a teflon and steel Millipore filter holder containing a Millipore filter (Cat. No. FGLP 013 00, Lot No. H1 BM92399 A), chosen for its solvent resistance. Glass syringes and stainless steel hypodermic needles were used to filter samples.

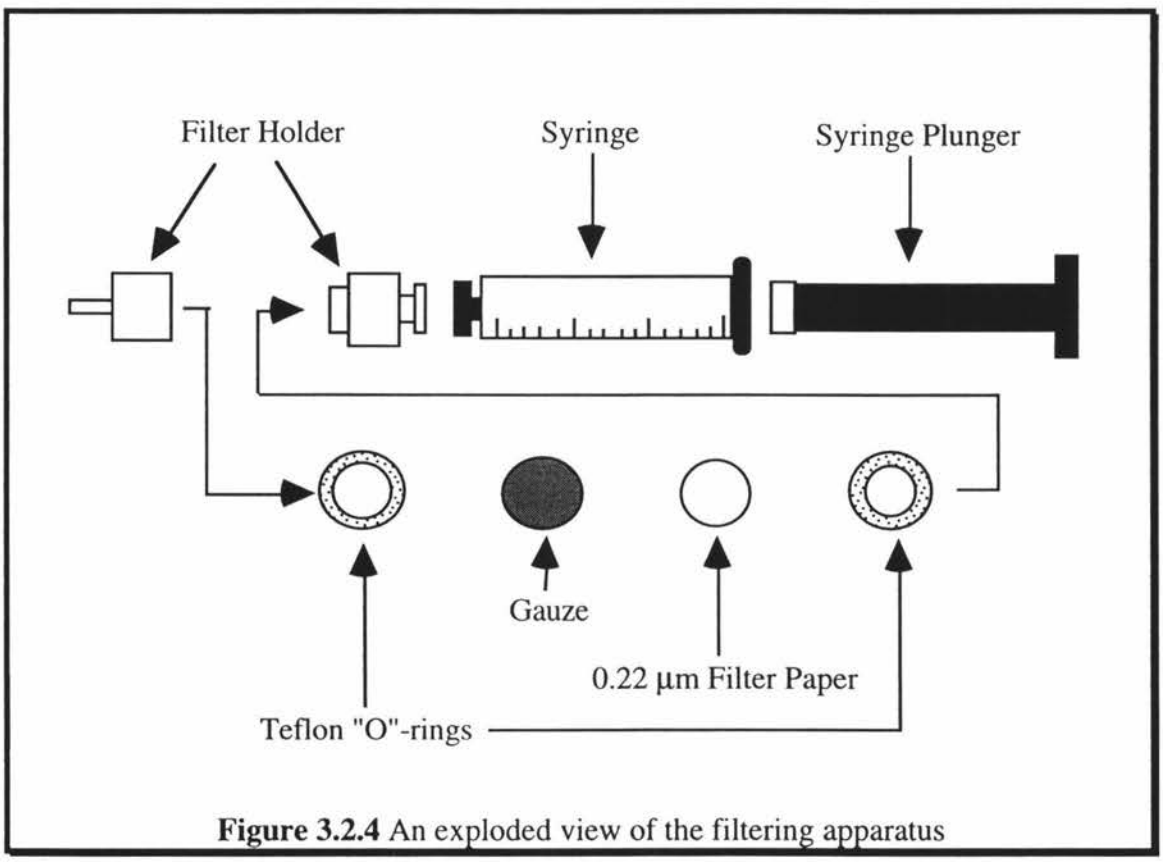

Figure 3.2.4 An exploded view of the filtering apparatus

The following procedure was used to filter samples: After cleaning and drying the filter holder, syringe and needle (as described in section 3.2.1) the current and the filtered (new) solution flasks were weighed, and the current polymer mass fractions were calculated from equation (3.2.2) (see section 3.2.7) (this step was unnecessary for pure solvent filtration). The sample to be filtered was transferred to the syringe, to which the filter holder was then attached. The first few drops of filtered sample were discarded, to avoid any risk of contamination from dust. The remaining sample was then filtered directly into the new solution flask, which was then sealed and the flask weighed. The mass of polymer transferred was then calculated using equation (3.2.2) and recorded.

3.2.5 Solution Preparation

Solutions were prepared using the following procedure. PS and PVME standard solutions were made in the appropriate solvent. These were then filtered and the mass of polymer remaining determined using equation (3.2.2). These standard solutions were combined into a third flask, in amounts appropriate to deliver the polymers in the correct quantities. The amount of solvent within this solution was then adjusted either by removing excess solvent using a rotary evaporator, or by adding filtered solvent as required.

In this work total polymer concentration was varied but the polymer composition was held constant. These solutions were prepared as follows: The samples were first concentrated until the solution was tactile or just after the solution had phase separated depending on the solvent. The solution was then diluted with filtered solvent (and left to equilibrate), samples being taken at each successive dilution. Values of x_{PS} investigated include 0.05, 0.125, 0.29 and 0.442, where

$$x_{PS} = \frac{m_{PS}}{m_{PS} + m_{PVME}} \qquad (3.2.1)$$

here x_{PS} is the PS composition parameter (or mass fraction) and m is the mass of the component of interest.

3.2.6 Sample delivery and storage

Samples were delivered directly into a 5 mm NMR tube (Wilmad Glass, USA), and sealed under a nitrogen atmosphere. Dilute samples were syringed directly into the

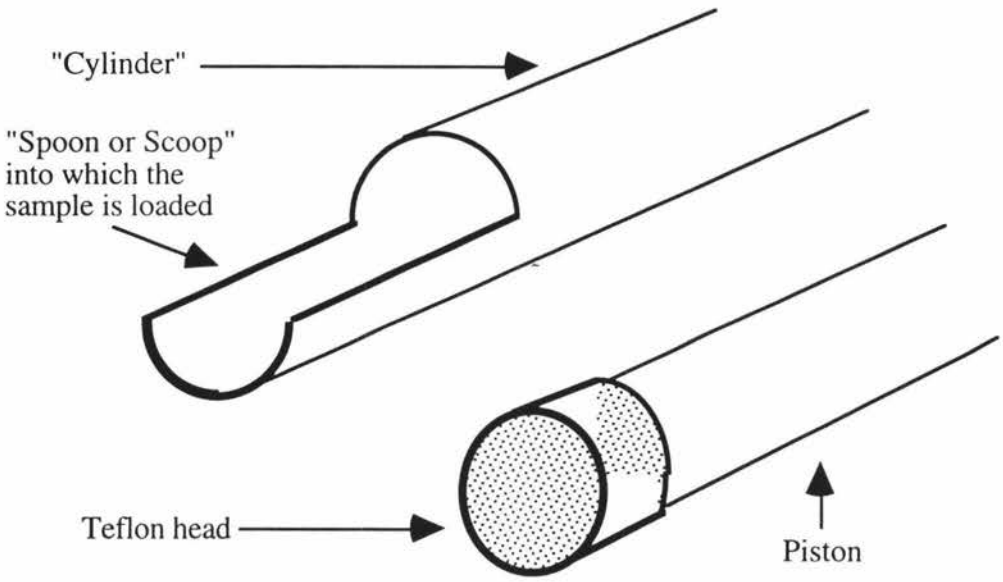

Fig 3.2.5 Apparatus for transferring high concentration solutions

NMR tube. High polymer concentration samples were so viscous that a special apparatus was designed to transfer the solution to the NMR tube. This is shown in figure 3.2.4. It consisted of a 4 mm diameter stainless steel tube forming a "cylinder," and a steel piston complete with teflon head. This apparatus was "loaded" with a micro-spatula and then inserted into the NMR tube, and the piston pushed to release the "load." This was repeated until the desired quantity of polymer solution was deposited in the NMR tube.

The NMR sample tubes were then wrapped in silver foil and left in order to come into thermal and chemical equilibrium before experimental work commenced.

3.2.7 Weighing

All masses were recorded on a five digit Mettler AT261 balance in a humidity and temperature controlled (25 °C) room. For new solution preparation the weighing procedure was as follows: The flask holder was weighed, and then the flask and holder

were weighed. The flask was then replaced by the standard solution, which was weighed and the polymer mass fraction determined from equation (3.2.2) (see below). This was then removed from the balance, and the appropriate amount of this standard solution was added. The original flask was reweighed and the mass of standard solution added calculated, as was the mass of polymer added from equation (3.2.2). The above steps were then repeated for the other standard solution, and finally the current mass fractions for each component were calculated.

For solution adjustment the weighing procedure was as follows: The weight of the flask holder was obtained and then the holder and solution flask together. The current mass fractions of the polymers were then calculated, and the amount of solvent or standard solution needed to adjust the original solution was calculated. This quantity of solvent or standard solution was then added and the flask reweighed. The masses of the polymers present were then calculated using equation (3.2.2).

Mass fractions were calculated for a particular component within the solution, using equation (3.2.2)

$$w_i = \frac{m_i}{\sum_{i,j,k} m} \qquad (3.2.2)$$

where w_i is the weight fraction of the component of interest, m is the mass of the component (i is the component of interest and j and k are the other components of the solution, of which k will be missing in a binary solution).

To calculate the concentrations of each polymer present within the solution of interest at anytime, first the solution was weighed, then using the previous mass data for each polymer, the weight fraction for each polymer was obtained. The weight fraction was then converted to a mass/volume concentration and volume fraction using equations (3.2.3)-(3.2.5) respectively

$$1/\rho = \sum_{i=1}^{3} w_i \bar{v}_i \qquad (3.2.3)$$

$$c_i = w_i \rho \qquad (3.2.4)$$

$$\phi_i = c_i \bar{v}_i \qquad (3.2.5)$$

Here, ρ is the solution density, w_i is the weight fraction of component i, $\bar{v}_i$ is the partial specific volume of component i, c_i is the mass/volume concentration of component i and ϕ_i is the volume fraction of component i. The partial specific volume fraction of polystyrene in toluene was given by Daivis [5] to be 0.916 m^3kg^{-1}, where this solution was taken at infinite dilution and interpolated using the temperature dependence given by Scholte [64]. The partial specific volume of PVME was taken as 0.983 x 10^{-3} m^3kg^{-1} [65]. The values of $\bar{v}$ for toluene, carbon tetrachloride and tetrachloroethylene were taken as the reciprocal of their densities at 25 °C. These are 1.1597 m^3kg^{-1}, 0.63111 m^3kg^{-1}, 0.6192 m^3kg^{-1} respectively [66]. The value for tetrachloroethylene was interpolated from data obtained from data given in Timmermans [66].

Chapter 4
Results and Discussion

4.1 Solutions Investigated and Sundry Information

4.1.1 Solutions Studied

This work was undertaken to investigate four aspects of the work previously presented by Daivis et al [5] [6] [7] [8] [9]. The first is the effect on the relationship between D_I and D_S of different mass fractions in the polymer system 110 000 Dalton PS/ 110 000 Dalton PVME/ solvent (where three different solvents were utilised:- toluene, carbon tetrachloride and tetrachloroethylene). The sample series *B1, MODB1A, A, B, C, and D were used in this study, the details of which are listed below. Secondly the effect of the polymer-polymer interaction parameter, χ, on the relationship between D_I and D_S is investigated. The sample series *B1, A, B, C and D were used in this study. Toluene data from Daivis [5] were also utilised to increase the range of polymer-polymer interaction parameters accessible in this study. Thirdly the effect of polymer molar mass on the relationship between D_I and D_S is investigated. The sample series *B1, A, B, C, D and Daivis's toluene data were utilised for this study. Fourthly the considerable discrepancy between D_I and D_S which is manifest in 110 000 Dalton PS/ 110 000 Dalton PVME/ toluene solutions at polymer volume fractions greater than 0.4 is investigated. The polymer series E and F were used for this study.

Daivis's [5] diffusion data from the system 110 000 Dalton PS/ 110 000 Dalton PVME/toluene obtained by Pulse Field Gradient Spin Echo Nuclear Magnetic Resonance (PGSE NMR) is utilised as a "control" in all the above investigations. Firstly it is well recognised [5] [9] that the diffusion coefficient obtained by PGSE NMR is the self diffusion coefficient. This self diffusion coefficient may then be contrasted by the diffusion coefficient, D_I, obtained by DLS for the systems under investigation.

Secondly these data are utilised as the solutions prepared by Daivis are identical to the solutions prepared in this work in both molar mass and preparation. These data therefore offer an excellent "control" to the data obtained in this work, with any discrepancy from the PGSE NMR data indicating a deviation from D_S, the self diffusion coefficient.

During the course of this study PS and PVME mixtures were solvated in three different solvents:- toluene, carbon tetrachloride and tetrachloroethylene at different polymer mass fractions and concentrations.

Details of the series of samples investigated are given below

Series Name	Solvent	x (g/g)	Comments
*B1	C_2Cl_4	0.05	
ModB1A	C_2Cl_4	0.44	
A	C_2Cl_4	0.125	
B	C_2Cl_4	0.29	
C	CCl_4	0.05	Phase separates above 12% polymer
D	CCl_4	0.29	Phase separates above 12% polymer
E	Toluene	0.29	Very high concentration
F	Toluene	0.05	Very high concentration

Table 4.1.1 Sample series investigated

Toluene is known to be a nearly equally good solvent for PS and PVME [6] (this is almost a unique case as most polymer blends are incompatible), while

tetrachloroethylene is an equally poor solvent for both PS and PVME. The solvent carbon tetrachloride is of unequally quality for these polymers.

Table 4.1.2 gives the polymer mass and weight fractions of these solutions as prepared

Solution Name	Solvent & Mass Fraction	w_{PS}	w_{PVME}
*B1A	C_2Cl_4 x=0.05	0.00535	0.09704
*B1B		0.00203	0.03685
*B1C		0.00501	0.04882
*B1D		0.01052	0.19090
*B1E		0.00866	0.15711
MODB1A1	C_2Cl_4 x=0.44	0.0588	0.10540
MODB1A2		0.03646	0.06535
MODB1A3		0.01781	0.03197
MODB1A4		0.00918	0.01646
A1	C_2Cl_4 x=0.125	0.08598	0.60185
A2		0.0699	0.48994
A3		0.05867	0.41067
A4		0.04506	0.31541
A5		0.02946	0.20625

A6		0.01455	0.10182
A7		0.00905	0.06332
B1		0.16471	0.39887
B2	C_2Cl_4	0.12220	0.29595
B3	x=0.29	0.9682	0.23450
B4		0.05981	0.14485
C1		0.02492	0.47241
C2		0.01177	0.22319
C3		0.00816	0.15460
C4		0.02452	0.46475
C5		0.01889	0.35816
C6		0.00634	0.12010
C7	CCl_4	0.00536	0.10163
C8	x=0.05	0.00409	0.07751
C9		0.00310	0.05869
C10		0.00206	0.03910
C11		0.00102	0.01931
C12		0.00731	0.13848

C13		0.00651	0.12342
C14		0.00530	0.10053
C15		0.00579	0.10970
D1		0.01301	0.03185
D2		0.09915	0.24273
D3		0.3578	0.08760
D4		0.03013	0.07376
D5	CCl_4	0.02355	0.05767
D6	x=0.29	0.01769	0.04332
D7		0.01181	0.02890
D8		0.00633	0.01551
D9		0.03613	0.08846
D10		0.03193	0.07816
D11		0.11710	0.03396
E1		0.20712	0.50717
E2		0.19089	0.46732
E3	Toluene	0.17389	0.42570
E4	x=0.29	0.16491	0.40372

E5		0.15084	0.36927
E6		0.13176	0.32257
E7		0.09934	0.24320
F1		0.03609	0.68543
F2	Toluene	0.03295	0.62581
F3	x=0.05	0.02911	0.55291
F4		0.02776	0.52725

Table 4.1.2 Solution series mass and weight fractions

4.1.2 Sundry information about results

All solutions were run under identical conditions, having first been given a period to come to thermal equilibrium, varying from one day to one week depending on the viscosity of the solution in question. Solutions were kept at 25°C, and if necessary data were adjusted to 30°C using the method previously discussed by Daivis [5].

Some of the samples were unstable and others close to phase separation, notably the carbon tetrachloride solutions suffered phase separation at concentrations greater than 12% polymer weight fraction.

According to the theories of Benmouna and Borsali et al presented in chapter 2 at least three parameters can effect the diffusion coefficient D_I (which is the observed diffusion found using DLS), mass fraction, x, interaction parameter, χ, and molar mass of the polymers, M. Section 4.2.1 investigates the variation of D_I with mass fraction, section 4.2.2 investigates the variation of D_I with interaction parameter by presenting data from solutions with similar mass fraction solutions but with different solvents. Lastly section

4.2.3 investigates the variation of D_I with molar mass (by utilising data from Daivis [5] and Martin [67])

This work seeks to extend on the work already completed by Daivis, hence this work utilises the same methods of polymer fractionation and solution preparation. This sometimes meant abbreviated solution runs, so as not to repeat work already completed, but with sufficient overlap to ensure continuity of results. We have included some of Daivis's results [5] from his work on the system 110 000 Dalton PS/ 110 000 Dalton PVME in toluene and his work with 929 000 Dalton PS/ 110 000 Dalton PVME in the solvents toluene and carbon tetrachloride as reference data

4.2 Results and Discussion

4.2.1 Investigation of the variation of D_I with Mass Fraction

The Borsali Benmouna theory applied to ternary polymer solutions formed with an equally good solvent, such as toluene with the PS and PVME, suggests that the diffusion coefficient should vary as

$$D_I \propto D_S[1-2x(1-x)\phi\chi NP(q)] \qquad (4.2.1)$$

(see equation 2.4.13). Hence if the polymer molar mass and the solution concentration are constant then it is expected that

$$D_I \propto D_S[1-\alpha x(1-x)\chi\phi] \qquad (4.2.2)$$

where α is a constant. Similar expressions can be obtained for an equally poor solvent (equations (4.2.3) and (4.2.4) and for a solvent of unequal quality (equation (4.2.5)). The form of these equations suggest that D_I/D_S should decrease with increasing concentration. Furthermore this decrease should be dependant on the Flory interaction parameter χ except in the last case (which must be viewed with extreme circumspection (see section 2.4)). In all cases a dependency on the mass fraction is shown. This section investigates this variation with x, while section 4.2.2 investigates the variation with χ.

Using the data collected we can compare the different mass fractions (in this work normally 0.05, 0.12 and 0.29) for each of the different solvent systems, keeping the molar mass constant at 110 000 Daltons for both PS and PVME. Graphing these results we can then directly correlate if the mass fraction affects the diffusion coefficient D_I. obtained by DLS. We can then compare these results with the self diffusion coefficient D_S of 110 000 Dalton PS/ 110 000 Dalton PVME/ toluene system found by PGSE NMR by Daivis.

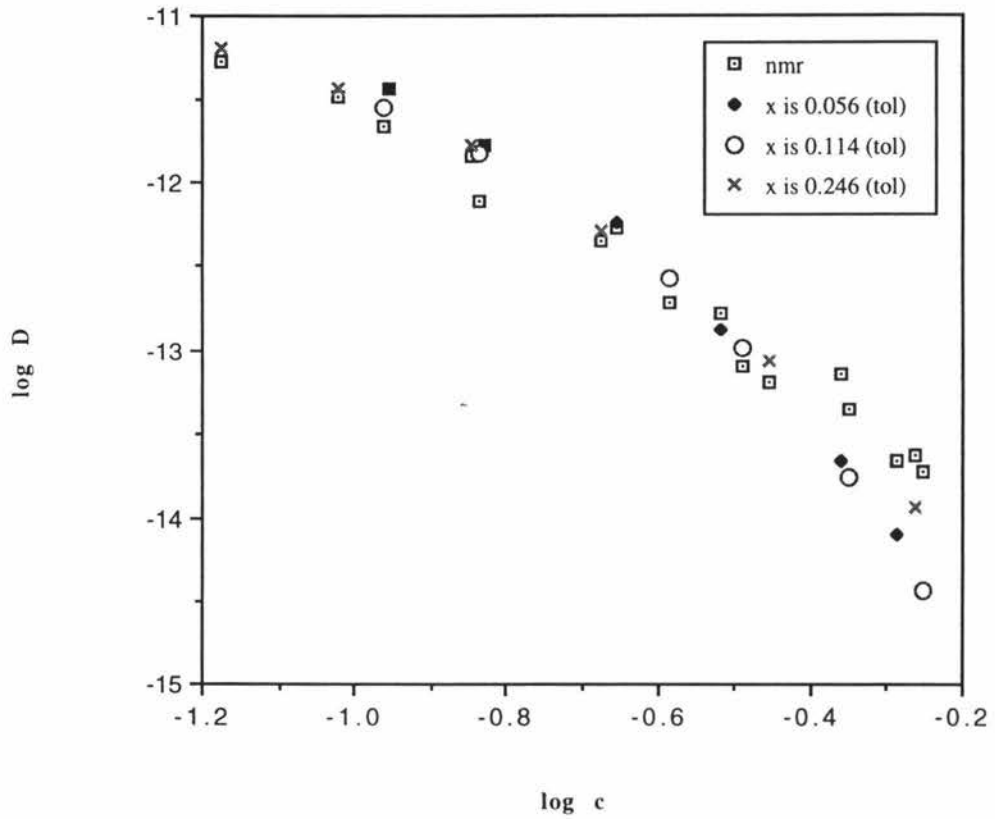

Figure 4.2.1 The concentration dependence of the diffusion coefficient of PS-PVME-toluene solutions of various mass fractions obtained from DLS experiments by Daivis. Both the PVME and the PS had molar masses of 110 000 $gmol^{-1}$. PS self diffusion coefficients of the same solutions probed by PGSE NMR are also shown. Relative sizes of the symbols indicate the errors associated with each datum point. Diffusion coefficients are presented in units of m^2s^{-1} while the concentration is expressed in kgm^{-3}.

The results are shown in figures 4.2.2 and 4.2.3 they closely mimic the form of the results of Daivis's shown in figure 4.2.1.

In figure 4.2.1 the apparent DLS diffusion coefficients closely follow the PGSE NMR polystyrene self diffusion coefficient up to a concentration of approximately 0.3 kgm^{-3}. Daivis speculated that the divergence at greater concentration was due to weak aggregation affects (since DLS is more sensitive to aggregation than PGSE NMR). He

suggested that the sample preparation procedure may have been responsible for the formation of these aggregates. "It is possible that strongly entangled clumps of polymer were formed during the evaporation of the solvent. These would have disentangled much more slowly than the surrounding solution in the concentrated samples."

The Benmouna theory predicts the dependence of D_I on x and χ for solutions formed with an equally bad solvent (ie. tetrachloroethylene). The diffusion coefficient should vary according to equations (2.4.74) and (2.4.71) with the form

$$D_I \propto D_S[1-\beta x\chi^2\phi] \quad - \quad \chi/\upsilon \to 0 \qquad (4.2.3)$$

or $$D_I \propto D_S[1-\gamma(x(1-x))^{1/2}\chi\phi] \quad x\chi^2/\upsilon^2 \text{ large} \qquad (4.2.4)$$

where β and γ are constants. Both predict a linear dependence on x if the polymer molar mass and solution concentration are held constant. These results are shown in figure 4.2.2.

Since the values of x investigated in this work are small (or in the case of tetrachloroethylene x=0.44 the largest value of ϕ is small) it is expected the predicted discrepancy of D_I with x as the concentration increases should be small (with data from the same solvent). They should follow the "master" curve of the PGSE NMR data, with gradual divergence (lowering) as the concentration increases. This is indeed the case, with the tetrachloroethylene data (figure 4.2.2) these recapitulated the toluene data (figure 4.2.1) almost exactly, with no noticeable variation on x. The carbon tetrachloride data however show considerable difference from the "master" curve of the PGSE NMR diffusion coefficient, however they too fail to show any significant dependence on x.

The diffusion coefficients obtained for the tetrachloroethylene solution with x equal to 0.29 are anomalous - uniformly too large compared with their toluene counterparts. However at low concentration this data set does converge to a "common" infinite dilution diffusion coefficient D_O. It is apparent that a systematic error has affected this

data set, probably the concentrations have been overstated. These results have been included in this section for completeness only.

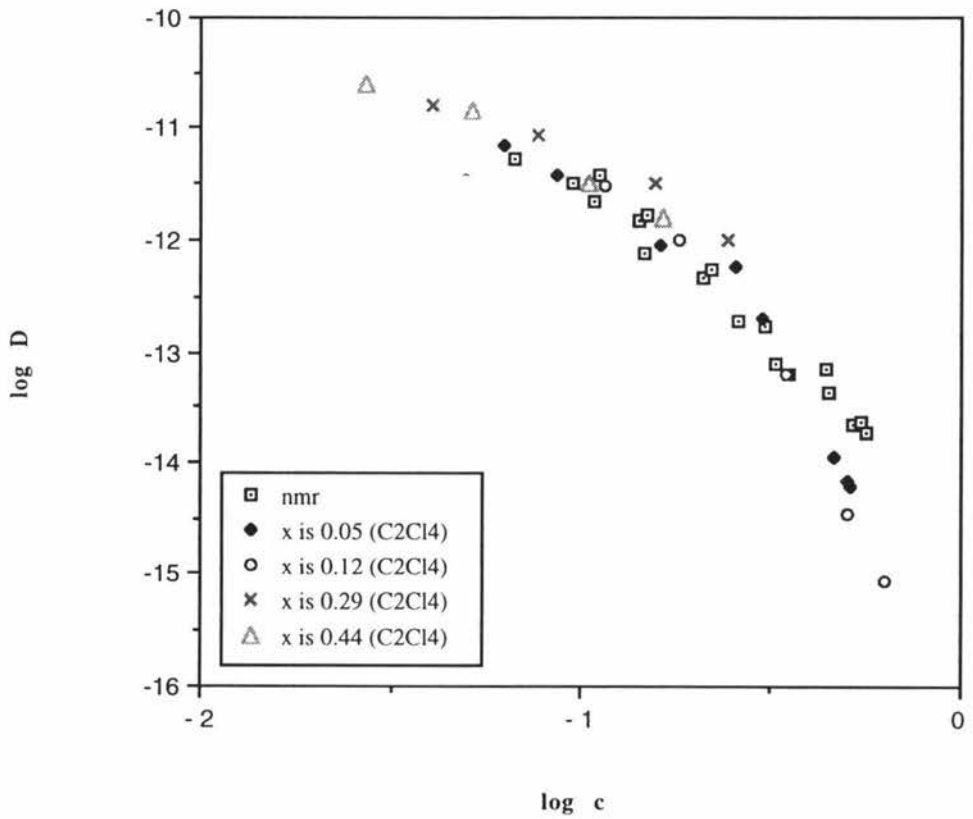

Figure 4.2.2 The concentration dependence of the diffusion coefficient of PS-PVME-tetrachloroethylene solutions of various mass fractions obtained from DLS experiments. Both the PVME and PS have molar masses of 110 000 $gmol^{-1}$. PS self diffusion coefficients of the system shown in figure 4.2.1, probed by PGSE NMR are also shown. Relative sizes of the symbols indicate the errors associated with each datum point. Diffusion coefficients are presented in units of m^2s^{-1} while the concentration is expressed in kgm^{-3}.

The Benmouna theory also predicts that for an unequal quality solvent (ie. carbon tetrachloride) D_I varies according to equation (2.4.76) with the form

$$D_I \propto D_S[1-\delta(x-x^2)\phi] \qquad (4.2.5)$$

where δ is a constant and the polymer molar mass and the solution concentration are not varied. The results associated with this theoretical prediction are shown in figure 4.2.3

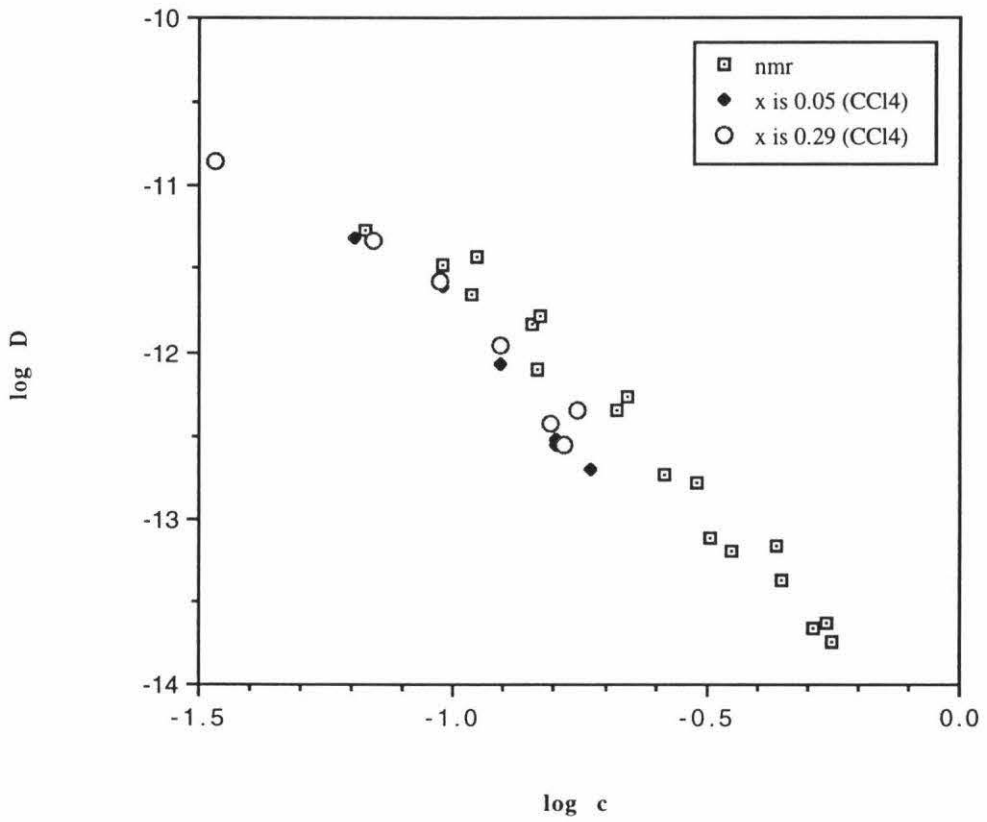

Figure 4.2.3 The concentration dependence of the diffusion in PS-PVME-carbon tetrachloride solutions of various mass fractions obtained from DLS experiments. Both PVME and PS had molar masses of 110 000 $gmol^{-1}$. PS self diffusion coefficients of the system shown in figure 4.2.1, probed by PGSE NMR are also shown. Relative sizes of the symbols indicate the errors associated with each datum point. Diffusion coefficients are presented in units of m^2s^{-1} while the concentration is expressed in kgm^{-3}.

The Benmouna theory also predicts that the low concentration apparent diffusion coefficient should approach the limit of the self diffusion coefficient of the trace polymer in the solvent of interest. However as figures 4.2.1-4.2.3 show the apparent diffusion coefficients tend toward the polystyrene self diffusion coefficient in a toluene solvent. This indicates that the solvent is not the "limiting" factor in the diffusion process (any solvent would do), but that the real inhibitor of diffusion in the solution is the difference between the component polymer's affinities (χ's) for one another and the solvent. This phenomena has been observed previously by Daivis [5] who noted, "it is a remarkable feature of these results that the PS self diffusion coefficient, ... is the same in PVME and toluene as it is in benzene and (in) carbon tetrachloride." More of this phenomena will be discussed in section 4.2.2

Physically, it is interesting to note that the carbon tetrachloride solutions phase separated at approximately 12% polymer weight fraction, while those of the toluene and the tetrachloroethylene solutions remained in a single phase until much higher polymer concentrations (approximately 65-70%) at which time they appeared to form glassy solids. This may offer a physical explanation of the deviation of the DLS observed diffusion coefficient from that of the PGSE NMR diffusion coefficient. The beginning of the formation of glassy solids or of the formation of two phases would effectively slow the diffusion of the probe polymer through the solution. The formation of networks effectively entangling and slowing down the probe polymer within the solution. More of this phenomena will be discussed in section 4.2.4

4.2.2 Investigation of the variation of D_I with the Flory Polymer-Polymer Interaction Parameter, χ

This work utilised the same (or similar) mass fractions across the three different polymer/solvent systems, so the data can be used to determine the effect of different χ's and $\Delta\chi$'s (where $\Delta\chi = |\chi_{13} - \chi_{23}|$ and χ_{13} is the interaction parameter for PS in the solvent and χ_{23} is the interaction parameter of PVME in the same solvent) on the DLS diffusion coefficient.

Patterson and Su [68] give values for the interaction parameters of both PS and PVME in various solvents at 40°C obtained by gas-liquid chromatography. They give the following results

Solvent	χ_{PS}	χ_{PVME}	$\Delta\chi$
Toluene	0.19	0.14	0.05
CCl_4	0.29	0.06	0.23
C_2Cl_4	0.36	0.34	0.02

Table 4.2.1 Interaction parameters for PS and PVME in various solvents

Patterson [69] also predicts that the compatibility of polymers not only reflects the interaction between the polymers themselves (ie. χ_{12}) but also any difference between the interaction between the polymers with the solvent. Since toluene has a similar interaction parameter values for both PS and PVME (and these values are low) it is an equally good solvent. Carbon tetrachloride is of unequal quality for the polymers and tetrachloroethylene is equally poor for the polymers.

Figures 4.2.4-4.2.6 show solutions formed with equal quality solvents have D_I nearly equal to D_S. But solutions formed with unequal quality solvents have D_I considerably less than D_S and of course such solutions suffer phase separation at lower concentration.

Figures 4.2.1 and 4.2.2 from section 4.2.1 indicate that it is not the value of χ that drives the mechanism of D_I divergence from D_S as both graphs show equivalent divergence from the polystyrene self diffusion coefficient data. From the relative magnitudes of the interaction parameter for each of these solutions we would expect the tetrachloroethylene solution to show a greater decrease in the diffusion coefficient when compared to its toluene equivalent. Clearly this is not the case.

It is tempting to forward the hypothesis that the difference between the interaction parameters for each of the polymers and the solvent has more influence on the diffusion coefficient and the stability of the solution than the actual value of the Flory polymer-polymer interaction parameters, since figure (4.2.3) shows that the carbon tetrachloride solvent system has a dramatically decreased the diffusion coefficient with increasing concentration. Since the magnitude of the Flory parameter is of the same size as that for the tetrachloroethylene interaction parameter we would expect similar curves for each of these two systems, however figures 4.2.1-4.2.3 show that toluene and tetrachloroethylene give similar results, while the carbon tetrachloride data deviates. One must urge caution in this hypothesis however as the validity of the theory for a solvent-polymer system with unequal Flory interaction parameters is "suspect." This theory also predicts the diffusion coefficient has no χ dependence (see section 2.4).

As previously noted, Zeeman and Patterson [69] have shown that the compatibility of polymers not only reflects the interaction between the polymers themselves (ie. χ_{12}) but also any difference between the interaction between the polymers with the solvent ($\Delta\chi$), ie. the solvent does not present a barrier to diffusion, but the polymer-solvent interaction (or attraction) does. As figures 4.2.1-4.2.3 show the apparent diffusion coefficients tend toward the polystyrene self diffusion coefficient in a toluene solvent. This indicates that the solvent is not the "limiting" factor in the diffusion process (any solvent would do), but that the real inhibitor of diffusion in the solution is the difference between the component polymers attractions (χ's) for one another and the solvent. This phenomena has been observed previously by Daivis [5] as noted in section 4.2.1 of this work. The results presented in figures 4.2.4-4.2.6 accentuate the above findings, each solution at the same mass fraction appears to converge at infinite dilution to a common D_O. While the difference in the affinity each polymer has for the solvent affects the fall in the apparent diffusion coefficient and the eventual point of "solidification" (glass transition or phase separation) of the solutions.

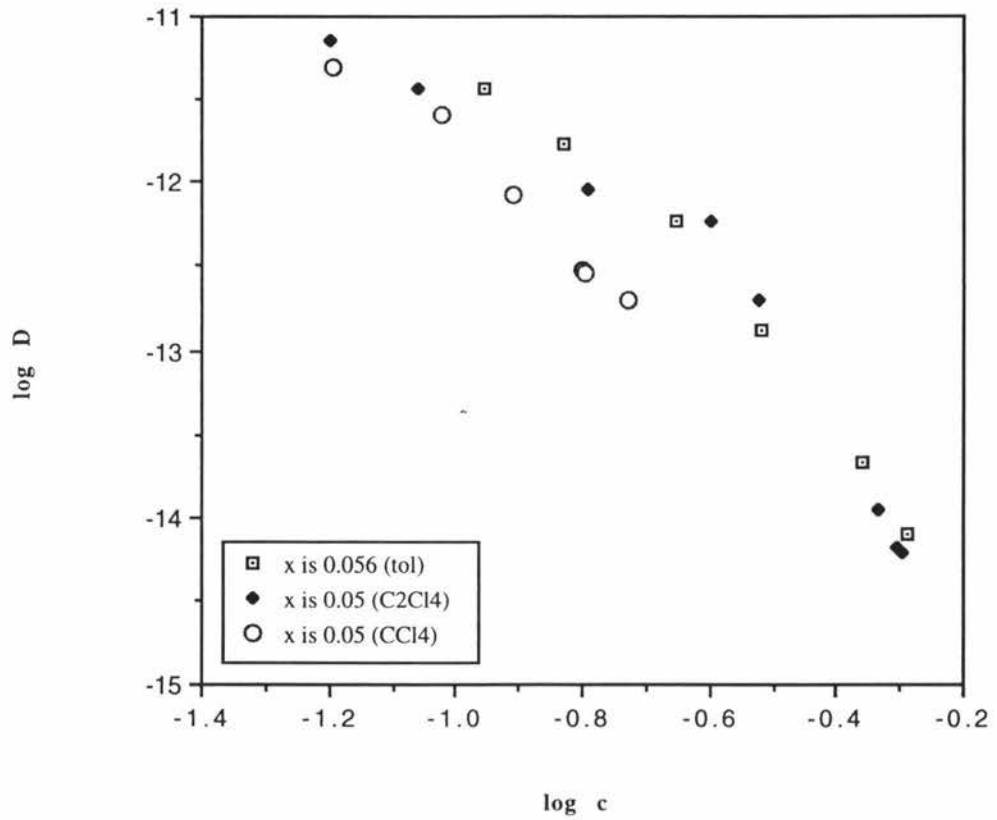

Figure 4.2.4 The concentration dependence of the diffusion coefficient found by DLS in the PS-PVME system with the solvents toluene, tetrachloroethylene and carbon tetrachloride at a polymer mass fraction of 0.05. PVME and PS both had a molar mass of 110 000 $gmol^{-1}$. Relative sizes of the symbols indicate the errors associated with each datum point. Diffusion coefficients are presented in units of m^2s^{-1} while the concentration is presented in kgm^{-3}.

The figures 4.2.4-4.2.6 also accentuate the slightly greater decrease of tetrachloroethylene with greater concentration than the its toluene counterpart. This may be in part due to the larger individual polymer solvent interaction found in the tetrachloroethylene solutions. This greater individual polymer solvent interaction parameter would tend to cause the solvent to repel the individual polymer which would then form "clusters" of "like affinity" with the other polymers, similar to soap micelles, as the concentration increases, to reduce the strength of the repulsive interaction with

the solvent. This would result in a localised (to the "micelle") slowing of the polymer diffusion coefficient as the polymer "cluster" then diffuses through the solution. Since DLS is sensitive to aggregative effects, it should differentiate between a "micelle" solution and similar "non-micelle" solution and return a reduced diffusion coefficient at higher concentration.

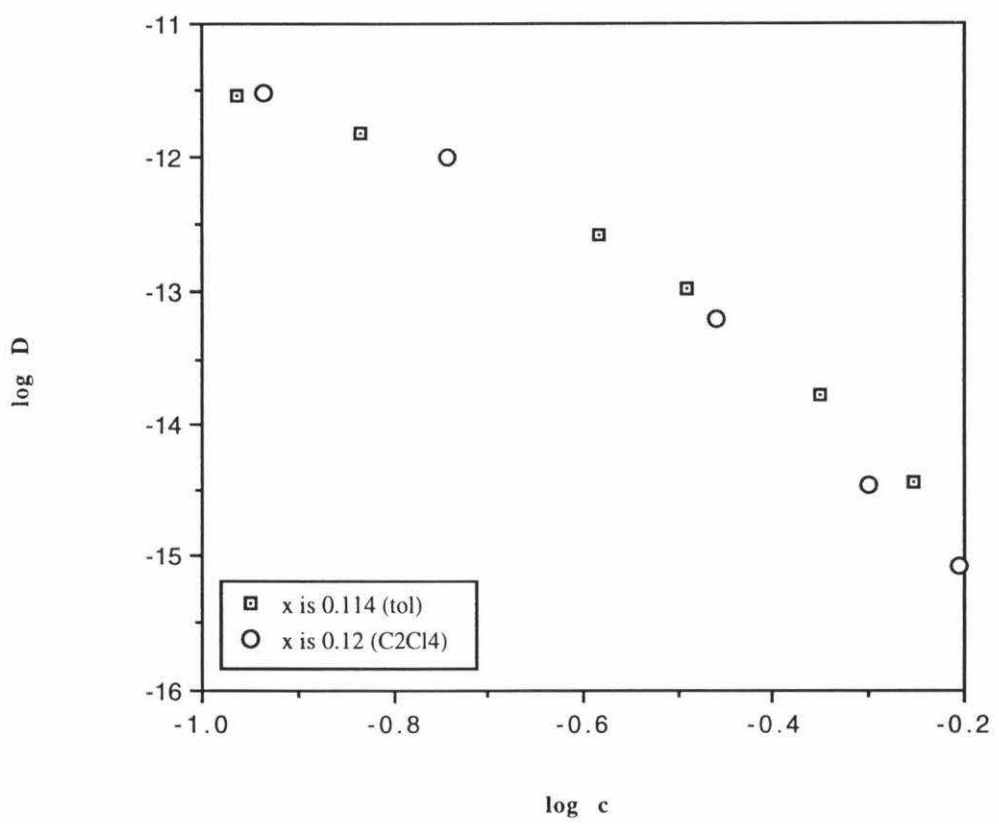

Figure 4.2.5 The concentration dependence of the diffusion coefficient obtained by DLS for the PS-PVME system with the solvents toluene and tetrachloroethylene at a polymer mass fraction of 0.12. PVME and PS both had a molar mass of 110 000 $gmol^{-1}$. Relative sizes of the symbols indicate the errors associated with each datum point. Diffusion coefficient is presented in units of m^2s^{-1} while the concentration is expressed in kgm^{-3}.

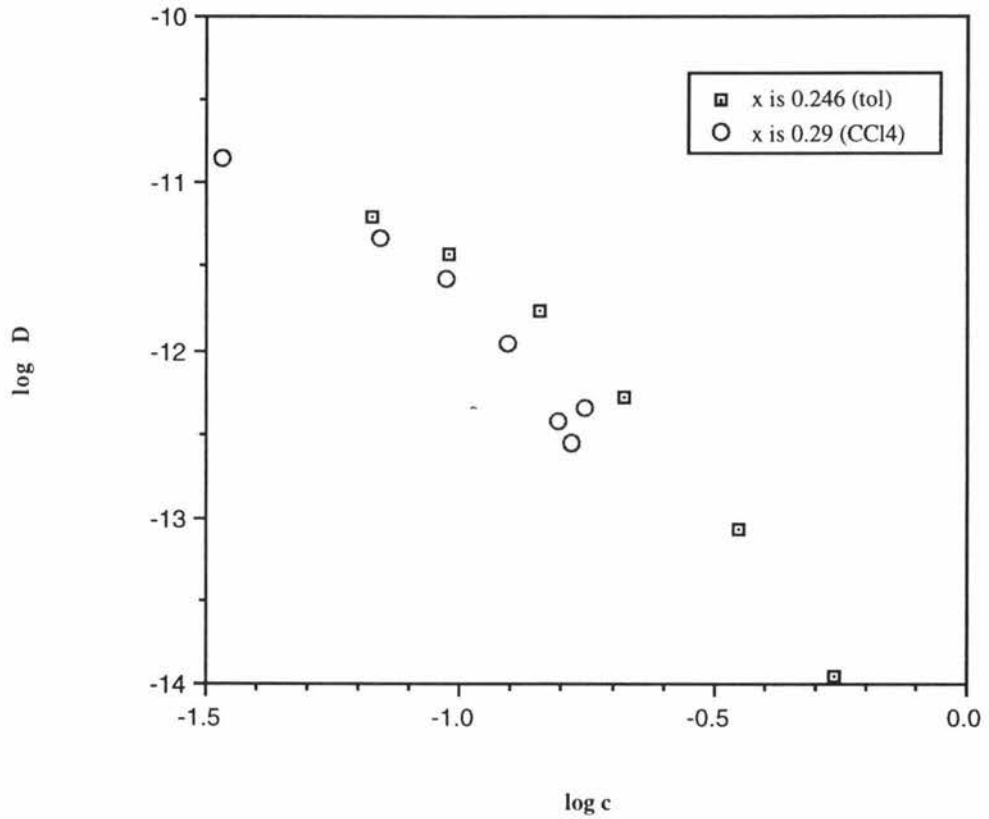

Figure 4.2.6 The concentration dependence of the diffusion coefficient found by DLS for the PS-PVME system with the solvents toluene and carbon tetrachloride at a polymer mass fraction of 0.29. PVME and PS both had a molar mass of 110 000 $gmol^{-1}$. Relative sizes of the symbols indicate the errors associated with each datum point. Diffusion coefficient is presented in units of m^2s^{-1} while the concentration is expressed in kgm^{-3}.

4.2.3 Investigation of the variation of D_f with Molar Mass

Daivis [5] produced data on the two systems toluene/PS/PVME and carbon tetrachloride/PS/PVME where PS has a molar mass of 929 000 Dalton and PVME had a molar mass of 102 000 Dalton (pre-fractionation-see chapter 3 of this work). These data and the data of Martin [67] when compared to the data of this work, allows the investigation of increasing the molar mass on the apparent diffusion coefficient.

M is expected to vary according to the relationship

$$\frac{D_1}{D_2} \propto \frac{M_2}{M_1} \qquad (4.2.6)$$

where D is the diffusion coefficient and M is the molar mass.

According to equation (4.2.6) the relative size of the diffusion coefficient obtained with the 110 000 Dalton PS solutions should be approximately nine times as large as those Daivis obtained with the 929 000 Dalton PS solutions. The apparent diffusion coefficients of the four systems are compared with the polystyrene self diffusion coefficient found by PGSE NMR (using data from Davis's 110 000 Dalton PS/ 110 000 Dalton PVME/toluene system).

As expected from theory (equation (4.2.6)), the 929 000 Dalton PS/ 110 000 Dalton PVME solutions are approximately one ninth of the size of the corresponding 110 000 Dalton PS/ 110 000 Dalton PVME solutions

The results given in figure 4.2.8 show the carbon tetrachloride data set has an interesting tendency to drop away with increasing concentration from the corresponding 110 000 Dalton PS/ 110 000 Dalton PVME/ toluene data set, this not being matched by the 929 000 Dalton PS/ 110 000 Dalton PVME/ carbon tetrachloride data set.

We may consider two possible sources of this deviation. The smaller (and more mobile) polymeric strands of the 110 000 Dalton PS are in transition to a new (slower) type of motion (ie. Rouse type to reptation type). Also it may be postulated that the concentration of the 929 000 Dalton PS solution set was not sufficiently large for the mechanism which restricts the motion of the 110 000 Dalton PS through the solution to become apparent in the 929 000 Dalton PS solution series (as the maximum concentration of these samples is less than that of the 110 000 Dalton PS solution at which the 110 000 Dalton PS solution starts to significantly deviate from the PGSE NMR results (D_S)). It is expected that any "common" mechanism slowing of diffusion in both solutions should occur first in the higher molar mass solution as the longer chain

length of the higher molar mass probe would lead to an enhancement of the "slowing" effect.

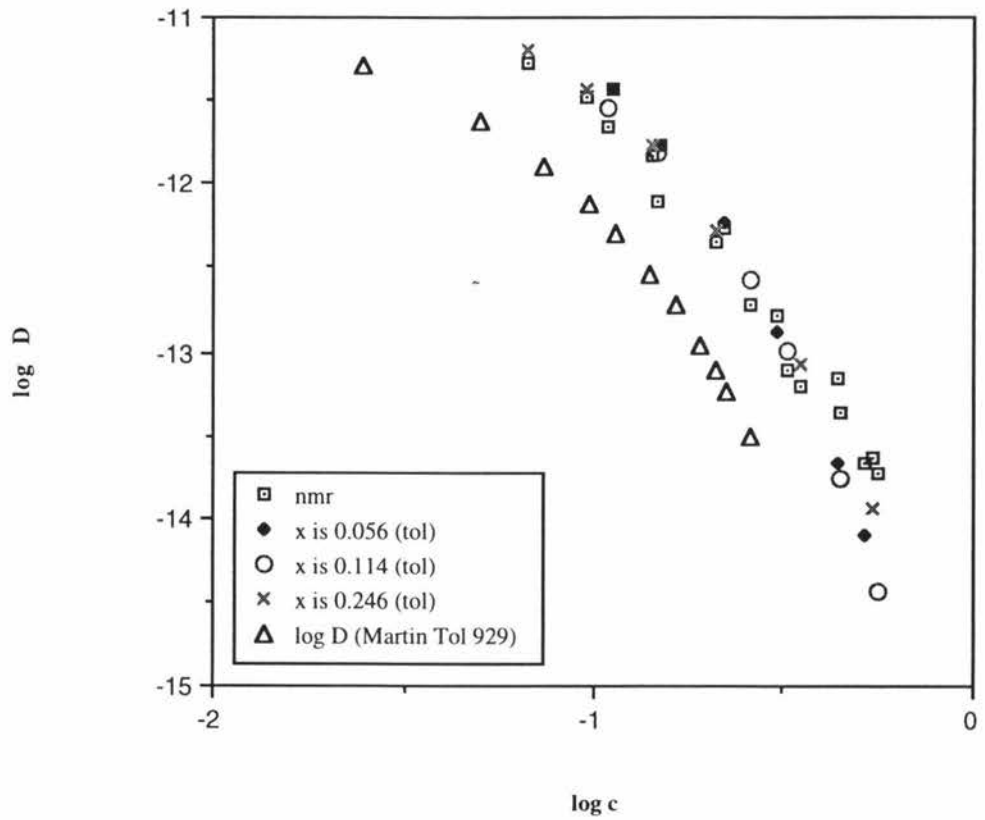

Figure 4.2.7 The concentration dependence of the diffusion coefficient obtained by DLS for the PS-PVME system with the solvent toluene at various polymer mass fractions and molar masses. PVME had a molar mass of 110 000 $gmol^{-1}$ while PS is varied between 110 000 and 929 000 (results from Daivis and Martin). Several solution runs of 110 000 $gmol^{-1}$ PS/PVME in toluene (with different x values) from this work were combined to give sufficient data (as D_I has been shown to have little variance with x) to aid evaluation of the discrepancy between $D_{I\,(929\,000\,)}$ and $D_{I\,(110\,000)}$. Relative sizes of the symbols indicate the errors associated with each datum point. Diffusion coefficients are presented in units of m^2s^{-1} while the concentration is expressed in kgm^{-3}.

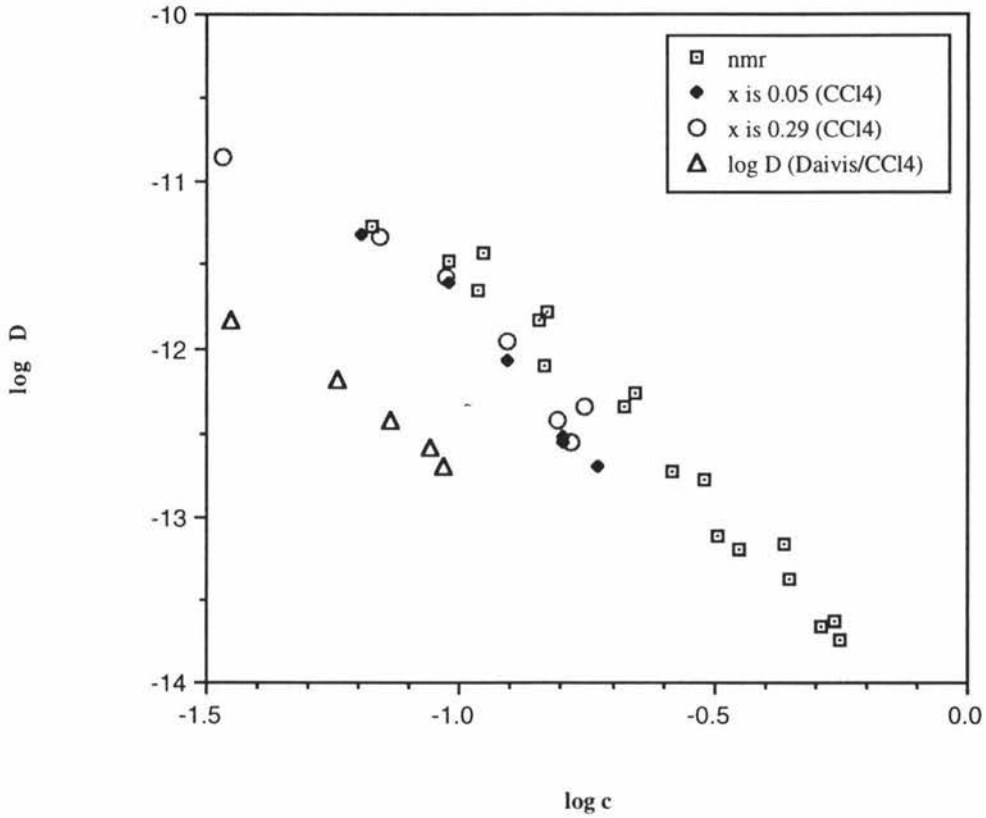

Figure 4.2.8 The concentration dependence of the diffusion coefficient obtained by DLS for the PS-PVME system with the solvent carbon tetrachloride at various polymer mass fractions and molar masses PVME had a molar mass of 110 000 $gmol^{-1}$ while PS is varied between 110 000 and 929 000 (929 000 $gmol^{-1}$ PS results from Daivis [5]). PS self diffusion coefficients of the system shown in figure 4.2.1, probed by PGSE NMR are also shown. Several solution runs of 110 000 $gmol^{-1}$ PS/PVME in carbon tetrachloride (with different x values) from this work were combined to give sufficient data (as D_I has been shown to have little variance with x) to aid evaluation of the discrepancy between $D_{I\,(929\,000)}$ and $D_{I\,(110\,000)}$. Relative sizes of the symbols indicate the errors associated with each datum point. Diffusion coefficients are presented in units of m^2s^{-1} while the concentration is expressed in kgm^{-3}.

The 110 000 PS/ 110 000 PVME/carbon tetrachloride solutions tendency to phase separate near the endpoint of these solution runs and the result discussed in the next

section (section 4.2.4) tend to support the insufficient concentration conclusion, however further probing with higher concentration 929 000 Dalton PS/ 110 000 Dalton PVME/ carbon tetrachloride solutions would be necessary to confirm this.

In figure 4.2.9 we show Martin's [67] data for the toluene system of 990 000 Dalton PS/ 110 000 Dalton PVME. This is contrasted by the equivalent carbon tetrachloride data and data for 110 000 Dalton PS /110 000 Dalton PVME system in both toluene and carbon tetrachloride. This highlights the 1/9th relationship of the molar mass/diffusion coefficient, but also invites questions as to the behaviour of the 929 000 Dalton probe PS in the carbon tetrachloride solvent. We can clearly see that the 110 000 Dalton PS system in carbon tetrachloride appears to have a similar D_O as the 110 000 Dalton PS system in toluene, yet the carbon tetrachloride data for this system fall rapidly from the toluene solution data with increasing polymer concentration.

The "929 000 Dalton PS" systems follow the basic shape of the PGSE NMR data, indicating similar constraint release mechanisms are at work in the solutions. However the 929 000 Dalton PS system in carbon tetrachloride shows a considerable decrease in the diffusion coefficient across similar concentrations as the Martin system. This systematic difference in diffusion coefficients across the concentration range available does not fit the pattern seen in the 110 000 Dalton PS data.

Daivis [5] gives possible reasons for this decrease in the apparent diffusion coefficient as being aggregation effects discussed in the proceeding section and also the slight difference in molar masses of the PS studied. According to equation (4.2.6) the difference in the molar masses of the Martin and Daivis systems would tend to increase diffusion coefficients of the carbon tetrachloride data, this however is not seen. Daivis's suggestion of aggregation would tend to "evenly" decrease the apparent diffusion coefficient across the range of concentration, with each aggregate acting as a polymer of larger molar mass (and hence slower diffusion).

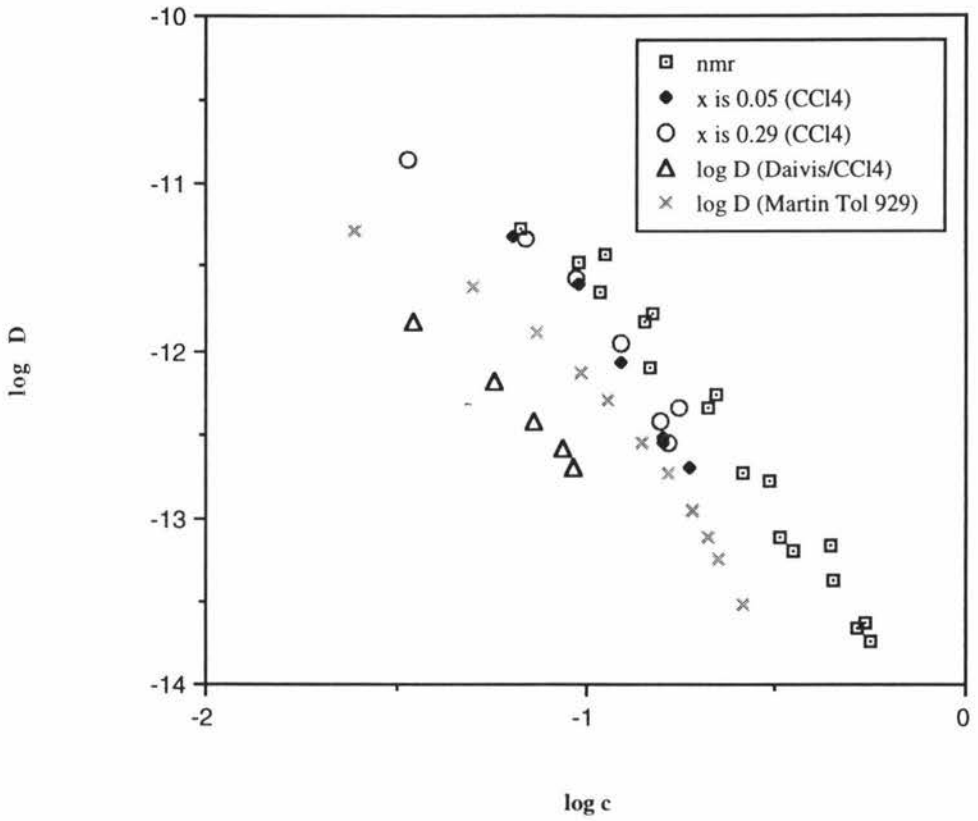

Figure 4.2.9 The concentration dependence of the diffusion coefficient found by DLS in the PS-PVME system for carbon tetrachloride and toluene at various polymer mass fractions and molar masses. PVME had a molar mass of 110 000 $gmol^{-1}$ while PS is varied between 110 000 and 929 000 (929 000 $gmol^{-1}$ PS results from Daivis [5]). PS self diffusion coefficients of the system shown in figure 4.2.1, probed by PGSE NMR are also shown. Several solution runs of 110 000 $gmol^{-1}$ PS/PVME in carbon tetrachloride (with different x values) from this work were combined to give sufficient data (as D_I has been shown to have little variance with x) to aid evaluation of the discrepancy between $D_{I\,(929\,000)}$ and $D_{I\,(110\,000)}$. Relative sizes of the symbols indicate the errors associated with each datum point. Diffusion coefficients are presented in units of m^2s^{-1} while the concentration is expressed in kgm^{-3}.

Each of the carbon tetrachloride polymer solutions (110 000 Dalton PS/ 110 000 Dalton PVME) appear to have critical solution points at approximately 12% polymer weight fraction. Each solution appears to phase separate into separate regions or phases. Interestingly the Benmouna extension near phase separation (section 2.4.3 case A) predicts a critical slowing down of the diffusion coefficient near phase separation. Equation (2.4.94) indicates that

$$D_I = D_O\left[1-\frac{\chi}{\chi_C}\right]+\frac{3}{4}\frac{k_BT}{6\pi\eta\xi} \qquad (4.2.7)$$

As the solution reaches the critical solution concentration the contribution from the first term slows down, this leads to a critical slowing down of the diffusion coefficient near phase separation to a value $D_I = \frac{3}{4}\frac{k_BT}{6\pi\eta\xi}$. Figures 4.2.7-4.2.9 clearly show that this does not happen.

Another prediction of the Benmouna theory is that D_I should be q dependent. This aspect of the theory was unable to be verified as these solutions were only run at 90° so as to give the largest signal, since the photon count and resulting diffusion coefficients obtained were very small.

4.2.4 Investigation into the discrepancy between D_I and D_S at high polymer concentrations

Lastly we have sought to extend the high concentration data Daivis obtained for the 110 000 Dalton PS/ 110 000 Dalton PVME/ toluene system. Daivis noted that above a volume fraction of approximately 0.4 the DLS diffusion coefficient (D_I) appears to fall more rapidly than the diffusion coefficient found by PGSE NMR (D_S). This last effect has not been resolved sufficiently to enable explanation of this observed phenomena.

Using the special apparatus described in section 3.2.6, high concentration solutions of samples E and F were loaded into NMR tubes. These samples were so viscous that on several runs the DLS apparent diffusion coefficient was too small to be measured.

Daivis [5] has already noted that the system toluene/PS/PVME has little or no variation with increasing x, hence the two solution sample runs (x=0.05 and 0.29) were combined to provide sufficient data for analysis. These were then added to Daivis's existing DLS low to middle concentration data for the same system, to give a high concentration extension of the known behaviour of this system.

Daivis attributed the discrepancy between D_I and D_S to aggregation effects, as DLS is more sensitive to aggregation than PGSE NMR because the average diffusion coefficient obtained from DLS is the z-average where as that for PGSE NMR is the weight average.

Figure 4.2.10 confirms Daivis's original data and indicate a rapid drop off in diffusion through the solution.

The "slowing down" of the diffusion coefficient could be the transition to another type of motion (ie. Rouse to reptation). Lodge and Wheeler [70] have noted a cross over from Stokes-Einstein to reptation polymer diffusion for the system PVME/ *o*-flourotoluene/3-Arm-Star PS at high concentration. They came to the conclusion that "reptation must be considered as a significant contribution to diffusion of linear polymers in thoroughly entangled solutions."

The reptation model suggests that the concentration scaling exponent should be -1.75 for a polymer in a good solvent and -3 for a polymer in a theta solvent. Daivis [5] was also able to show that the blob model also predicts a change in the scaling behaviour of the observed diffusion coefficient from DLS from -1.75 to -3 as the concentration increases.

Regression of log D vs. log c for the DLS diffusion data of Daivis, without the last five data points reveals a slope of -11±4, while regression of the data collected in this work reveals a slope of -14.9±0.7, which fits with the previously observed slope increase with increasing concentration of Wesson [71]. This indicates that reptation is not the

significant method of diffusion in either low (below a volume fraction of 0.4) or high concentration.

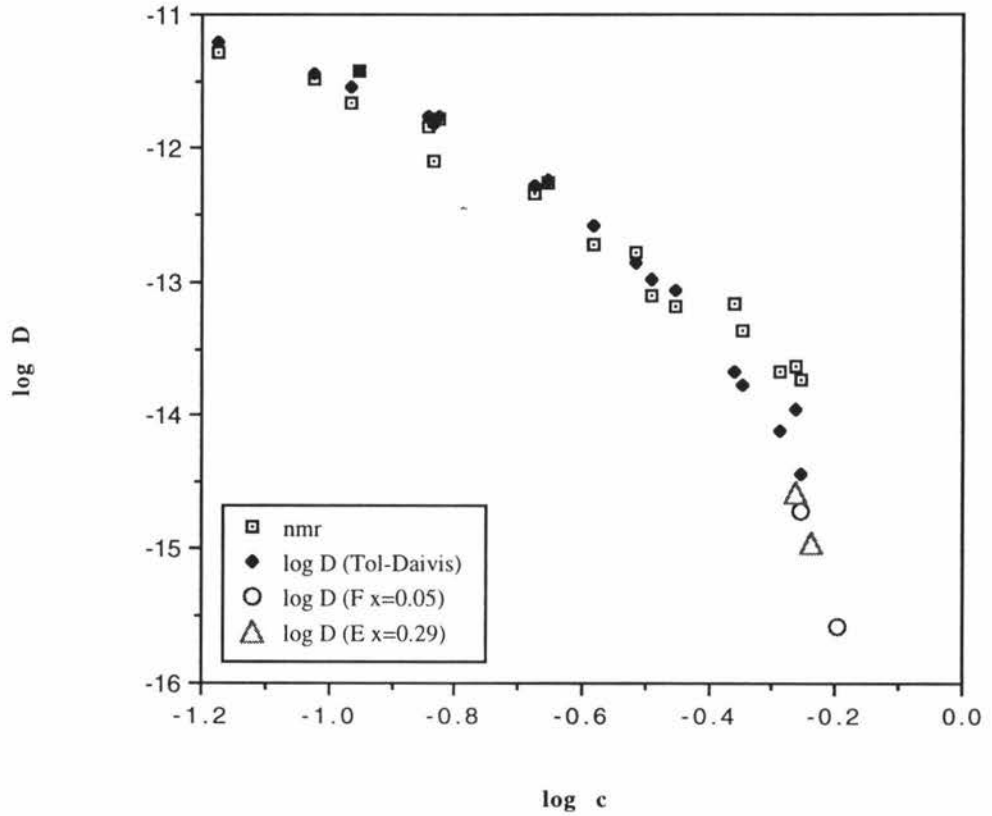

Figure 4.2.10 High concentration extension of Daivis's 110 000 $gmol^{-1}$ PS / 110 000 $gmol^{-1}$ PVME in toluene system. PS self diffusion coefficients of Daivis's solution probed by PGSE NMR are also shown. Relative sizes of the symbols indicate the errors associated with each datum point. Diffusion coefficient is presented in units of m^2s^{-1} while the concentration is expressed in kgm^{-3}.

Clearly the polymer was severely restricted, possibly due to localised networks forming close to the onset of the glass transition. These latter solutions were nearly solidlike hence the onset of glass transition and its associated local viscosity effects is the most likely explanation available for the observed rapid decrease in diffusion.

Several other results from literature are interesting to note. Experimental data in the semi dilute region have yielded some apparently conflicting results. Leger et al [72] measured D for the system polystyrene in benzene by forced Rayleigh scattering and found $D \propto M^{-2}c^{-1.75}$ as predicted by scaling theory. Callaghan and Pinder [73] however report that for the system polystyrene in carbon tetrachloride using PGSE NMR to obtain D, found that while log D vs. log c curves exhibit a slope of approximately -1.75 at concentrations above $c/c^* \approx 5$, D scales as $M^{-1.4}$. In 1984, Wesson et al reported diffusion data with a consistent M^{-2} dependence for the system polystyrene in tetrahydrofuran, also using forced Rayleigh scattering [71]. However the concentration dependence did not fit a unique power law, and the slope of log D vs. log c became increasingly negative at high concentrations, reaching values of -13.

The experimentally observed deviation from predicted scaling behaviour indicates that several different mechanisms may be at work in the diffusion of the polystyrene probe polymer through the solution matrix and these should be considered.

Constraint release is a mode of relaxation that describes the lateral freedom of a test chain due to the reptation of neighbouring chains. There is good evidence in melt data for both linear and branched polymers that constraint release can be quite significant [74][75]. Alternatively, the coupled motion of polymer chains has recently been modelled in terms of the "noodle effect," in which parts of the constraining chains are dragged along with a primary chain; this leads to a diffusion coefficient that varies as $D \propto M^{-2.5}c^{-1.5}$ [76]. As in the dilute limit, polymers may also exhibit Stokes-Einstein type diffusion, governed by the macroscopic solution viscosity and the hydrodynamic radius of the test chain. An additional diffusion process to be considered is the random Brownian motion of a particle though a field of obstacles which generate hydrodynamic screening.

Some or all these mechanisms may play some part in the diffusion of the probe polymer through the matrix of the solution as the concentration increases. These may account for some of the observed variation in solution behaviour, as one mechanism becomes

dominant in a particular concentration range (due to increasing constraints as the solution becomes more concentrated), the solution dynamics will change to take account of this (and hence plots of log D vs. log c will change slope according to the dominant mechanism operating in the solution through that concentration range). Hence we should expect to see several different slopes throughout the concentration range of a plot of log D vs log c.

Further investigation is required on several different systems with several different probe molar masses to confirm which (or if any of these) mechanisms contribute to the observed behaviour, as seen in figure 4.2.10, the most likely being Rouse-like followed by the strong entanglement owing to glass transition.

Chapter 5
Conclusion

5.1 Conclusion

Chapter 2 mainly summarised existing results which could be found in literature. In particular this chapter presented an overview of polymer solution molecular movement theory, and gave the important properties of polymers needed for this work. Also included was a brief overview of DLS theory and recent developments in this field. This was extended to give a recent theory of ternary polymer solutions developed by Benmouna and Borsali et al [1] [2] [3] [4] [34] [35] [36]. Recent work by Pinder and Daivis [5] [6] [7] [8] [9] has extended further Benmouna's theory for specific specialised cases, their work is also summarised in this chapter, along with Benmouna's own extension to ternary solutions close to phase separation and some of Pinder's recent unpublished extensions [38].

Chapter 3 described the experimental set-up and techniques involved in this work. This involved the set-up and testing of DLS equipment, the cleaning of glassware (where a new method of cleaning loosely based on that of Daivis [5] is described), and solution preparation. A new method of preparation of polymer solutions, to prevent dust contamination is described (also loosely based on that of Daivis). A new apparatus to transfer high concentration polymer solutions to 5 mm NMR tubes is shown.

Chapter 4 discloses the results of four investigations into the PS/PVME/solvent system. This system has previously been examined by Daivis [5] who made some introductory investigations. This chapter extends these investigations by examining;

a) the relationship of D_I to the mass fraction of polymer in the solution,

b) the relationship of D_I to the Flory polymer-polymer interaction parameter,

c) the relationship of D_I to the molar mass,

d) a high concentration investigation of the discrepancy between D_I and D_S found by Daivis.

The investigation into the diffusion coefficient and its variation with mass fraction were presented in section 4.2.1. The measurements made in this work confirmed Daivis [5] proposition that there is no appreciable variation of D_I with increasing mass fraction. Further it was shown that all solutions investigated in this section appear to converge to a common infinite dilution diffusion coefficient. This has previously been noted by Daivis [5] for solutions containing PS in various solvents (carbon tetrachloride and benzene). The data for PS/PVME/carbon tetrachloride diverged significantly from that of the corresponding toluene and carbon tetrachloride solutions. This was interpreted as a change in the type of polymer diffusion mechanics consistent with the approach of phase separation.

Section 4.2.2 investigated the variation of the DLS diffusion coefficient with the Flory polymer-polymer interaction parameter, χ. The data presented in this section and those presented in the proceeding section indicated that solutions formed with equal quality solvents have D_I nearly equal to D_S. But solutions formed with unequal quality solvents have D_I considerably less than D_S and that such solutions suffer phase separation at lower concentrations. These data also indicate $\Delta\chi$, the difference between polymer-solvent interaction parameters for each polymer in a ternary polymer solution have a large effect on the solution dynamics. Specifically large $\Delta\chi$ solutions (where carbon tetrachloride was the solvent for the polymers PS and PVME) resulted in "early" phase separation and reduced D_I when compared to their small $\Delta\chi$ counterparts (toluene and tetrachloroethylene solvents).

In the third section of chapter 4 the variation of D_I with molar mass was investigated. Using data from this work and comparing it to data from Daivis [5] and Martin [67] the diffusion coefficients obtained from 110 000 Dalton PS solutions were contrasted with those from "929 000" Dalton PS solutions (both using 110 000 Dalton PVME). The solvents used in these investigations were toluene and carbon tetrachloride allowing two

sets of molar mass contingent diffusion coefficient data to be produced. Both sets of data revealed the 110 000 Dalton PS solution diffusion coefficients to be approximately nine times larger than their corresponding "929 000" Dalton PS counterparts, in agreement with theory. The 110 000 Dalton PS solution in carbon tetrachloride shows a concentration dependent decrease in D_I that is not observed in the corresponding 929 000 Dalton PS solution. This is attributed to the 110 000 Dalton PS solutions closeness to phase separation and in part to the data from the 929 000 Dalton PS solution only reaching to the semi dilute region. Also the 929 000 Dalton PS solution in carbon tetrachloride solvent does not follow the data obtained for the 110 000 Dalton PS solution in carbon tetrachloride solvent, in that the infinite dilution diffusion coefficient, D_O, for the 929 000 Dalton PS in carbon tetrachloride does not tend to D_O for the same molar mass toluene solvent counterpart. This is in part attributed to aggregation effects in the data of Daivis [5]. The extension of Bemouna near phase separation predicts a critical slowing down of the diffusion coefficient obtained by DLS near pase separation. This is not observed experimentally.

Section 4.2.4 investigates the high concentration deviation of D_I from D_S. Daivis's [5] earlier work on the system 110 000 PS/ 110 000 PVME/ toluene was extended in solutions of concentrations up to 70% polymer weight fraction. This extension confirms Daivis's results, showing that D_I deviates from D_S above a volume fraction of approximately 0.4, this deviation rapidly increases with increasing concentration. The concentration dependence of D_I does not fit a unique power law. Regression of the diffusion data shows the concentration power law dependence varies from -11±4 to -14.9±0.7 as the concentration increases from a volume fraction of 0.4 into the concentrated domain. These results are in agreement with those of Wesson et al [71] who found the concentration dependence did not fit a unique power law, and that the slope of log D vs. log c became increasingly negative, reaching values of -13. The change in power law indicates changes in the dominant diffusion mechanism. The concentration dependence power law indicates that reptation is not the significant method of diffusion at these solution concentrations, but that the solution is severely

constrained. These constraints are postulated to be localised polymer networks formed on the onset of glass transition.

5.2 Suggestions for Further Work

The similarity of diffusion coefficients found for solutions with similar quality solvents, and that D_I is considerably less than D_S for solutions with unequally poor quality solvents invites investigation of solutions with unequally good quality solvents. Such measurements would provide valuable information about the importance of $\Delta\chi$ to solution dynamics.

The failure of the 929 000 Dalton PS/ 110 000 Dalton PVME/ carbon tetrachloride solution to converge to the toluene equivalent's infinite dilution diffusion coefficient as shown in section 4.2.3 makes it highly desirable to "re-run" the original data of Daivis [5] and Martin [67] with the same polymers used in both ternary polymer solutions. Confirmation of the high molecular weigh solution diffusion coefficients is desirable, to enable understanding of the solution dynamics throughout the concentration range, and to find out if the decrease in D_I observed in the 110 000 Dalton PS/ 110 000 Dalton PVME/ carbon tetrachloride solutions is a "universal" feature of these solutions or if the decrease has a more simple explanation, that of internal diffusion mechanism changes brought about by the onset of phase separation.

During the course of this work the Autocorrelator described and used in this work was superseded by a Multiple Tau Log Autocorrelator built by Luo [43]. This Autocorrelator allows a greater diffusion time span to be investigated than the current 50 channel Autocorrelator built by O'Driscoll [51]. This would allow the investigation of the so called "fast mode" of diffusion (described in chapter 2) along side the "slow mode" currently investigated. Current Autocorrelator technique deliberately tries to remove this "fast mode" through careful solution preparation and selection, the Multiple Tau Log Autocorrelator can potentially allow the resolution of both the "fast" and "slow" mode diffusion allowing investigation of D_C, hitherto uninvestigated, and it's relationship with mass fraction, polymer-polymer interaction parameter, molar mass and the self diffusion coefficient.

Appendices: Publications

Appendix 1

Dynamic Light Scattering from Ternary Polymer Solutions

New Zealand Institute of Physics Conference Poster (1992)

Appendix 2

Studies of Ternary Polymer Solutions by Dynamic Light Scattering and Pulsed Field Gradient Nuclear Magnetic Resonance

***Macromolecular Reports*, A31(Suppls. 6&7), 1119-1126 (1994)**

References

[1] R. Borsali, M. Duval, H. Benoit and M. Benmouna, *Macromolecules*, **20**, 1112-1115 (1987)

[2] M. Benmouna, H. Benoit, M. Duval and Z. Akcasu, *Macromolecules*, **20**, 1107-1112 (1987)

[3] G. Foley and C. Cohen, *Macromolecules*, **20**, 1891-1896 (1987)

[4] H. Benoit and M. Benmouna, *Macromolecules,* **17**, 535-540 (1984)

[5] P. J. Daivis, Ph D Thesis, Massey University (1989)

[6] P. J. Daivis, D. N. Pinder, *Macromolecules*, **26**, 3381-3390 (1993)

[7] P. J. Daivis, D. N. Pinder, *Polymer International*, **27**, 261-265 (1992)

[8] D. N. Pinder, D. T. Clark, P. J. Daivis, *Macromolecular Reports*, **A31(SUPPLS, 6 & 7)**, 1119-1126 (1994)

[9] P. J. Daivis, D. N. Pinder, P. T. Callaghan, *Macromolecules,* **25**, 170-178 (1992)

[10] U. Eisele, *Introduction to Polymer Physics*, Springer-Verag, New York (1990)

[11] M. Daoud, G. Jannink, *J. Physique*, **37**, 973-979 (1976)

[12] M. Doi, S. F. Edwards, *The Theory of Polymer Dynamics*, Oxford University Press, Oxford (1986)

[13] P. G. de Gennes, *Scaling Concepts in Polymer Physics*, Cornell University Press, Ithaca (1979)

[14] P. J. Flory, *Principles of Polymer Chemistry*, Cornell University Press, Ithaca (1953)

[15] H. Fujita, *Polymer Solutions*, Elsevier, Amsterdam (1990)

[16] W. Kuhn, *Kolloid Z.*, **68**, 2 (1934)

[17] P. J. Flory, *J. Chem Phys.*, **17**, 303 (1949)

[18] D. W. Schaefer, *Polymer*, **25**, 387-394 (1984)

[19] A. Z. Akcasu, C. C. Han, *Macromolecules*, **12**, 276-280 (1979)

[20] M. Huggins, *J. Phys. Chem.*, **46**, 151 (1942), M. Huggins, *Ann N. Y. Acad. Sci.*, **41**, 1 (1942), M. Huggins, *J. Am. Chem. Soc.*, **64**, 1712 (1942)

[21] F. Gundert, B. A. Wolf, "Polymer-Solvent Interaction Parameters", in *Polymer Handbook,* Second Edition, Ed J. Brandrup and E. H. Immergut, John Wiley and Sons, New York (1975)

[22] J. Pouchly, D. Patterson, *Macromolecules*, **6**, 465-467 (1973)

[23] P. E. Rouse, *J. Chem Phys.*, **21**, 1272 (1953)

[24] E. H. Zimm, *J. Chem. Phys.*, **24**, 269-278 (1956)

[25] J. G. Kirkwood, *Macromolecules*, Gordon and Breach, New York (1967)

[26] B. J. Berne, R. Pecora, *Dynamic Light Scattering*, John Wiley and Sons, N.Y. (1976)

[27] D. E. Koppel, *Journal of Chemical Physics*, **57**,4814-4820 (1972)

[28] P. N. Pusey, "Measurement of diffusion coefficients of poly disperse solutes by intensity fluctuation spectroscopy", in *Industrial Polymers Characterisation by Molecular Weight*, Ed. J. H. S. Green and R. Deitz, Transcripta Books, London (1973) and J. C Brown, P. N. Pusey, R. Dietz, *J. Chem. Phys.*, **62**, 1136-1144 (1975)

[29] T. A. King and M. F. Treadaway, *Journal of The Chemical Society Faraday Transactions II*, **73**, 1616-1626 (1977).

[30] P. G. de Gennes, *Macromolecules*, **9**, 587-593 and 594-598 (1976)

[31] Bloomfield in *Dynamic Light Scattering*, Ed R. Pecora, Plenum Press, New York (1985)

[32] G. D. J. Philles, *J. Chem. Phys.*, **60**, 983-987 (1974)

[33] P. N. Pusey, H. M. Fijnaut and A. Vrij, *J. Chem. Phys.*, **77**, 4270-4281 (1982)

[34] R. Borsali, M Duval, M. Benmouna, *Macromolecules*, **22**, 816-821 (1989)

[35] L. Giebel, R. Borsali, E. W. Fisher and G. Meier, *Macromolecules*, **23**, 4054-4060, (1990)

[36] A. Z. Akcasu, G. Nagele, R. Klein, *Macromolecules*, **24**, 4408-4422 (1991)

[37] E. L. Cussler, *Multi component Diffusion*, Elsevier Scientific Publishing Company, Amsterdam (1976)

[38] D. N. Pinder, Massey University, New Zealand, Private Correspondence

[39] M. Benmouna, J. Seils, G. Meier, A Patkowski and E. W. Fisher, *Macromolecules*, **26**, 668-678 (1993)

[40] S. Saeki, S. Tsubotani, H. Kominami, M. Tsubokawa, *J. Polym. Sci., Polym. Phys. Ed.*, **24**, 325 (1986)

[41] R. Borsali, "Scattering properties of ternary polymer solutions," in *Light Scattering-Principles and Development,* Ed by W. Brown, Oxford University Press Inc., New York (1996)

[42] A. Z. Akcasu, "Dynamic scattering from multi component polymer mixtures in solution and in bulk", in *Dynamic Light Scattering-The Method and Some Applications*, Ed by W. Brown, Oxford University Press Inc, New York (1993)

[43] Y. Luo, Ph D Thesis, Massey University, New Zealand (1996)

[44] E. R. Pike, *The Theory of Light Scattering in Photon Correlation and Light Beating Spectroscopy*, Eds H. Z. Cummins and E. R. Pike, Plenum Press, New York (1974)

[45] R. Hanbury-Brown, R. Q. Twiss, *Nature*, **177**, 27 (1956)

[46] R. Pecora, *J. Chem. Phys.*, **40**, 1604 (1964)

[47] H. Z. Cummins, N. Knable, Y. Yeh, *Phys. Rev. Letts.*, **12**, 150 (1964)

[48] R. C. O'Driscoll, D. N. Pinder, *J. Phys. E.:Sci. Instrum.*, **13**, 192-200 (1980)

[49] C. M. Trotter, Ph D Thesis, Massey University, New Zealand (1980)

[50] D. Jolly, H. Eisenberg, *Biopolymers*, **15**, 61-95 (1976)

[51] R. C. O'Driscoll, Ph D Thesis, Massey University, New Zealand (1982)

[52] T. Raj, W. H. Flygare, *Biopolymers*, **16**, 545-549 (1977)

[53] P. Nieuwenhuysen, *Macromolecules*, **11**, 832-834 (1978)

[54] R, Foord, E, Jakeman, C. J. Oliver, E. R. Pike, R. J. Blagrove, E. Wood, A. R. Peacocke, *Nature*, **227**, 242-245 (1970)

[55] C. J. Oliver, in *Photon Correlation and Light Beating Spectroscopy*, Eds H. Z. Cummins and E. R. Pike, Plenum Press, New York (1974)

[56] A. Mole, E. Giessler, *J. Phys. E,: Sci. Instrum.*, **8**, 417-420 (1975)

[57] E. Jakeman, in *Photon Correlation and Light Beating Spectroscopy*, Eds H. Z. Cummins and E. R. Pike, Plenum Press, New York (1974)

[58] H. Z. Cummins and P. N. Pusey, "Dynamics of Macromolecular Motion" from *Photon Correlation Spectroscopy and Velocimetry*, Ed H. Z. Cummins and E. R. Pike, Plenum Press, New York (1977)

[59] S. W. Provencher, J. Hendrix and L. De Mayer, *J. Chem. Phys.*, **69**, 4273-4276 (1978)

[60] P. R. Bevington, *Data Reduction and Error Analysis for the Physical Sciences*, McGraw-Hill Book Company (1969)

[61] B. E. Tabor, "Preparation and Clarification of Solutions", from *Light Scattering from Polymer Solutions*, Ed M. B. Huglin, Academic Press, London (1972)

[62] E. H. Zimm, *J. Chem. Phys.*, **16**, 1099-1114

[63] J. A. Manson and G. J. Arquette, *Macromolekulare Chemie*, **37**, 187-197 (1960)

[64] Th. G. Scholte, *Journal of Polymer Science*, **A2**, 841-868 (1970)

[65] *Polymer Handbook*, Second Edition, Ed J. Brandrup and E. H. Immergut, John Wiley and Sons, New York (1975)

[66] J. Timmermans, *Physico-Chemical Constants of Pure Organic Compounds*, Elsevier Publishing Company, Amsterdam (1950)

[67] J. E. Martin, *Macromolecules*, **17**, 1279-1283 (1984)

[68] C. S. Su, D. Patterson, *Macromolecules*, **10**, 708-710 (1977)

[69] L. Zeeman, D. Patterson, *Macromolecules*, **5**, 513 (1972)

[70] T. P. Lodge, L. M. Wheeler, *Macromolecules*, **19**, 2983-2986 (1986)

[71] J. A. Wesson, I. Noh, T. Kitano, H. Yu, *Macromolecules*, **17**, 782 (1984)

[72] L. Leger, H. Hervet, F. Rondelez, *Macromolecules*, **14**, 1732 (1981)

[73] P. T. Callaghan, D. N. Pinder, *Macromolecules*, **17**, 431 (1984)

[74] P. F. Green, E. J. Kramer, *Macromolecules*, **19**, 1108 (1986)

[75] C. R. Bartels, B. Crist (Jr), L. J. Fetters, W. W. Graessley, *Macromolecules*, **19**, 785 (1986)

[76] H. Fujita, Y. Einaga, *Polym. J. (Tokyo)*, **17**, 1131 (1985)